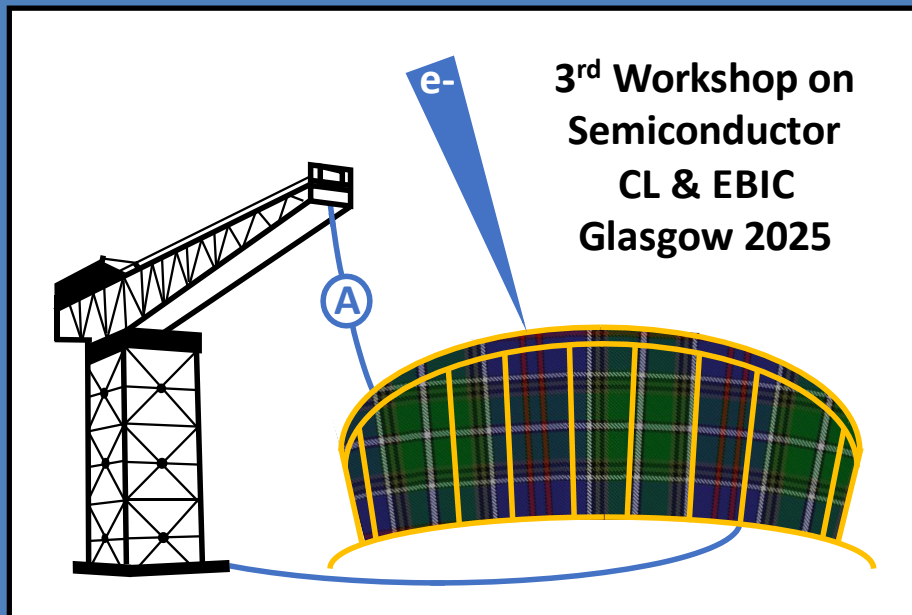


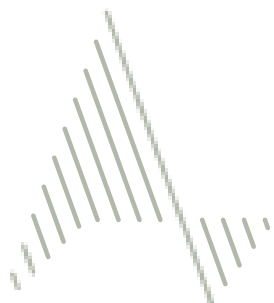
# 3rd Workshop on Semiconductor Cathodoluminescence and Electron Beam Induced Current



9–11 April 2025  
Technology & Innovation Centre  
99 George St, Glasgow  
Scotland, UK

## Conference Sponsors

Gold Sponsor



# attolight™

Silver Sponsor



Bronze Sponsors



**ThermoFisher**  
SCIENTIFIC

**Wednesday 9<sup>th</sup> April**
**AM** Arrival and coffee from 11:00, tours, 12:30 lunch

**Session A: STEM-CL**
**13:30** Nanometer Resolution Cathodoluminescence Imaging of Individual Quantum Emitters in Twisted hBN  
**A1** Hanyu Hou,<sup>1,2</sup> Muchuan Hua,<sup>1</sup> Kaijun Yin,<sup>2</sup> Jian-Min Zuo,<sup>2</sup> Benjamin T. Diroll,<sup>1</sup> Thomas E. Gage,<sup>1</sup> Jianguo Wen<sup>1</sup>
<sup>1</sup>Argonne National Laboratory, Lemont, IL, USA

<sup>2</sup>University of Illinois at Urbana-Champaign, Urbana, IL, USA

**14:05** Time-resolved Cathodoluminescence using an Ultrafast Transmission Electron Microscope  
**A2** M. Moreira,<sup>1</sup> C. Santini,<sup>1</sup> N. Van Nielsen,<sup>5</sup> F. Castioni,<sup>2</sup> D. Lagarde,<sup>3</sup> R. Cours,<sup>1</sup> S. Weber,<sup>1</sup> T. Hungria,<sup>6</sup> A.V. Sakharov,<sup>4</sup> A. F. Tsatsulnikov,<sup>4</sup> A. E. Nikolaev,<sup>4</sup> A. Polman,<sup>5</sup> A. Balocchi,<sup>3</sup> N. Cherkashin,<sup>1</sup> L. Tizei,<sup>2</sup> S. Meuret<sup>1</sup>
<sup>1</sup>CEMES/CNRS, Toulouse, France

<sup>2</sup>Université Paris Saclay/CNRS, Orsay, France

<sup>3</sup>LPCNO, Toulouse, France

<sup>4</sup>Ioffe Institute, St Petersburg, Russia

<sup>5</sup>NWO-institute AMOLF, Amsterdam, The Netherlands

<sup>6</sup>Centre Castaing - Centre de microcaractérisation Raimond Castaing, Toulouse, France

**14:25** Quantum Confined Luminescence in Two Dimensions

**A3** Luiz H. G. Tizei

*Université Paris-Saclay/CNRS, Orsay, France*
**14:45** Single Dot Spectroscopy: Carrier Capture into Individual InP Quantum Dots Directly Imaged by  
**A4** Nanoscale Cathodoluminescence Microscopy

F. Bertram,<sup>1</sup> G. Schmidt,<sup>1</sup> P. Veit,<sup>1</sup> J. Christen,<sup>1</sup> A. Ćutuk,<sup>2</sup> M. Jetter,<sup>2</sup> P. Michler<sup>2</sup>
<sup>1</sup>Otto-von-Guericke-University Magdeburg, Germany

<sup>2</sup>University of Stuttgart, Germany

**15:05** Insights into Carrier Transport and Recombination in a Cascaded InGaN LED: A Nanoscale Correlation  
**A5** of EBIC and CL

G. Schmidt, K. Wein, H. Eisele, F. Bertram, P. Veit, O. August, C. Berger, A. Dadgar,  
A. Strittmatter, J. Christen

*Otto-von-Guericke-University Magdeburg, Germany*
**15:25** Coffee

**Session B: Power and electronic devices**
**16:00** High-Resolution Cathodoluminescence Mapping for Doping Quantification Across a Wide Range of  
**B1** Silicon Concentrations in GaN Epitaxial Layers

Z. M'qaddem<sup>1</sup>, N. Rochat<sup>1</sup>, G. Jacopin<sup>2</sup>, B. Mohamad<sup>1</sup>, T. Kaltsounis<sup>1</sup>, M. Charles<sup>1</sup>, J. Buckley<sup>1</sup>, Ł. Borowik<sup>1</sup>
<sup>1</sup>Univ. Grenoble Alpes, CEA-LETI, France

<sup>2</sup>Univ. Grenoble Alpes, CNRS, Grenoble INP, Institut Néel, France

**16:20** Defect Analysis in Diamond Schottky Barrier Diodes for Beta-Voltaic Applications

**B2** H. Ribeiro,<sup>1,2</sup> D.Z. Nusimovici,<sup>1,3</sup> L. Valera,<sup>1</sup> M. Jacquemin,<sup>1</sup> G. Jacopin,<sup>2</sup>
<sup>1</sup>DIAMFAB SAS, Grenoble, France

<sup>2</sup>Institut Néel CNRS, Univ. Grenoble Alpes, France

<sup>3</sup>Univ. Grenoble Alpes, CNRS, Grenoble INP, SIMaP, France

**16:40** Cathodoluminescence Study of CdSeTe/CdTe Solar Cells using FIBSEM and STEM and Site-Specific  
**B3** Selection

Stuart Robertson, Zhaoxia Zhou, Sam Machin, Kieran  
Curson, Michael Walls

*Loughborough University, UK*
**17:00** Investigation of Ag Alloying Effect in Cu(In,Ga)S<sub>2</sub> Solar Cells Absorber by CL-EBSD

**B4** Y.Hu,<sup>1</sup> A.V.Oli,<sup>2</sup> Z.S.Pehlivan,<sup>1</sup> G.Kusch,<sup>1</sup> S.Sieberttritt,<sup>2</sup> R.A.Oliver<sup>1</sup>
<sup>1</sup>University of Cambridge, UK

<sup>2</sup>University of Luxembourg, Luxembourg

**17:20** Close


	Evening reception at National Piping Centre <b>30–34 McPhater St, G4 0HW</b>
<b>19:00</b>	Drinks reception
<b>19:20</b>	Conference banquet and ceilidh



#### Thursday 10<sup>th</sup> April

Session C: Quantum emitters and nanostructures I	
<b>09:00</b>	<b>Cathodoluminescence Study on a Surface-Emitting Nano-Ridge Laser</b>
C1	Toon Coenen, <sup>1</sup> E. M. B. Fahmy, <sup>2</sup> Z. Ouyang, <sup>2</sup> D. Colucci, <sup>2,3</sup> J. Van Campenhout, <sup>3</sup> B. Kunert, <sup>3</sup> D. Van Thourhout <sup>2</sup> <i><sup>1</sup>DELMIC B.V, Delft, The Netherlands</i> <i><sup>2</sup>Ghent University - IMEC, Belgium</i> <i><sup>3</sup>IMEC, Heverlee, Belgium</i>
<b>09:35</b>	<b>Cathodoluminescence Investigation of InGaN Buffer Layer Inclusion in InGaN/GaN Nanowire Superlattice: A way Towards High Efficiency Red Light Emission</b>
C2	Krishnendu Sarkar, Stefano Pirota, Nidel Tchoulayeu, Quang-Chieu Bui, Omar Saket, Stephane Collin, Laurent Travers, Martina Morassi, François H. Julien, Jean-Christophe Harmand, Noëlle Gogneau, Maria Tchernycheva <i>University Paris-Saclay, University Paris-City, CNRS, Palaiseau, France</i>
<b>09:55</b>	<b>Influence of Surface Modification on the Properties of GaN nanowires – Cathodoluminescence and Electron Microscopy Studies</b>
C3	A. Reszka, <sup>1</sup> S. Piotrowska, <sup>1</sup> Tomasz Plocinski, <sup>2</sup> Radosław Szymon, <sup>3</sup> Eunika Zielony, <sup>3</sup> Aleksandra Wierzbicka, <sup>1</sup> Sylwia Gierałtowska, <sup>1</sup> Marta Sobanska, <sup>1</sup> Zbigniew R. Zytkeiwicz, <sup>1</sup> B.J. Kowalski <sup>1</sup> <i><sup>1</sup>Polish Academy of Sciences, Warsaw, Poland</i> <i><sup>2</sup>Warsaw University of Technology, Warsaw, Poland</i> <i><sup>3</sup>Wrocław University of Science and Technology, Wrocław, Poland</i>
<b>10:30</b>	<b>Coffee</b>
Session D: Quantum emitters and nanostructures II	
<b>11:10</b>	<b>Cathodoluminescence Investigations of Nano-LEDs Based on Micron Sized III Nitride Platelets</b>
D1	A. Gustafsson, <sup>1,2</sup> H. Usman, <sup>1</sup> Z. Bi, <sup>3,4</sup> L. Samuelson, <sup>1,2,3</sup> <i>1) Southern University of Science and Technology, Shenzhen, China</i> <i>2) Lund University, Lund, Sweden</i> <i>3) Hexagem AB, Lund, Sweden</i> <i>4) Future Display Institute of Xiamen, Xiamen, China</i>
<b>11:45</b>	<b>Correlative Scanning Electron Microscopy for Exploring Quantum Emitters in Cubic GaN</b>
D2	K. Nicholson, <sup>1</sup> R. Alshammary, <sup>1</sup> J.K. Cannon, <sup>2</sup> J. Lee, <sup>3</sup> K. Chang, <sup>3</sup> Y.C Chiu, <sup>3</sup> C. Bayram, <sup>3</sup> R.W. Martin, <sup>4</sup> P.R. Edwards, <sup>4</sup> N. Gunasekar <sup>1</sup> <i><sup>1</sup>School of Physics and Astronomy, Cardiff University, UK</i> <i><sup>2</sup>School of Engineering, Cardiff University, UK</i> <i><sup>3</sup>University of Illinois at Urbana-Champaign, Champaign, Illinois, 61801, USA</i> <i><sup>4</sup>University of Strathclyde, Glasgow, UK</i>
<b>12:05</b>	<b>Polarisation-Resolved Cathodoluminescence Study of a Zincblende InGaN/GaN Single Quantum Well</b>
D3	X. Xu, <sup>1</sup> M. Frentrup, <sup>1</sup> G. Kusch, <sup>1</sup> Z. S. Pehlivan, <sup>1</sup> M. J. Kappers, <sup>1</sup> D. J. Wallis, <sup>1,2</sup> R. A. Oliver <sup>1</sup> <i><sup>1</sup>University of Cambridge, UK</i> <i><sup>2</sup>University of Cardiff, UK</i>
<b>12:25</b>	<b>Characterization of InGaN/GaN Nanowires by Wavelength &amp; Angle Resolved Cathodoluminescence</b>
D4	T. Lassiak, R. Vermeersch, A. Rooney, J. Brochet, M. Charbonnier, B. Amstatt, P. Tchoulfian, M. Daanoune <i>Aledia, Echirrolles, France</i>
<b>12:45</b>	<b>Lunch</b>

Thursday 10<sup>th</sup> April

## Session E: Time-resolved CL

- 14:00** Recombination Dynamics of Oxygen-Related Defects in AlN Layers Studied with Time-Resolved Cathodoluminescence Spectroscopy  
E1  
B. Szafranski, L. Peters, C. Margenfeld, S. Wolter, A. Waag, T. Voss  
*Technische Universität Braunschweig, Germany*
- 14:35** Study of Nanolaser Optical and Structural Properties at the Nanometre Scale  
E2  
C. Santini,<sup>1</sup> N. Van Nielen,<sup>2</sup> T.H Ngo,<sup>3</sup> V. Brändli,<sup>3</sup> S. Chenot,<sup>3</sup> P.M. Coulon,<sup>3</sup> S. Vézian,<sup>3</sup> J. Brault,<sup>3</sup> P.A. Shields,<sup>5</sup> A. Polman,<sup>2</sup> B. Damilano,<sup>3</sup> C. Brimont,<sup>4</sup> T. Guillet,<sup>4</sup> S. Meuret<sup>1</sup>  
<sup>1</sup>CEMES, CNRS, 31055 Toulouse, France  
<sup>2</sup>AMOLF, Amsterdam, Netherlands  
<sup>3</sup>Université Côte d'Azur, CNRS, CRHEA, Valbonne, France  
<sup>4</sup>L2C, Montpellier, France  
<sup>5</sup>University of Bath, UK
- 14:55** V-pits as a Source of Emission Heterogeneity in InGaN/GaN Micro-LEDs Studied by Photon-Correlation Cathodoluminescence Spectroscopy  
E3  
P. Sáenz de Santa María Modroño<sup>1</sup>, C. Le Maout<sup>2</sup>, N. Bernier,<sup>2</sup> D. Vaufrey,<sup>2</sup> G. Jacopin<sup>1</sup>  
<sup>1</sup>Univ. Grenoble Alpes, CNRS, Institut Néel, Grenoble, France  
<sup>2</sup>Univ. Grenoble Alpes, CEA-LETI, Grenoble, France
- 15:15** Effects of Lamella Preparation on InGaN Quantum Well Luminescence  
E4  
N. van Nielen,<sup>1</sup> D. Lagard,<sup>2</sup> C. Santini,<sup>3</sup> F. Castioni,<sup>4</sup> R. Cours,<sup>3</sup> A. Balocchi,<sup>2</sup> T. Hungria,<sup>5</sup> A. Tsatsulnikov,<sup>6</sup> A. Sakharov,<sup>6</sup> A. Nikolaiev,<sup>6</sup> N. Cherkashin,<sup>3</sup> L. Tizei,<sup>4</sup> A. Polman,<sup>1</sup> S. Meuret<sup>3</sup>  
<sup>1</sup>AMOLF, Amsterdam, The Netherlands  
<sup>2</sup>CNRS, LPCNO, Toulouse, France  
<sup>3</sup>CEMES/CNRS, Toulouse, France  
<sup>4</sup>Laboratoire de Physique des Solides, Orsay, France  
<sup>5</sup>CNRS, Centre de Microcaractérisation Raimond Castaing, Toulouse, France  
<sup>6</sup>Ioffe Institute, Saint-Petersburg, Russia

15:35 Coffee

## Session F: Time-resolved &amp; steady-state CL

- 16:05** Carrier Diffusion in Ga(As,Sb) Nanowires Investigated by Continuous and Time-Resolved Cathodoluminescence Spectroscopy  
F1  
M. Gómez Ruiz,<sup>1</sup> G. Kusch,<sup>2</sup> V. Kaganer,<sup>1</sup> A. Ajay,<sup>3</sup> H. W. Jeong,<sup>3</sup> G. Koblmüller,<sup>3</sup> R. A. Oliver,<sup>2</sup> O.Brandt,<sup>1</sup> J. Lähnemann<sup>1</sup>  
<sup>1</sup>Paul-Drude-Institut für Festkörperelektronik, Berlin, Germany  
<sup>2</sup>University of Cambridge, United Kingdom  
<sup>3</sup>Walter-Schottky-Institut, Technische Universität München, Germany
- 16:25** Steady-State and Time-Resolved Cathodoluminescence of III-Nitride Semiconductors  
F2  
K. Loeto, A. F. Campbell, D. Spallek, J. Lähnemann  
*Paul-Drude-Institut für Festkörperelektronik, Berlin, Germany*
- 16:45** CLEBIC characterisation of deep UV emitting LEDs  
F3  
Douglas Cameron,<sup>1,2</sup> Marcel Schilling,<sup>3</sup> Gunnar Kusch,<sup>4</sup> Paul R. Edwards,<sup>2</sup> Veisturs Spulis,<sup>4</sup> Tim Wernicke,<sup>3</sup> Michael Kneissl,<sup>3</sup> Rachel A. Oliver,<sup>4</sup> Robert W. Martin<sup>2</sup>  
<sup>1</sup>Gatan, Inc., Pleasanton, USA  
<sup>2</sup>University of Strathclyde, Glasgow UK  
<sup>3</sup>Technische Universität Berlin, Germany  
<sup>4</sup>University of Cambridge, Cambridge, UK

**17:05** HyperSpy/LumiSpy update  
Jonas Lähnemann

17:45 Close

**19:00** Civic reception at Glasgow City Chambers:  
George Square, G2 1DU

With thanks to the Lord Provost of Glasgow and Glasgow City Council



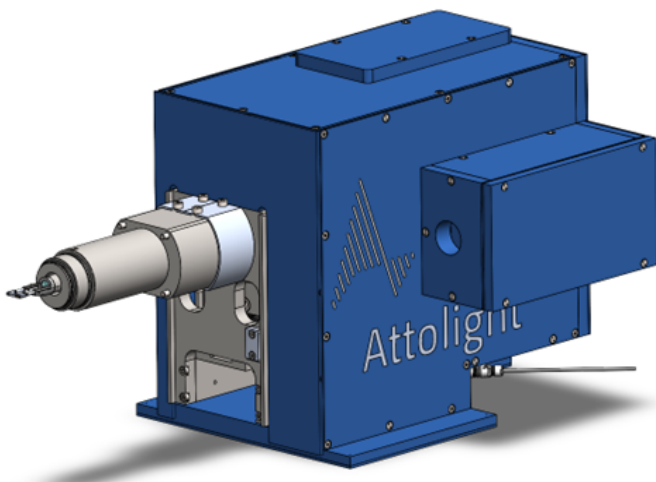
Friday 11<sup>th</sup> April

Session G: Emerging semiconductors	
<b>09:00</b> G1	Cathodoluminescence of Triplet Excitons in Organic Light Emitting Diode Materials B.G. Mendis, <sup>1</sup> A. Danos, <sup>1,2</sup> A.P. Monkman <sup>1</sup> <sup>1</sup> Durham University, UK <sup>2</sup> Queen Mary University of London, UK
<b>09:35</b> G2	Morphological Effect on Cathodoluminescence Outcoupling in Perovskite Thin Films R. Schot, I. Schuringa, S. Fiedler, T. Veeken, B. Ehrler, A. Polman AMOLF, Amsterdam, The Netherlands
<b>09:55</b> G3	Luminescence Properties of Dislocations in $\alpha$ -Ga <sub>2</sub> O <sub>3</sub> M. Maruzane, <sup>1</sup> Y. Oshima, <sup>2</sup> O. Makydonska, <sup>1</sup> P. R. Edwards, <sup>1</sup> R. W. Martin, <sup>1</sup> F. Massabuau <sup>1</sup> <sup>1</sup> University of Strathclyde, Glasgow, UK <sup>2</sup> National Institute for Materials Science, Tsukuba, Japan
<b>10:15</b> G4	Temperature-Dependent Interplay between Surface GaN Quantum Wells and Two-Dimensional MoS <sub>2</sub> D. Chen, J. Jiang, J.-F. Carlin, M. Banerjee, N. Grandjean Ecole polytechnique fédérale de Lausanne (EPFL), Switzerland
<b>10:35</b>	Coffee
Session H: Novel CL techniques	
<b>11:05</b> H1	Cathodoluminescence Excitation Spectroscopy and the Quest of Filtering Transition Radiation A. Freilinger, F. Castioni, Y. Auad, J.-D. Blazit, X. Li, M. Kociak, L. Tizei Université Paris Saclay/CNRS, Orsay, France
<b>11:25</b> H2	Determination of LED External Quantum Efficiency by Electron Pumping in a SEM C. Guérin, <sup>1,2</sup> F. Donatini, <sup>2</sup> Bruno Daudin, <sup>1</sup> G. Jacopin <sup>2</sup> <sup>1</sup> Univ. Grenoble Alpes, CNRS, CEA Grenoble, France <sup>2</sup> Univ. Grenoble Alpes, CNRS, Institut Néel, France
<b>11:45</b> H3	Photo-Enhanced Cathodoluminescence Nicolas Tappy, <sup>1</sup> Aurélie Coppex, <sup>1</sup> Stefano Marinoni, <sup>2</sup> Nicholas Morgan, <sup>1</sup> Christian Monachon <sup>1</sup> <sup>1</sup> Attolight SA, Ecublens, Switzerland <sup>2</sup> Ecole Polytechnique Fédérale de Lausanne (EPFL), Switzerland
<b>12:05</b> H4	Towards Laser-Driven Semiconductor Electron Sources: Field-Induced Negative Electron Affinity Gallium Nitride Photocathodes S. Marinoni, <sup>1</sup> N. Tappy, <sup>2</sup> V. Piazza, <sup>1</sup> A. Fontcuberta i Morral, <sup>1</sup> C. Monachon <sup>2</sup> <sup>1</sup> Ecole Polytechnique Fédérale de Lausanne (EPFL), Switzerland <sup>2</sup> Attolight SA, Ecublens, Switzerland
<b>12:25</b> H5	Cathodoluminescence Hyperspectral Imaging without an Electron Microscope Paul R. Edwards, Robert W. Martin University of Strathclyde, Glasgow, UK
<b>12:45</b>	Closing remarks



# MÖNCH

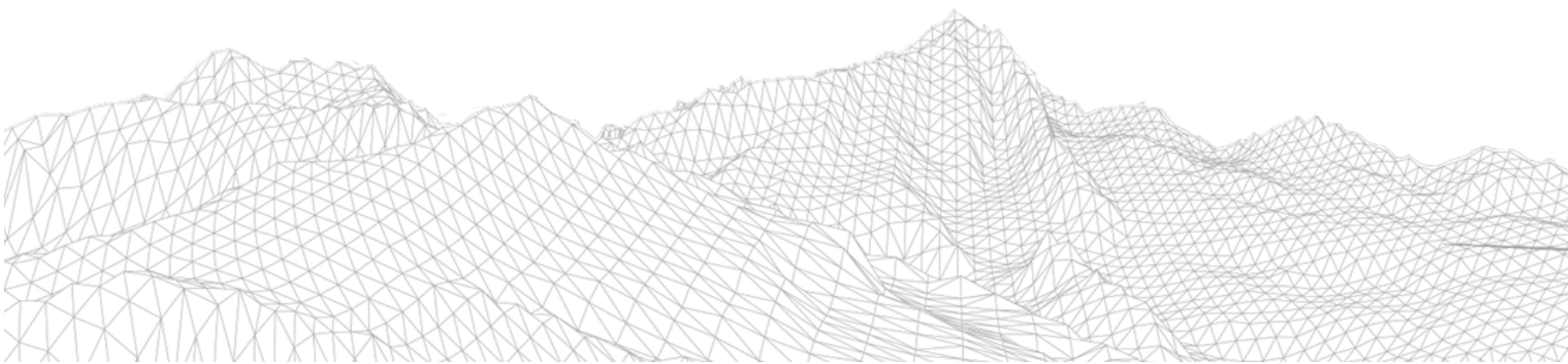
## Light Collection/Injection add-on for STEM



- Unique system for light collection and injection in STEM
- High Numerical Aperture for efficient light collection
- Free-space coupling to preserve light intensity and spectral resolution
- Mirror independent of the sample to analyse the entire sample area
- Beam spot size down to 10µm-diam (injection mode)
- Compatible with most TEM models (including HR pole pieces)
- Equipped with stage touch alarm and X-Ray protection

- Cathodoluminescence
- Photoluminescence
- Light excitation
- Pump & Probes analysis

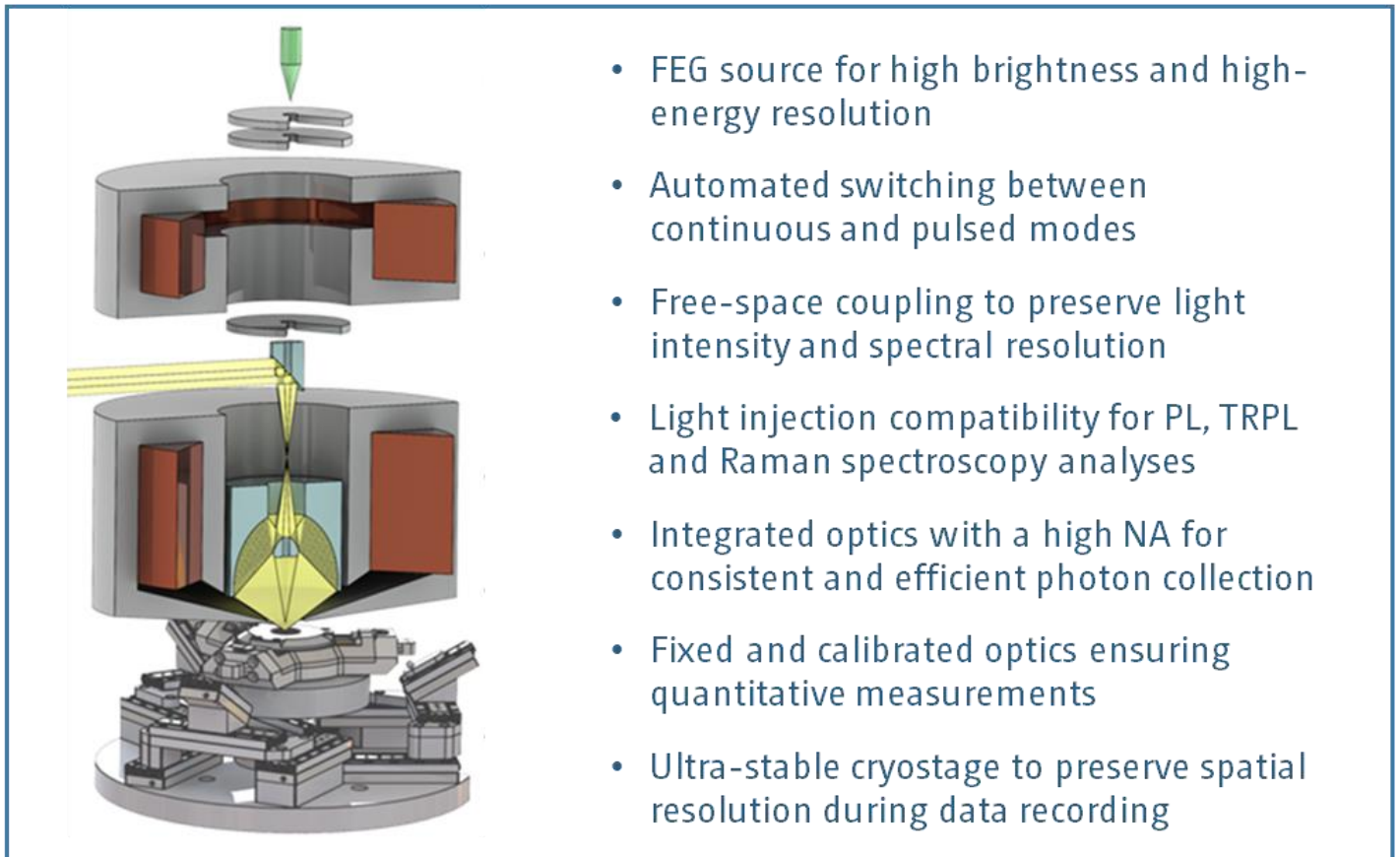
- Electronics & Opto-electronics
- Photovoltaic cells
- Light Emitting Diodes
- 2D materials
- Plasmonic
- Nanomaterials
- Organic, biological samples





# ALLALIN

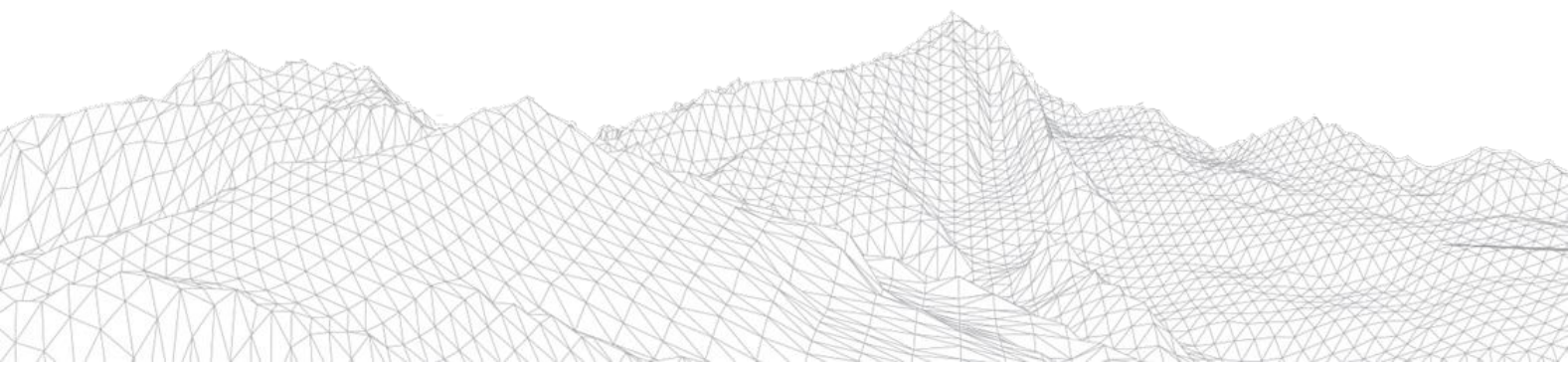
## Hybridized SEM- Spectroscopic platform



- FEG source for high brightness and high-energy resolution
- Automated switching between continuous and pulsed modes
- Free-space coupling to preserve light intensity and spectral resolution
- Light injection compatibility for PL, TRPL and Raman spectroscopy analyses
- Integrated optics with a high NA for consistent and efficient photon collection
- Fixed and calibrated optics ensuring quantitative measurements
- Ultra-stable cryostage to preserve spatial resolution during data recording

- SEM
- Cathodoluminescence
- Photoluminescence
- Raman
- Nanoprobes
- Electrical measurements
- Time-resolved analyses
- Cryo-compatibility

- Electronics & Opto-electronics
- Photovoltaic cells
- Light Emitting Diodes
- 2D materials
- Plasmonic
- Nanomaterials
- Organic, biological samples



## Nanometer resolution cathodoluminescence imaging of individual quantum emitters in twisted hBN

Hanyu Hou<sup>1,2</sup>, Muchuan Hua<sup>1</sup>, Kaijun Yin<sup>2</sup>, Jian-Min Zuo<sup>2</sup>, Benjamin T Diroll<sup>1</sup>, Thomas E Gage<sup>1</sup>, Jianguo Wen<sup>1\*</sup>

<sup>1</sup> Center for Nanoscale Materials, Argonne National Laboratory, Lemont, IL, United States of America

<sup>2</sup> Department of Materials Science and Engineering, 2. Materials Research Laboratory, University of Illinois at Urbana-Champaign, Urbana, IL, United States of America

\*Corresponding author: [jwen@anl.gov](mailto:jwen@anl.gov)

Establishing a direct correlation between the atomic structures of quantum emitters and their optical properties is essential for advancing quantum information science, with applications in quantum computing, communication, and sensing. Until now, such correlations have primarily relied on density functional theory (DFT) calculations, as no experimental method has been available for nanoscale studies. Combining atomic-resolution scanning transmission electron microscopy (STEM) with cathodoluminescence (CL)—a technique where electron beams, rather than photons, are used to excite luminescence—offers a promising avenue to explore the structure-property relationships of quantum emitters.

Cathodoluminescence (CL) detects photons emitted as a result of electron beam excitation. Conventional scanning electron microscopy (SEM)-based CL achieves spatial resolutions of tens of nanometers [1], which, while significantly higher than the hundreds of nanometers typical of photoluminescence, remains insufficient for precisely correlating atomic structures with optical properties due to SEM's large interaction volume. Moreover, achieving this goal using STEM-CL faces two critical challenges: (1) Current STEM-CL microscopy lacks the spatial resolution needed to resolve and precisely localize individual quantum emitters, and (2) the sample thickness suitable for CL is often incompatible with the structural and chemical requirements of STEM analysis.

In this study, we use two-dimensional (2D) exfoliated hexagonal boron nitride (hBN), a material with a bandgap near 6 eV [2], as a model system to correlate atomic structures with emission properties. hBN has been extensively engineered to host quantum emitters, with a diverse library of emission lines reported, spanning the ultraviolet to near-infrared spectrum, depending on fabrication methods and treatments [2].

Figure 1 presents preliminary results obtained using STEM-CL on carbon-implanted hBN. A CL line scan using a nanoprobe electron beam reveals significant CL enhancement in twisted hBN areas [3-5]. This approach enables the observation of numerous isolated emitters in twisted area with significantly improved spatial resolution, facilitating the identification of corresponding defect structures. The spatial resolution of CL is influenced by the probe size, plasmon wave, and charge carrier diffusion length [1][4]. When the CL resolution is reduced to just a few nanometers, the precise spatial location of the defect can be determined. Since the emission signal in STEM-CL is proportional to the number of activated defects, the use of a small electron probe allows for highly localized defect excitation. As shown in Fig. 1, the CL spectrum obtained from the defect region reveals carbon-related emission at 440 nm, with a spatial resolution of 2–3 nm for mapping the blue emitter. These results demonstrate that blue and ultraviolet light emitters in thin twisted hBN (approximately 20 nm thick) can be probed with sufficient intensity and high spatial resolution.

To investigate the chemical composition and structure of the emitter, we employ correlative electron energy loss spectroscopy (EELS) and quantitative high-angle annular dark-field (HAADF) imaging. By acquiring scanning transmission electron microscopy cathodoluminescence (STEM-CL) and STEM-EELS data from the same region, we identify that the 440 nm blue emission originates from substituted carbon atoms. Atomic-resolution HAADF imaging (Fig. 2) allows us to distinguish contrast differences between boron and nitrogen sites in a three-layer AA' stacking configuration of hBN. Intensity histograms of the atomic columns, combined with quantitative HAADF contrast analysis, reveal that the bright defect corresponds to a vertical carbon dimer, which is responsible for the observed 440 nm blue emission.

This talk will report on our use of aberration-corrected STEM and CL to identify and characterize the optical properties, chemical and structural information of the quantum emitter embedded in 2D-exfoliated hBN. In addition, we will report on density-functional theory (DFT) calculations to study the intrinsic properties of the defects, such as the formation energy. The correlation between quantum emitters' emission and its structure provides the fundamental insights for the fabrication of stable, bright, and long-lifetime quantum emitters [6].

## References

- [1] "High spatial resolution cathodoluminescence | Gatan, Inc." Accessed: Feb. 10, 2024. [Online]. Available: <https://www.gatan.com/high-spatial-resolution-cathodoluminescence>
- [2] I. Aharonovich, J.-P. Tetienne, and M. Toth, "Quantum Emitters in Hexagonal Boron Nitride," *Nano Lett.*, vol. 22, no. 23, pp. 9227–9235, Dec. 2022, doi: 10.1021/acs.nanolett.2c03743.
- [3] B. Shevitski et al., "Blue-light-emitting color centers in high-quality hexagonal boron nitride," *Phys. Rev. B*, vol. 100, no. 15, p. 155419, Oct. 2019, doi: 10.1103/PhysRevB.100.155419.
- [4] H. Zhang, D. R. Glenn, R. Schalek, J. W. Lichtman, and R. L. Walsworth, "Efficiency of Cathodoluminescence Emission by Nitrogen-Vacancy Color Centers in Nanodiamonds," *Small*, vol. 13, no. 22, p. 1700543, 2017, doi: 10.1002/sml.201700543.
- [5] C. Su et al., "Tuning colour centres at a twisted hexagonal boron nitride interface," *Nat. Mater.*, vol. 21, no. 8, Art. no. 8, Aug. 2022, doi: 10.1038/s41563-022-01303-4.
- [6] Work performed at the Center for Nanoscale Materials, a U.S. Department of Energy Office of Science User Facility, was supported by the U.S. DOE, Office of Basic Energy Sciences, under Contract No. DE-AC02-06CH11357. The correlation of point defects with optical behavior is supported by QIS research funding from the U.S. Department of Energy, Office of Science User Facility.

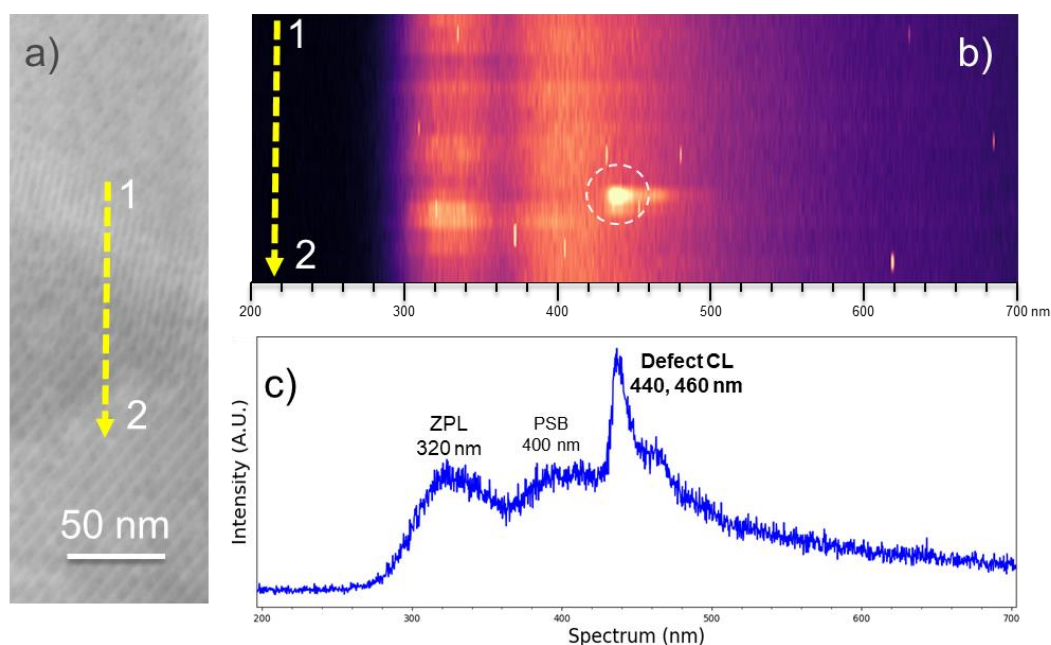


Fig. 1: a) STEM image of twisted interface with Moiré pattern. b) STEM-CL line scan showing a 440 nm blue emitter. c) CL spectrums of the circled positions with corresponding to the blue emitter with ZPL at 440 nm.

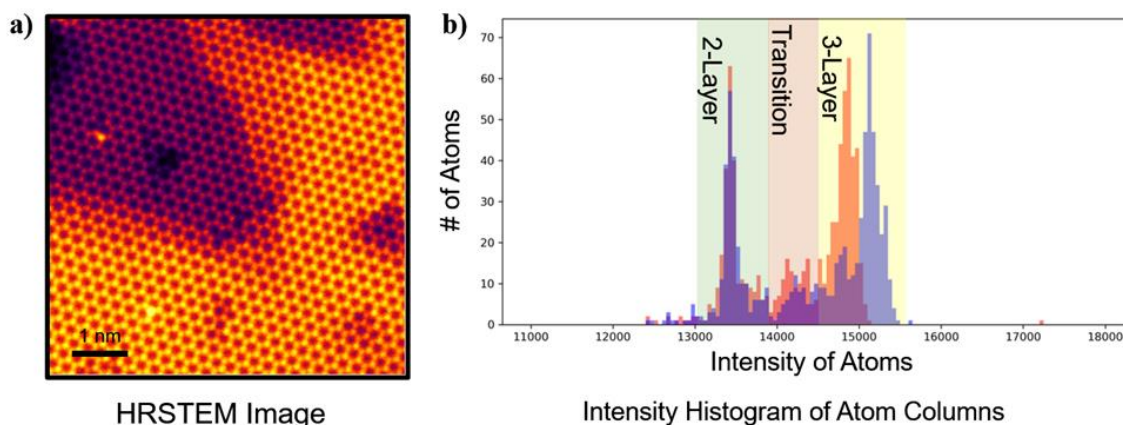


Fig. 2: a) Atomic resolution STEM imaging of few-layer hBN. b) Intensity histogram of atomic columns in 2-layer and 3-layer AA' stacking configurations of hBN (right), showing that Boron and Nitrogen can be distinguished in the odd-numbered layers.

## Time-resolved cathodoluminescence using an Ultrafast Transmission Electron Microscope

M. Moreira<sup>1</sup>, C. Santini<sup>1</sup>, N. Van Nielen<sup>5</sup>, F. Castioni<sup>2</sup>, D. Lagarde<sup>3</sup>, R. Cours<sup>1</sup>, S. Weber<sup>1</sup>, T. Hungria<sup>6</sup>, A.V. Sakharov<sup>4</sup>, A. F. Tsatsulnikov<sup>4</sup>, A. E. Nikolaev<sup>4</sup>, A. Polman<sup>5</sup>, A. Balocchi<sup>3</sup>, N. Cherkashin<sup>1</sup>, L. Tizei<sup>2</sup>, S. Meuret<sup>1,\*</sup>

<sup>1</sup>) CEMES/CNRS, Toulouse, France

<sup>2</sup>) University Paris Saclay/CNRS, Orsay, France

<sup>3</sup>) LPCNO, Toulouse, France

<sup>4</sup>) Ioffe Institute, St Petersburg, Russia

<sup>5</sup>) NWO-institute AMOLF, Amsterdam 1098 XG, The Netherlands

<sup>6</sup>) Centre Castaing - Centre de microcaractérisation Raimond Castaing

Time-resolved cathodoluminescence (TRCL) is an emerging technique that combines high spatial resolution with ultrafast optical characterization. By synchronizing electron beam excitation with time-resolved luminescence detection, TRCL captures rapid emission events that can be used to study charge carrier dynamics and material defects engineering. It is an essential technique for characterizing semiconductor materials for the direct correlation of their structural (defects, composition heterogeneities, strains, etc.) and optical/electronic properties.

Traditionally implemented in scanning electron microscopes (SEMs), TRCL has enabled sub-wavelength resolution studies—such as elucidating the effects of stacking faults in GaN excitons, silver layer interactions in YAG crystals, and stress influences in ZnO nanowires [1-3]. Recently, advances in transmission electron microscopy (TEM) have further pushed TRCL's capabilities, offering enhanced spatial resolution and integration with complementary electron-based spectroscopies [4,5]. Our TRCL experiments are performed in a unique Ultrafast TEM (UTEM) based on a cold-FEG electron gun [6]. This technology allows, among other things, the spatial resolution of a few nanometers to be reached.

In this presentation, we will discuss the advantages and inconveniences of TRCL in a UTEM using different heterostructures as examples. The presentation will focus on our experiments' instrumentation and technical aspects, discussing spurious effects such as transition radiation and the impact of fiber collection on time and angular resolution. Finally, discussing how to deal with these challenges, aiming to go further in temporal and spatial resolution with high-quality signal-to-noise ratios.

### References

- [1] P. Corfdir *et al.*, "Exciton localization on basal stacking faults in a-plane epitaxial lateral overgrown GaN grown by hydride vapor phase epitaxy," *J. Appl. Phys.*, vol. 105, no. 4, p. 043102, 2009.
- [2] R. J. Moerland, I. G. C. Weppelman, M. W. H. Garming, P. Kruit, and J. P. Hoogenboom, "Time-resolved cathodoluminescence microscopy with sub-nanosecond beam blanking for direct evaluation of the local density of states," *Opt. Express*, vol. 24, no. 21, p. 24760, 2016.
- [3] X. Fu *et al.*, "Exciton Drift in Semiconductors under Uniform Strain Gradients: Application to Bent ZnO Microwires," *ACS Nano*, vol. 8, no. 4, pp. 3412–3420, 2014.
- [4] S. Meuret *et al.*, "Time-resolved cathodoluminescence in an ultrafast transmission electron microscope," *Appl. Phys. Lett.*, vol. 119, no. 6, p. 6, 2021.
- [5] Y. J. Kim and O. H. Kwon, "Cathodoluminescence in Ultrafast Electron Microscopy," *ACS Nano*, vol. 15, no. 12, pp. 19480–19489, 2021.
- [6] F. Houdellier, G. M. Caruso, S. Weber, M. Kociak, and A. Arbouet, "Development of a high brightness ultrafast Transmission Electron Microscope based on a laser-driven cold field emission source," *Ultramicroscopy*, vol. 186, pp. 128–138, 2018.

## Quantum Confined Luminescence in Two Dimensions

Luiz H. G. Tizei<sup>1)\*</sup>

<sup>1)</sup>Université Paris-Saclay, CNRS-UMR 8502, Laboratoire de Physique des Solides, Orsay 91405, France

\*Corresponding author: luiz.tizei@cnrs.fr

Nanothermometry Nanoscale light emitters have emerged as a cornerstone of nanophotonics, promising revolutionary advances in lasers, light-emitting devices, and photodetectors. Conventional approaches to achieving localized emission have relied on quantum dots, nanowires, quantum wells, and point defects embedded within semiconductors or wide-bandgap materials. The spatial confinement inherent in these structures gives rise to quantized energy levels and unique emission properties, including single-photon emission in certain cases. These characteristics hold immense potential for applications in quantum communication, quantum cryptography, and advanced quantum light sources. This work introduces a new class of confined emitters: two-dimensional quantum dots (2DDots). These 2DDots consist of MoSe<sub>2</sub> islands embedded in a continuous WSe<sub>2</sub> monolayer (Figure 1). This unique heterostructure was realized through metal-organic chemical vapor deposition (MOCVD) by sequentially introducing 2DDots and matrix precursors. To confirm the formation of 2DDots exhibiting quantum confinement, we investigated the size-dependence of excitonic transitions. Cathodoluminescence (CL) spectra were acquired from MoSe<sub>2</sub> islands of varying lateral dimensions (Figure 1b). Due to the type-II band alignment in this heterostructure, electrons localize in the MoSe<sub>2</sub> islands while holes reside in the surrounding WSe<sub>2</sub> matrix. This spatial separation leads to a reduced exciton transition energy compared to that of bulk MoSe<sub>2</sub>. Crucially, we observed a blueshift in the X<sub>Mo/W</sub> transition energy with decreasing MoSe<sub>2</sub> island size (Figure 1b and [1]). This size-dependent energy shift provides strong evidence of quantum confinement, confirming the 2D quantum dot nature of the MoSe<sub>2</sub> islands. The observed size-dependence of the 2DDot transition energy agrees well with theoretical calculations [1]. Furthermore, a phenomenological model successfully describes the ring patterns observed in energy-filtered CL maps [1]. Cathodoluminescence (CL) and monochromated electron energy loss spectroscopy (EELS) measurements were performed using a Nion Hermes 200 (Chromatem) scanning transmission electron microscope (STEM), with the samples cooled down to 100 K. This system is equipped with a Nion electron spectrometer, an Attolight Mönch light detection/injection system, and direct electron detectors (Medipix3 or Timepix3) for EELS. If time allows, nanosecond-resolved nanothermometry experiments with the same experimental setup will be described [2].

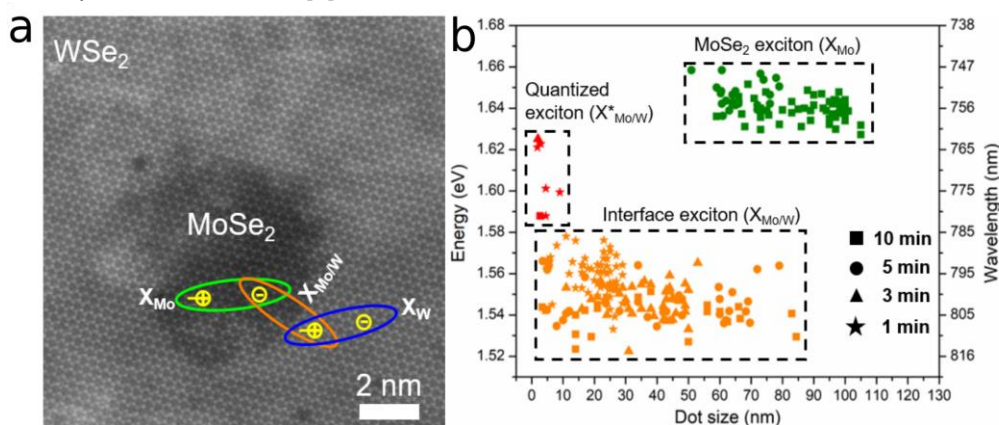


Fig. 1: a) Image of a MoSe<sub>2</sub> 2D quantum dot in a WSe<sub>2</sub> matrix. b) CL emission energy versus 2D dot island size, showing confinement for the smallest dots [4].

### References

- [1] S. Bachu, *et al.* ACS Photonics **12**, 364 (2025).  
 [2] F. Castioni, *et al.* Nano Letters **25**, 1601 (2025).

## Single Dot Spectroscopy: Carrier Capture into Individual InP Quantum Dots Directly Imaged by Nanoscale Cathodoluminescence Microscopy

F. Bertram,<sup>1)\*</sup> G. Schmidt,<sup>1)</sup> P. Veit,<sup>1)</sup> J. Christen,<sup>1)</sup> A. Ćutuk,<sup>2)</sup> M. Jetter,<sup>2)</sup> and P. Michler<sup>2)</sup>

<sup>1)</sup> Institute of Physics, Otto-von-Guericke-University Magdeburg, Germany

<sup>2)</sup> Institut für Halbleitertechnik und Funktionelle Grenzflächen, Center for Integrated Quantum Science and Technology (IQST) and SCoPE, University of Stuttgart, Germany

\*Corresponding author: frank.bertram@ovgu.de

We present a nanoscopic investigation of the carrier capture into individual InP quantum dots (QDs) by means of highly spatially resolved cathodoluminescence spectroscopy directly performed in a scanning transmission electron microscope (STEM-CL). Single dot spectroscopy using low temperature STEM-CL provides a detailed insight into the energy structure of individual QDs and directly correlates those properties with the real structure on a nanoscale. In this study, we comprehensively characterize the vertical and lateral transfer of carriers within a 7-fold stack of layers containing high-density InP quantum dots.

Grown by metal-organic vapor-phase epitaxy, the active region consists of 7 InP QD layers embedded in 20.0 nm  $\text{Al}_{0.1}\text{GaInP}$  barriers, an  $\text{Al}_{0.55}\text{GaInP}$  cladding layer of 31.6 nm and an  $\text{AlInP}$  layer of 12.0 nm thickness as an electron blocking layer. The cladding layer at the bottom and the top of the stack is slightly thicker (64.8 nm) than the other layers. A 12.0 nm  $\text{AlInP}$  and a 10.0 nm thick  $\text{Al}_{0.1}\text{GaInP}$  layer completes the active region. The QD layers were grown via Stranski-Krastanov mode achieving a high QD density of  $10^{10}/\text{cm}^2$ .

Low-temperature CL imaging and spectroscopy was performed to correlate the structural and optical properties of the separate confinement heterostructure. STEM-CL taken at a relatively thick specimen region averages in the depth of the sample slice over a large number of QDs, i.e., representing ensemble properties. This ensemble luminescence of the seven quantum dot layers exhibits a broad and intense emission band, which is composed of overlapping sharp emission lines in the spectral range from  $\lambda = 610$  to 680 nm, with an overall maximum around  $\lambda = 627$  nm. The competition of individual quantum dots in capturing of excess carriers is directly visualized.

Taking advantage of the ultra-high spatial resolution of our STEM-CL setup ( $\delta x < 5$  nm) in thinner parts of the TEM lamella exciting fewer dots within the specimen depth allows us to perform single dot spectroscopy and image different excitonic transitions of an individual InP dot. The nanoscopic lateral transport is investigated by a spectrum linescan across an isolated single InP QD, where we observe a characteristic change of the excitonic lines during this linescan. This directly correlates to the change of the numbers of excess carriers reaching the dot - i.e. altering the quantum dot population. The shift of emission energies visualizes the renormalization of the ground-state energy of the single dot and the intensity ratio of the excitonic recombinations verifies this change of the occupation and the state-filling.

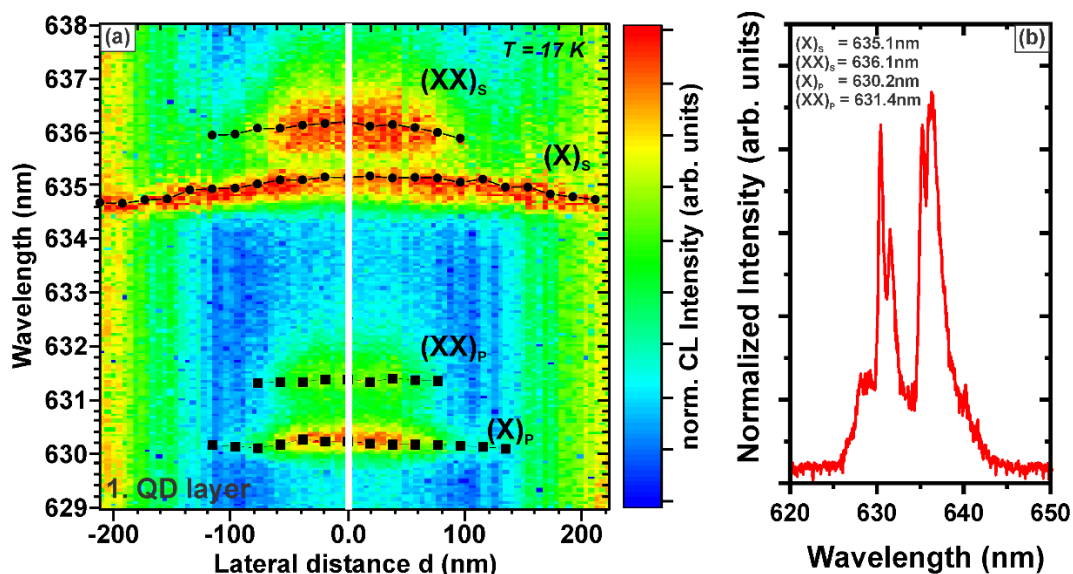


Fig. 1: (a) lateral CL line scan across a single quantum dot along the first QD layer at  $T = 17$  K. Depicted are the normalized local spectra from  $\lambda = 629$  to 638 nm versus the lateral distance from the QD position. (b) local spectrum the dot position ( $d = 0$  nm).

## Insights into Carrier Transport and Recombination in a Cascaded InGaN LED: A Nanoscale Correlation of EBIC and CL

G. Schmidt,\* K. Wein, H. Eisele, F. Bertram, P. Veit, O. August, C. Berger, A. Dadgar, A. Strittmatter, and J. Christen

*Institute of Physics, Otto-von-Guericke-University Magdeburg, 39106 Magdeburg, Germany*

\*Corresponding author: [gordon.schmidt@ovgu.de](mailto:gordon.schmidt@ovgu.de)

By correlating electron beam-induced current (EBIC) and cathodoluminescence (CL) measurements in a scanning transmission electron microscope (STEM), we present an in-depth characterization of a triple-cascaded InGaN/GaN LED. Each segment consists of a p-n junction with multiple quantum wells (MQW) and an AlGaIn electron-blocking layer (EBL), separated by a GaN:Ge/GaN:Mg tunnel junction (TJ). We analyze the impact of internal electric fields on carrier transport, recombination, and injection dynamics at the nanoscale providing insights into carrier diffusion and drift along the vertical direction of the device.

Each LED comprises a Si-doped n-GaN layer ( $8 \times 10^{18} \text{ cm}^{-3}$ ), an MQW region with five  $\text{In}_{0.11}\text{Ga}_{0.89}\text{N}$  QWs of 2.5 nm thickness separated by undoped GaN barriers, and a 17 nm Mg-doped  $\text{Al}_{0.18}\text{Ga}_{0.82}\text{N}$  EBL embedded between 23 nm and 210 nm thick Mg-doped p-GaN layers ( $2 \times 10^{19} \text{ cm}^{-3}$ ). Together with the p-doped layer, a highly n-doped GaN:Ge layer ( $1 \times 10^{20} \text{ cm}^{-3}$ ) forms the TJ, enabling efficient carrier injection into the next segment. Every LED is completed with an AlGaIn layer preventing from Mg diffusion from the underlying p-layers.

EBIC linescans along the growth direction reveal the highest current within the p-n junction of each segment. However, due to significant carrier recombination in the MQWs, the maximum EBIC signal shifts toward the EBL. This shift is attributed to (i) efficient carrier capture and recombination in the MQWs, reducing carriers from EBIC current, (ii) band discontinuities at the AlGaIn/GaN interface, impeding carrier transport in the space charge region, and (iii) polarization-induced charge separation at the AlGaIn:Mg/GaN:Mg interface. These combined effects contribute to the observed EBIC maximum toward the AlGaIn/GaN interface. These findings are supported by STEM-CL linescans at  $T = 17 \text{ K}$ . We observe a maximum intensity of the spectrally integrated MQW emission at the 3<sup>rd</sup> QW and an abrupt MQW intensity drop at the EBL, indicating the underlying carrier separation and blocking.

In contrast, a weak EBIC response is detected at the TJ, despite its simulated electric field of  $\sim 4 \text{ MV/cm}$ , far exceeding any other electric field amplitude in the structure. Drastically reduced CL intensity near the TJ interface suggests a locally low quantum efficiency due to efficient carrier separation. However, a tunnel current opposite in sign is assumed to reduce the overall EBIC signal.

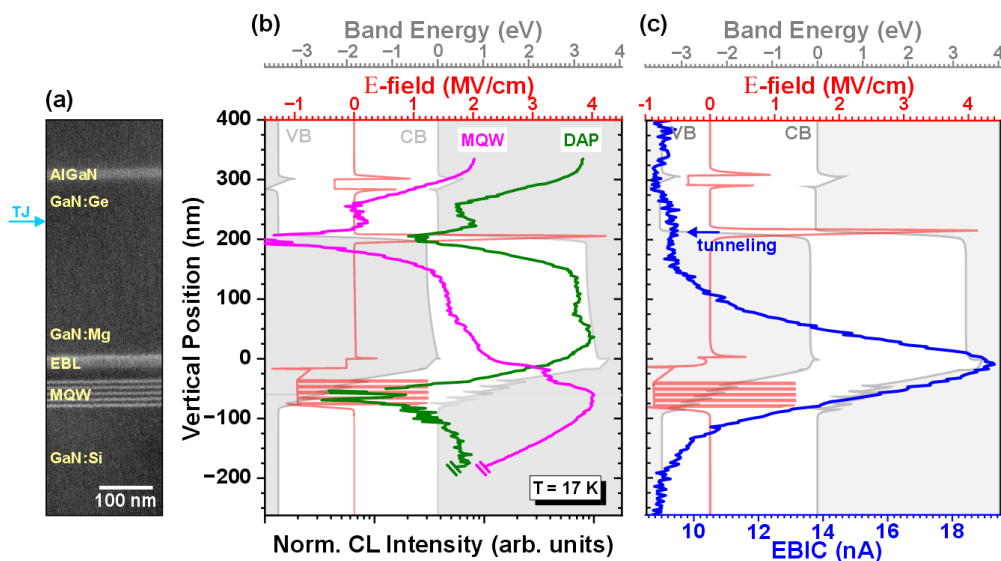


Fig. 1: STEM-EBIC vs. STEM-CL nanoscale correlation of an individual LED segment: (a) STEM image, (b) monochromatic CL intensity profiles of MQW and donor-acceptor pair (DAP) recombination, and (c) EBIC current across the middle LED section with simulated electric field and valence / conduction band energies (*nextnano*).

## High-Resolution Cathodoluminescence Mapping for Doping Quantification Across a Wide Range of Silicon Concentrations in GaN Epitaxial Layers

Z. M'qaddem, N. Rochat, G. Jacopin, B. Mohamad, T. Kaltsounis, M. Charles, J. Buckley, Ł. Borowik

1) Univ. Grenoble Alpes, CEA-LETI, Grenoble 38000, France  
2) Univ. Grenoble Alpes, CNRS, Grenoble INP, Institut Néel, 38000 Grenoble, France

\*Corresponding author: zakariae.mqaddem@cea.fr

Power electronic devices are crucial for electrical energy conversion, with gallium nitride (GaN) emerging as a promising material due to its high critical electric field. Optimizing device performance requires precise control of silicon (Si) doping, as vertical power devices operating above 1 kV necessitate thick GaN drift layers with low doping concentrations[1]. These structures can be grown by localized epitaxial growth, which mitigates tensile stress, facilitating the growth of these thick GaN layers. While several techniques exist for mapping Si concentration, they often suffer from limitations in spatial resolution and accuracy, especially for low doping concentrations. Cathodoluminescence (CL) presents a compelling alternative, offering nanoscale resolution for visualizing local doping variations.

This study introduces CL hyperspectral mapping as high-resolution technique for analyzing silicon doping in GaN layers. By correlating energy shifts ( $E$ ) and linewidth broadening Half Width Half Maximum (HWHM) of the near-band-edge (NBE) emission with doping concentrations, we achieve nanoscale-resolution mapping of local carrier densities in a calibration sample with doping ranging from unintentionally doped GaN to  $5 \times 10^{18} \text{ cm}^{-3}$ . Calibration with Secondary Ion Mass Spectrometry (SIMS) confirms the accuracy of our doping quantification, providing a reliable means to assess doping uniformity. Moreover, we demonstrate superior sensitivity compared to SIMS for doping below  $5 \times 10^{16} \text{ cm}^{-3}$ . This approach is then applied to a quasi-vertical PN diode structure.

Two models were developed to link both spectral parameters to doping while accounting for temperature, and epitaxial quality [2]–[5]. Discrepancies between doping estimates from  $E$  and HWHM values were observed. It is well known that  $E$  is influenced by strain, whereas HWHM is sensitive to doping levels down to  $10^{16} \text{ cm}^{-3}$  without strain interference. This distinction is critical for advancing device architectures. By combining these two data and separating the effects of strain and doping on energy shifts, we successfully mapped both doping and tensile strain relaxation at mesa edges, highlighting the significant potential of CL mapping for enhancing understanding of GaN-based power electronic devices.

This work, carried out on the Platform for Nanocharacterisation (PFNC), was supported by the “Recherche Technologique de Base”, “France 2030 - ANR-22-PEEL-0014” programs of the French National Research Agency (ANR). This work is part of the ELEGaNT project (ANR-22-CE05-0010).

### References

- [1] J. A. Cooper and D. T. Morissette, *IEEE ELECTRON DEVICE Lett.*, vol. 41, no. 6, p. 829, 2020,
- [2] M. Feneberg *et al.*, *Phys. Rev. B - Condens. Matter Mater. Phys.*, vol. 90, no. 7, pp. 1–10, 2014, d
- [3] A. Cremades, L. Gorgens, O. Ambacher, and M. Stutzmann, *Phys. Rev. B*, vol. 46, no. 11, pp. 1499–1508, 2014,
- [4] Y. P. Varshni, *Physica*, vol. 34, no. 1, pp. 149–154, 1967, doi: 10.1016/0031-8914(67)90062-6.
- [5] G. Pozina, S. Khromov, C. Hemmingsson, L. Hultman, and B. Monemar, *Phys. Rev. B - Condens. Matter Mater. Phys.*, vol. 84, no. 16, p. 165213, 2011

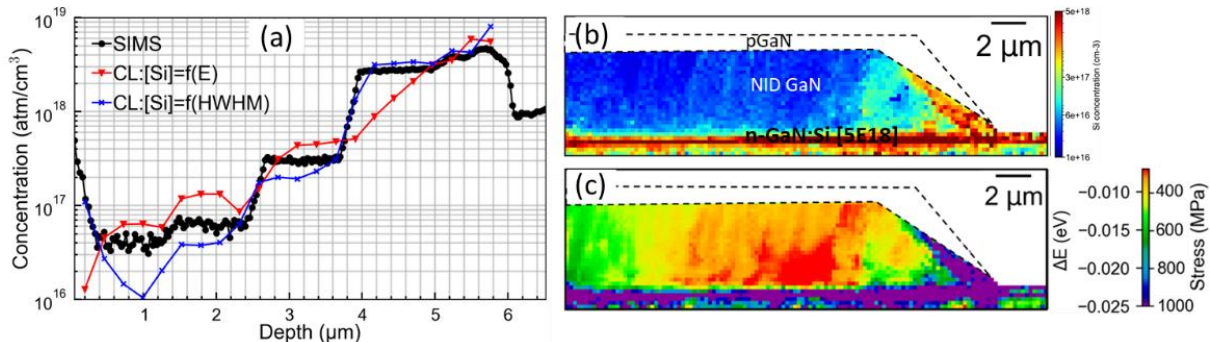


Fig. 1: (a) Si concentration profiles from SIMS, compared with doping maps using HWHM and energy-based calibration. (b) Cross-sectional Si doping map at the mesa edge of quasi-vertical PN diodes (HWHM model). (c) Strain-induced BE peak shift ( $\Delta E$ ) and corresponding strain values, derived from near-bandgap luminescence under biaxial stress.

## Defect Analysis in Diamond Schottky Barrier Diodes for beta-voltaic applications

H. Ribeiro,<sup>1),2),\*</sup> D.Z. Nusimovici,<sup>1),3)</sup> L. Valera,<sup>1)</sup> M. Jacquemin,<sup>1)</sup> G. Jacopin,<sup>2)</sup>

<sup>1)</sup> DIAMFAB SAS, 25 avenue des martyrs, 38042 Grenoble, France

<sup>2)</sup> Institut Néel CNRS, Univ. Grenoble Alpes, 38042, Grenoble, France

<sup>3)</sup> Univ. Grenoble Alpes, CNRS, Grenoble INP, SIMaP, 38000 Grenoble, France

\*Corresponding author: hugo.ribeiro@diamfab.com

Beta-voltaic (BV) cells aim to deliver a reliable current with constant discharge for several decades, only depending on the half-life of the radioactive element used, while requiring no maintenance. The principle of these BV generators is rather simple: they convert the kinetic energy of  $\beta^-$  particles into electrical energy in a semiconductor, similar to the photovoltaic effect. Thanks to its ultra-wide and indirect band gap of 5.45 eV, along with long carrier diffusion length, diamond emerges as the ultimate semiconductor for BV applications. However, structural defects in diamond – such as dislocations, impurities, and vacancies – are believed to significantly influence material's electronic properties. In the context of BV cells, specific defects contribute to the degradation of electrical performance, manifesting as a reduction of the charge collection efficiency (CCE), the open-circuit voltage, the fill factor, therefore of the semiconductor efficiency. Consequently, extensive research has been dedicated to investigate these defects and assessing their impact using both destructive and non-destructive techniques [1][2].

Here, we report on the fabrication and characterization of a diamond pseudo-vertical Schottky barrier diode p-/p++ stack grown on a (100)-oriented diamond single crystal. The heavy boron-doped layer has a hole concentration above  $6 \times 10^{20} \text{ cm}^{-3}$  and a thickness of 730 nm. In contrast, the drift layer has an effective concentration of  $3 \times 10^{14} \text{ cm}^{-3}$  and a thickness of about 2.2  $\mu\text{m}$ . Ti/Pt/Au and Mo/Pt/Au were deposited on p++ and p- layers to form respectively, Ohmic and Schottky contacts.

In order to characterize structural defects and BV devices, we use the field emission gun of a scanning electron microscopy (SEM) to mimic the  $\beta^-$  radiation. Through electron beam induced current (EBIC) analysis, we identify two types of electrically active defect (Fig. 1a and Fig. 1b), and we quantify the efficiency of our BV devices. First, we observe a CCE drop of 4% near linear defects at 0 V. In addition, we identified a strong persistent photoconductivity of 178 ms near non-epitaxial crystallite. By performing current-voltage characteristics under e-beam irradiation, we deduce for the best cell a charge collection efficiency of more than 90% at 20 kV, an open circuit voltage of 1.54 V and a fill factor of 85.4%. The semiconductor conversion efficiency was estimated to be up to 10.1%, close to the state of art for diamond Schottky diodes [3]. To further identify the origin of these defects, a mapping of the A-band (Fig. 1c) by cathodoluminescence (CL) has been performed. As the A-band is associated with dislocations [2], we suggest that the linear defect observed in EBIC are related to dislocations. Finally, selective etching with molten salt allows us to correlate and identify the defects observed in EBIC and CL with the type of dislocation present on the surface (Fig 1d).

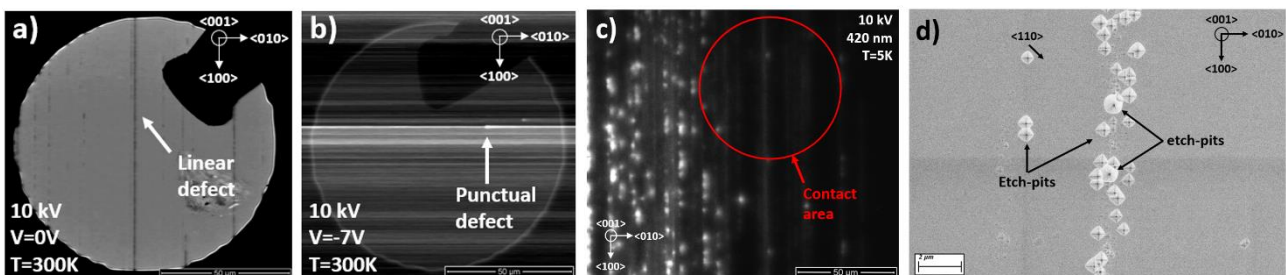


Fig. 1: (a) EBIC cartography of Schottky contact at 10 kV, (a) at 0 V, (b) at -7V, (b) CL mapping of the diamond A-band (420 nm), the circle indicates the contact area, (c) SEM image after selective etching using molten salt.

- [1] N. Akashi, N. Fujimaki, S. Shikata, *Diamond and Related Materials*. **109**, 108024 (2020).
- [2] T. Shimaoka, T. Teraji, K. Watanabe, S. Koizumi, *Physica Status Solidi (a)*. **11**, 1700180 (2017).
- [3] C. Delfaure, M. Pomorski, J. de Sanoit, P. Bergonzo, et S. Saada, *Appl. Phys. Lett.* **108**, 252105 (2016).

## Cathodoluminescence study of CdSeTe/CdTe Solar cells using FIBSEM and STEM and site-specific selection

Stuart Robertson, Zhaoxia Zhou, Sam Machin, Kieran Curson, and Michael Walls

Loughborough University, Loughborough, LE11 3TU, United Kingdom

\*Corresponding author: s.robertson@lboro.ac.uk

CdTe is the leading second-generation solar technology among thin-film solar cells, offering cost-effective solar electricity production. Extensive research in academia and industry continues to push CdTe solar cells toward the maximum efficiency predicted by the Shockley-Queisser model [1]. Typical processes focus on incorporating a gradient selenium (Se) in CdTe, CdCl<sub>2</sub> treatment, and doping in the absorber aiming to tune the band gap and passivating grain boundaries [2]. At Loughborough, polycrystalline CdSeTe/CdTe thin film solar cells have been routinely analysed using FIB-SEM/EBSD (xenon Helios G4 plasma FIB, FEI) and STEM/EDS (Talos 200i, ThermoFisher Scientific) to develop a statistical understanding of film microstructures and the solar cell performance.

With the newly funded cathodoluminescence (CL) detectors (CCD and InGaAs) integrated into both the FIB-SEM (Monarc Pro, Gatan) and STEM (Mönch, Attolight) systems with cryo-holders, researchers can now investigate light emission (i.e. band gap) from microscale to nanoscale and correlate the photoactivity directly with grain orientation, defects, and chemical composition. Site-specific sections either parallel (in-plane) or perpendicular (edge) to the film surface can be in-situ extracted based on CL or EBSD maps for further STEM. Figure 1 presents an example of a CdSeTe/CdTe absorber on an industrial SnO<sub>2</sub>-coated glass substrate, demonstrating the potential of TEM-CL. The STEM bright-field image of the cross-section highlights grain boundaries, interior twins and stacking faults. For brevity, only the key selenium and chlorine net-count EDX maps are shown. The selenium map reveals a gradient in selenium distribution throughout the device, while the chlorine map indicates its concentration at grain boundaries and the front interface. The CL map, displaying intensity at a wavelength of  $839 \text{ nm} \pm 25 \text{ nm}$ , shows that bright lines align with twin boundaries in the high-angle annular dark field (HAADF) image, as well as with regions of higher selenium concentration in the EDX map. The correlation between CL and STEM images suggests that twin boundaries exhibit a lower band gap and stronger CL contrast, potentially obstructing diffusion and causing selenium accumulation. Compared to SEM-CL, TEM-CL offers higher spatial resolution and the advantage of directly correlating CL maps with EDS and STEM images at the same location. Typical workflow from large area cross sectional SEM/CL, site-specific FIB extraction and STEM/CL will be presented.

### References

[1] S Rühle, Sol. Energy 2016, 130, 139–147.

[2] MA Scarpulla, B McCandless, AB Phillips, *et al*, Solar Energy Materials and Solar Cells, 2023, 255, 112289.

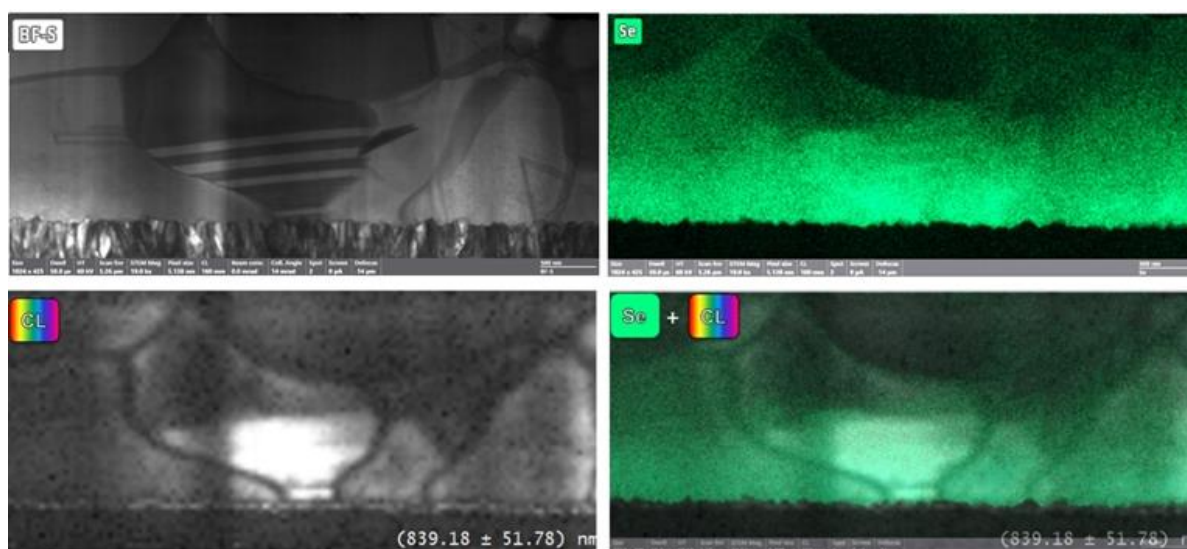


Fig. 1: Cross section of a CdSeTe/CdTe solar cell characterized by STEM/EDX, and CL.

## Investigation of Ag Alloying Effect in Cu(In,Ga)S<sub>2</sub> Solar Cells Absorber by CL-EBSD

Y.Hu<sup>1)\*</sup>, A.V.Oli<sup>2)</sup>, Z.S.Pehlivan<sup>1)</sup>, G.Kusch<sup>1)</sup>, S.Siebert<sup>2)</sup>, R.A.Oliver<sup>1)</sup>

1) University of Cambridge, 27 Charles Babbage Road, Cambridge, CB3 0FS, United Kingdom

2) University of Luxembourg, 41 rue du Brill, L-4422 Belvaux, Luxembourg

\*Corresponding author: [yh478@cam.ac.uk](mailto:yh478@cam.ac.uk)

Cu(In,Ga)S<sub>2</sub> (CIGS) is a wide bandgap polycrystalline semiconductor suitable for absorber layers in the top cells of tandem solar cells. Currently, single junction CIGS solar cells has a recorded efficiency of 15.5%[1], which is much lower than its selenide analogue, Cu(In,Ga)Se<sub>2</sub> (CIGSe), at 23.6%[2]. To improve the efficiency of CIGS solar cells, reducing the open circuit voltage deficit, primarily caused by interface and bulk recombination, is important. Methods, such as adjusting buffer layer composition and through-thickness absorber compositional gradient, have been applied before. Ag alloying can also be a potential strategy. However, systematic research on Ag alloying in CIGS is limited. We employed a multi-microscopy approach on bevel cross sections of four Ga-graded absorbers with different Ag content, as shown in Figure 1a, to reveal the impact of Ag-alloying on the microstructure, opto-electronic and compositional properties of CIGS absorbers.

An example multi-microscopy dataset combining SEM, electron backscatter diffraction (EBSD) and cathodoluminescence (CL) on an Ag alloyed CIGS is shown in Figure 1. The SEM image on a bevel cross section of the absorber prepared using a focused ion beam, reveals the presence of voids, which become less dense with increasing Ag content. The EBSD map gives additional microstructure information, including grain structure and grain boundary (GB) orientation. The comparison between different absorbers shows that the Ag alloying will significantly enlarge the average grain size. Via correlation of EBSD and CL data, it may be observed that at random grain boundaries (RGBs) defect-related emission (DE) dominates, and near-band-edge emission is strongly inhibited, while twin boundaries (TBs) are mostly opto-electronically neutral. The reduction of GB length by Ag alloying effectively reduces the bulk DE centres. Additionally, the DE intensity at RGBs is reduced with Ag alloying, suggesting the passivation of GBs. The improvement in microstructure and the GB passivation both contribute to improved CL intensity of the Ag alloyed absorber. The fitted near band edge emission (NBE) energy extracted from CL shows the flattened through-thickness bandgap and improved compositional homogeneity in absorbers with high Ag alloy content. The improved microstructure, enhanced opto-electronic properties, and greater elemental homogeneity achieved by Ag alloying of the absorber material will all contribute to the improvement of performance of CIGS solar cells.

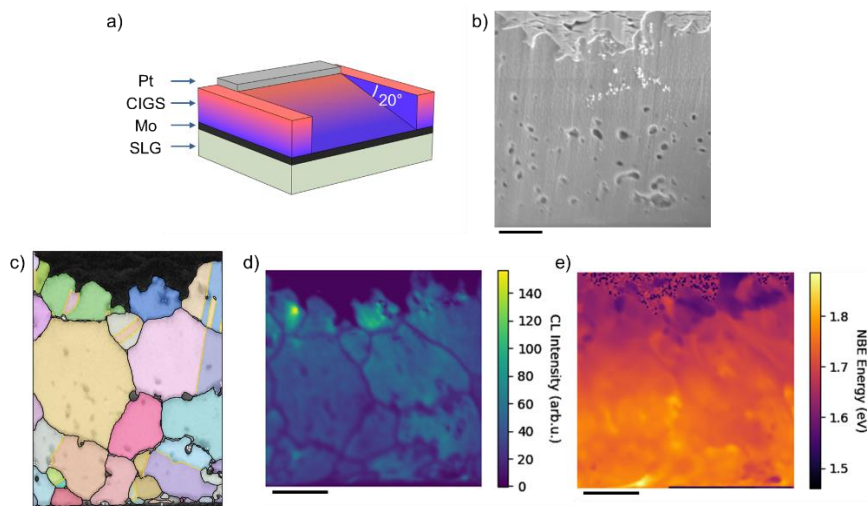
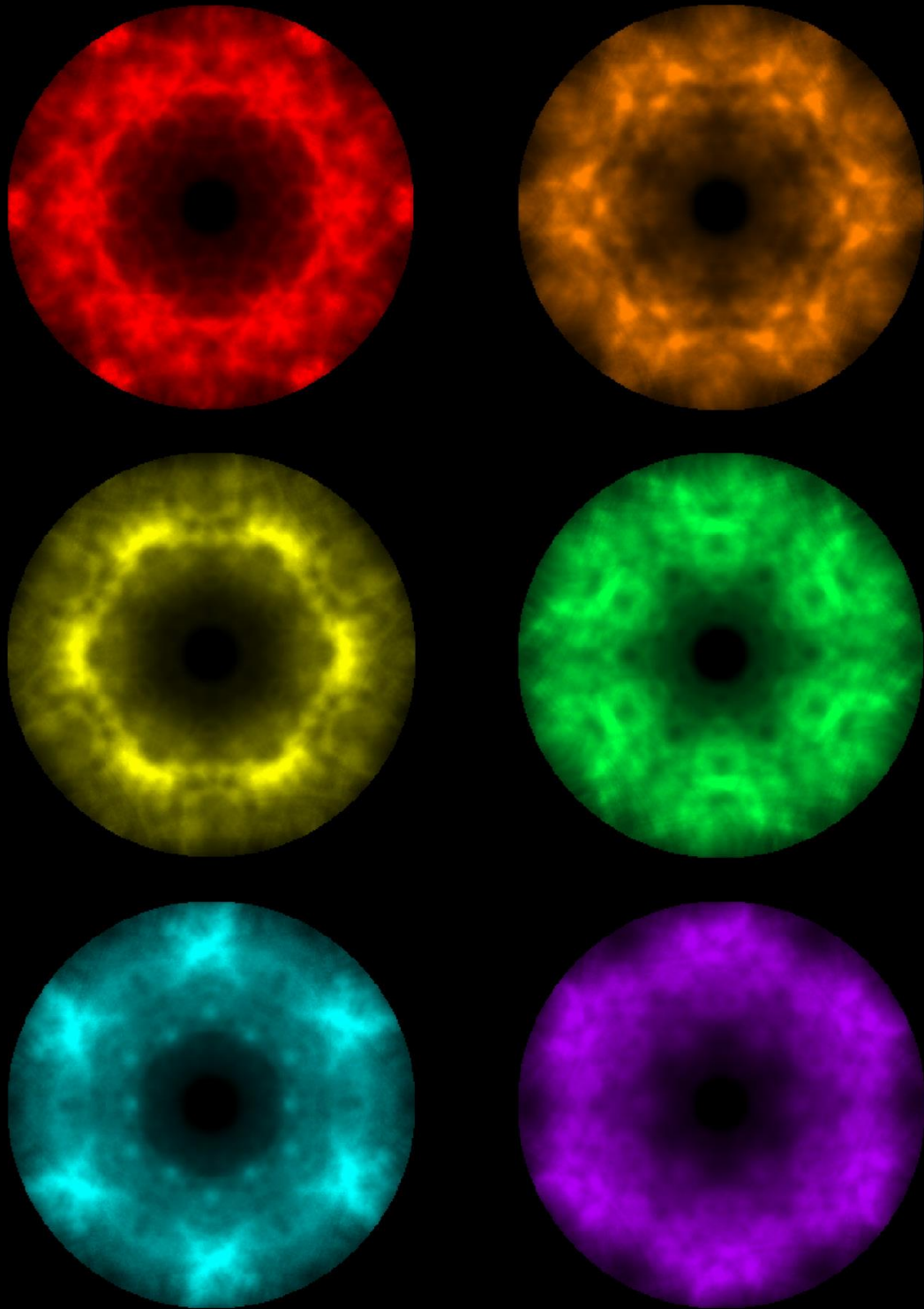


Figure 1. a) bevel cross section schematic; b) top-view SEM image; c) EBSD map; d) panchromatic CL intensity map; e) NBE energy map extracted from CL data. Scalebar size: 2  $\mu$ m.

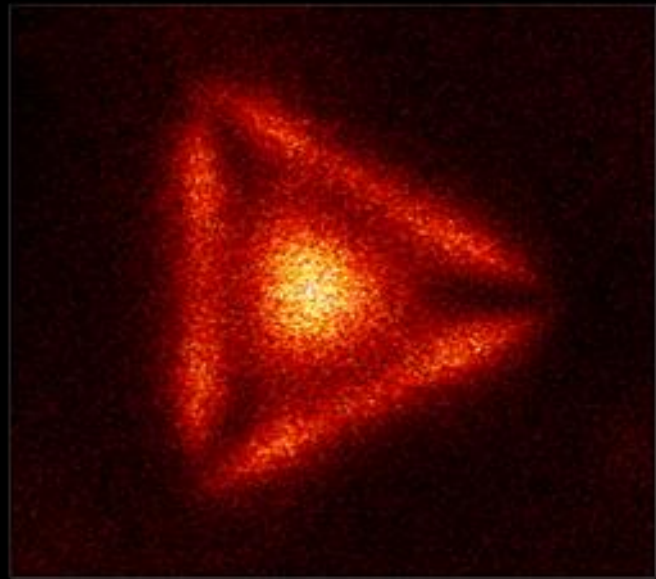
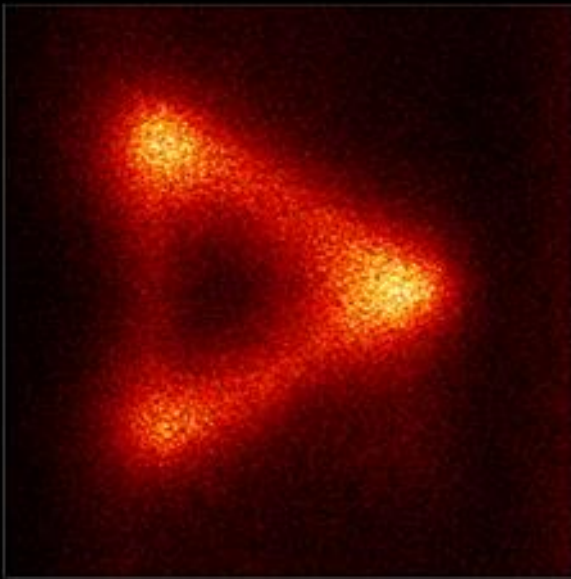
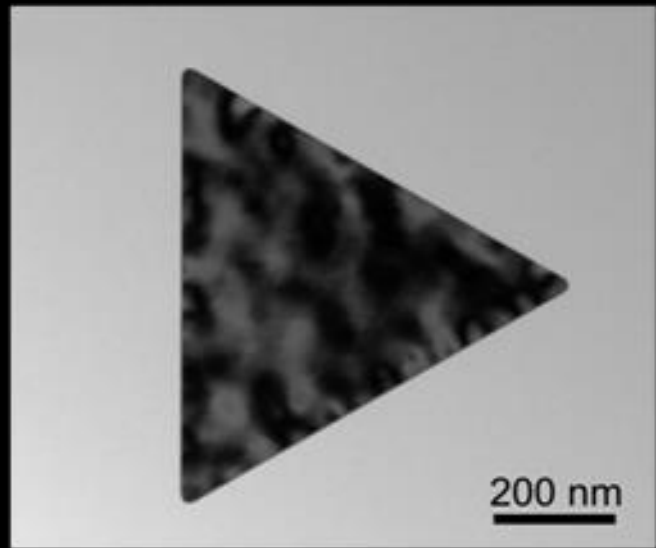
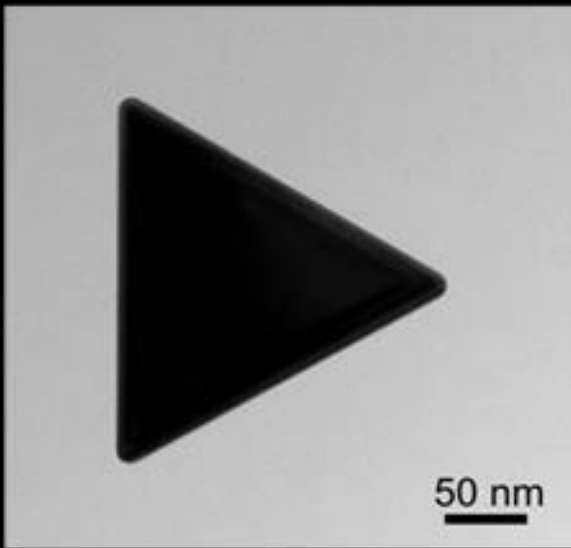
1. Shukla, S. *et al.* Joule 5, 1816–1831 (2021). 2. Jan, K. *et al.* Nature Energy 9, 467-478 (2024).



## Energy-momentum spectroscopy of sub-diffraction limit structures

Monarc<sup>®</sup> offers the most powerful analysis of optical properties below the diffraction limit. The system can be used to reveal wavelength, angle, and polarization distributions of luminescence, and can directly correlate them with sample structure and composition at high spatial resolutions.

Image: Selected emission patterns from a microLED pillar array extracted from the reconstructed wavelength- and angle-resolved cathodoluminescence data set. Each emission pattern has been colorized according to the emission wavelength and normalized by intensity to aid clarity.



## Optically-coupled transmission electron microscopy

The Monarc<sup>®</sup> Pro T is the most flexible STEM-CL solution, utilizing a modular holder-based dual mirror design. This system enables light collection or injection, discrimination between upper and lower hemispheres, and simultaneous EELS and CL measurements.

Image: STEM-CL measurements on two different sized gold prisms. The top row displays bright field images, while the bottom row shows CL intensity maps. The distinct dimensions of the prisms result in two unique plasmon resonance patterns being observed. Data was collected on a FEI Titan at 300 kV. Special thanks to Dr. M. Bosman, A\*STAR IMRE, Singapore for allowing us to share this data.

[gatan.com](http://gatan.com)



## Cathodoluminescence Study on a Surface-Emitting Nano-Ridge Laser

Toon Coenen<sup>1\*</sup>, E. M. B. Fahmy<sup>2\*</sup>, Z. Ouyang<sup>2</sup>, D. Colucci<sup>2,3</sup>, J. Van Campenhout<sup>3</sup>, B. Kunert<sup>3</sup>, and D. Van Thourhout<sup>2</sup>

1. DELMIC B.V, Kanaalweg 4, Delft 2628 EB, The Netherlands

2. Photonics Research Group, Department of information technology (INTEC), Ghent University - IMEC, Belgium

3. IMEC, Kapeldreef 75, 3001 Heverlee, Belgium

\* Equal contribution

\*Corresponding author: coenen@delmic.com

Nano-ridge technology is a promising solution to address the challenges facing current micro-laser technologies [1]. It allows the growth of high quality, defect free active materials on silicon substrates without the need for thick buffer layers [2]. Here, we present a novel laser design based on an array of nano-ridges arranged in a photonic crystal configuration, where each nano-ridge is spaced with a period of 380 nm and has three quantum wells (Fig. 1a). This architecture supports a bound state in the continuum (BIC) mode across the nano-ridge array, providing both strong in-plane confinement and surface emission. To gain insight into the underlying physics of the lasing mechanism, we use cathodoluminescence (CL) measurements to construct experimental band-structure maps [2]. The angle- and spectrally-resolved CL data enable us to visualize the photonic modes and directly confirm the presence of the BIC mode. Although CL uses an electron beam to locally excite only a single nano-ridge, the observation of the complete band structure in our measurements highlights that the laser action arises from collective coupling across the nano-ridge array. The experimentally measured band structure obtained from CL exhibits excellent agreement with FDTD simulations along both the  $k_x$  and  $k_y$  directions, including a close match in the frequency of the lowest band mode at the  $\Gamma$  point as well as in the curvature of the band (Fig. 1b). Under optical pumping, a prominent lasing peak emerges near the predicted wavelength of around 990 nm. As shown in Fig. 1c, when increasing the pump power, the device displays a distinct threshold at about  $10 \text{ kW/cm}^2$ , confirming robust laser action near the designed operating wavelength. This new approach to achieving lasing combined with in depth characterisation through CL offers unprecedented flexibility, as the BIC mode can be tuned by adjusting key design parameters—such as the array period and nano-ridge width. This versatility not only enables operation at wavelengths beyond the near-infrared, but also paves the way for cost-effective, integrated, mass-manufactured lasers on standard silicon wafers.

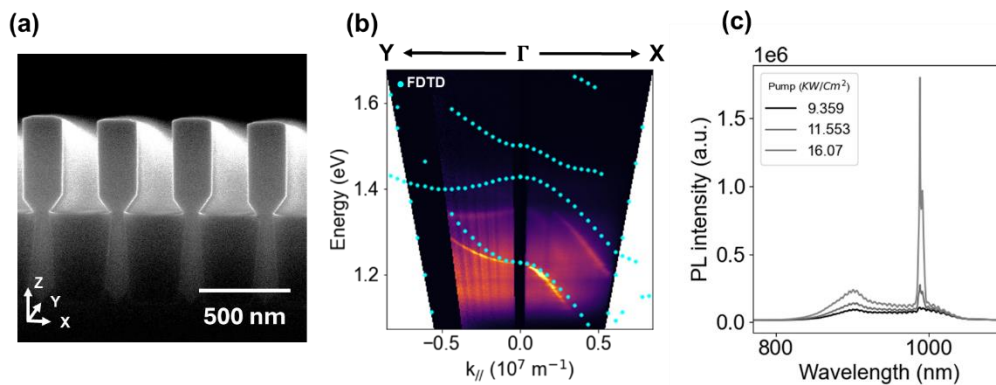


**Fig. 1** (a) Scanning electron microscope (SEM) image of an array of coupled nano-ridges forming the laser device. (b) Angle-resolved cathodoluminescence measurement showing the band structure of the coupled nano-ridge array, obtained by locally exciting a single nano-ridge with an electron beam. The measured data is overlaid with the band diagram simulations from FDTD simulations (cyan) (c) Lasing spectrum under different pump powers, measured using a micro-PL setup with a 532 nm laser as the pump source. A strong peak at 986 nm is observed, with a threshold pump power of approximately  $10 \text{ kW/cm}^2$ .

### References

- [1] Y. De Koninck, C. Caer, D. Yudistira, et al., *Nature* 637, 63–69 (2025).
- [2] D. Van Thourhout, Y. Shi, M. Baryshnikova, Y. Mols, N. Kuznetsova, Y. De Koninck, M. Pantouvaki, J. Van Campenhout, R. Langer, B. Kunert, *Future Directions in Silicon Photonics* 283, 283–304 (2019).
- [3] T. Coenen and N. M. Haegel, *Appl. Phys. Rev.* 4, 031103 (2017).

## Cathodoluminescence investigation of InGaN buffer layer inclusion in InGaN/GaN Nanowire Superlattice: A way towards high efficiency red light emission

Krishnendu Sarkar<sup>1</sup>, Stefano Pirota<sup>1</sup>, Nidel Tchoulayeu<sup>1</sup>, Quang-Chieu Bui<sup>1</sup>, Omar Saket<sup>1</sup>, Stephane Collin<sup>1</sup>, Laurent Travers<sup>1</sup>, Martina Morassi<sup>1</sup>, François H. Julien<sup>1</sup>, Jean-Christophe Harmand<sup>1</sup>, Noëlle Gogneau<sup>1</sup>, Maria Tchernycheva<sup>1</sup>

<sup>1)</sup> Centre de Nanosciences et Nanotechnologies, University Paris-Saclay, University Paris-City, CNRS, UMR9001, 10 Boulevard Thomas Gobert, 91120, Palaiseau, France

\*Corresponding author: [krishnendu.sarkar@universite-paris-saclay.fr](mailto:krishnendu.sarkar@universite-paris-saclay.fr)

Nanowire (NW) axial InGaN/GaN heterostructures are building blocks for light emitting diodes (LED). In particular, thanks to the stress relaxation through NW sidewalls, GaN NWs are promising pseudo-substrates for epitaxially growing In-rich InGaN axial nanostructures [1]. While InGaN/GaN NW based blue/green LEDs have been mastered by many groups, extending the spectral emission towards red with a high efficiency is challenging due to the large lattice mismatch between the In-rich InGaN and GaN. The resulting strain makes difficult the incorporation of high concentration of In atoms in the InGaN lattice leading to the so-called compositional pulling effect [2]. Moreover, crystallographic point defects detrimental for the LED efficiency are prone to appear in InGaN.

In the present contribution, our endeavor is to find a solution to both counterbalance the compositional pulling effect for achieving In-rich InGaN insertions while at the same time to reduce the point defects in the InGaN/GaN superlattice. For this, InGaN/GaN NW superlattice has been grown by PAMBE on an InGaN buffer with a low In content on a GaN NW base, separated from the superlattice with a very thin GaN insertion (Fig. 1). The influence of the InGaN buffer on trapping the defects from the InGaN/GaN superlattice has been investigated with high resolution cathodoluminescence spectroscopy at room temperature and at 10 K. The NW heterostructure is spatially mapped along the NW axis. A statistical study of the luminescence spectra recorded for InGaN/GaN NW superlattice with InGaN buffer demonstrates a considerable reduction in the point defects spectral signatures at both RT and 10 K. We discuss the impact of the InGaN buffer growth conditions on the optical properties of the InGaN superlattice. We show that the InGaN buffer functions as a strain counterbalancing and defect trapping layer to simultaneously compensate the pulling effect and to reduce the defects in red-emitting InGaN insertions.

### References

- [1] M. Morassi et al., Cryst. Growth Des. 18, 2545 (2018)  
 [2] S. Pereira et al., Phys. Rev. B, 64, 205311 (2001)

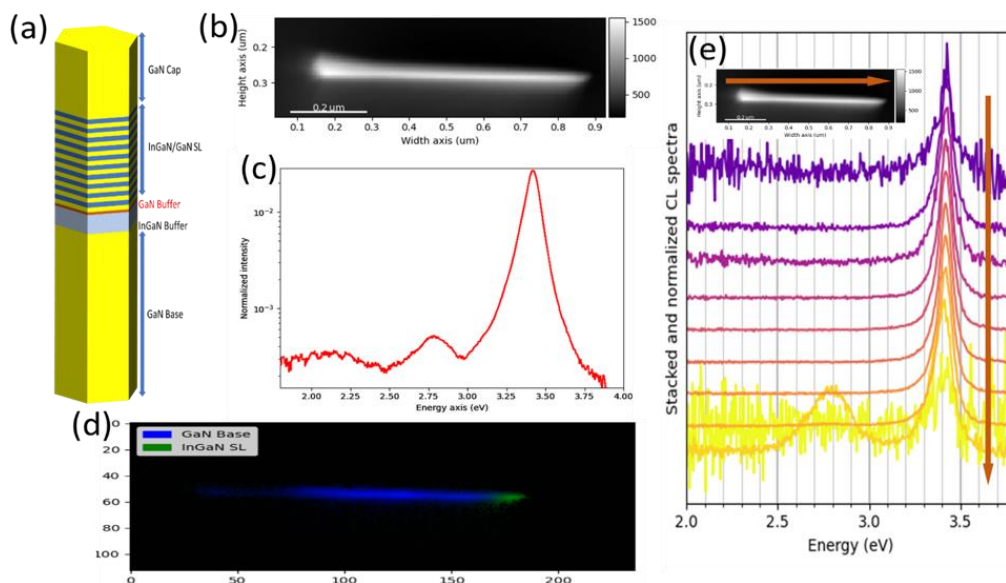


Fig. 1: (a) Schematic of the NW structure. (b) SEM of the NW. (c) Average CL spectra recorded from the NW. (d) Spatial mapping along the length of the NW. (e) Line scan and corresponding luminescence spectra along the length of the NW.

## **Influence of surface modification on the properties of GaN nanowires – cathodoluminescence and electron microscopy studies**

**A. Reszka,<sup>1)\*</sup> S. Piotrowska,<sup>1)</sup> Tomasz Plocinski,<sup>2)</sup> Radosław Szymon,<sup>3)</sup> Eunika Zielony,<sup>3)</sup>  
Aleksandra Wierzbicka,<sup>1)</sup> Sylwia Gieraltowska,<sup>1)</sup> Marta Sobanska,<sup>1)</sup> Zbigniew R. Zytkeiwicz,<sup>1)</sup>  
and B.J. Kowalski <sup>1)</sup>**

<sup>1)</sup> *Institute of Physics, Polish Academy of Sciences, Aleja Lotnikow 32/46, PL-02668 Warsaw, Poland*

<sup>2)</sup> *Warsaw University of Technology, Faculty of Materials Science and Engineering, Woloska 141, PL-02507 Warsaw, Poland*

<sup>3)</sup> *Department of Experimental Physics, Faculty of Fundamental Problems of Technology, Wrocław University of Science and Technology, Wybrzeże Wyspiańskiego 27, PL-50370 Wrocław, Poland*

\*Corresponding author: [rezka@ifpan.edu.pl](mailto:rezka@ifpan.edu.pl)

Although a clear influence of surface conditions on the transport and optical properties of semiconductor nanowires (NWs) was noticed already in the first decade of this century, methods of controlling surface states and inhibiting their harmful impact on the characteristics of NWs still remain an important and current subject of research. This applies especially to nanowires made of group III nitrides. Passivating by wet chemical treatments or coating of NWs with oxide layers are considered suitable means of protecting and passivating the NW sidewalls. Since low-dimensional nanostructures containing gallium nitride (GaN) and its alloys with aluminum nitride or indium nitride are promising structural elements of novel optoelectronic devices, such modifications of the NW surface may also significantly affect the operating parameters of NW-based devices.

Group III nitride NWs are of exceptional interest in materials engineering due to their specific microstructure with a wide range of possible structural defects, such as inversion domains, structural stacking faults etc. The luminescent properties of NWs depend on factors such as the surface conditions, NW diameter, presence and distribution of point or extended defects. At the same time, the optical properties of NWs define many of their applications. Research on the relationship between the material properties of nanowires, such as luminescence characteristics, and their microstructure requires the parallel use of several complementary experimental techniques. The results presented in this work are the outcome of the cooperation of an interdisciplinary team using various electron microscopy techniques – from high-resolution transmission electron microscopy, through scanning electron microscopy, to cathodoluminescence spectroscopy and microscopy.

The first part of the talk will present the results of multi-technique research on GaN NWs grown by plasma-assisted MBE and coated with hafnium oxide shells using atomic layer deposition method. Detailed TEM and SEM studies revealed the structure and morphology of the prepared GaN/HfO<sub>x</sub> core-shell NWs. Light emission from individual NWs were observed using of cathodoluminescence microscopy and spectroscopy. The results made it possible to correlate the spectral characteristics of cathodoluminescence with the properties of the hafnium oxide shell - its thickness, morphology and structure. Shell parameters leading to the optimal cathodoluminescence of the structures are assessed.

In the second part we will report the results obtained for GaN NWs modified by etching their surfaces in KOH and HCl solutions. Since both processes are used to etch, deoxidize, or passivate nitride surfaces, we applied them to evaluate their effect on the luminescence of GaN NWs. SEM observations revealed significant changes in the morphology, structure and surface conditions of the NWs, while STEM allows an insight into atomic structure of the NWs at high resolution. A correlation of the results acquired by different electron microscopy based techniques and the structural changes detected by complementary XRD studies was successfully achieved.

This work was partially supported by the Polish NCN grants 2022/45/B/ST5/02876, 2021/43/D/ST7/01936 and 2022/04/Y/ST7/00043.

## Cathodoluminescence Investigations of Nano-LEDs Based on Micron Sized III Nitride Platelets

A. Gustafsson,<sup>1),2)</sup> H. Usman,<sup>1)</sup> Z. Bi,<sup>3),4)</sup> and L. Samuelson,<sup>1),2),3)</sup>

<sup>1)</sup> Institute of Nanoscience and Applications, Southern University of Science and Technology, Shenzhen, China

<sup>2)</sup> Solid State Physics and NanoLund, Lund University, Box 118, Lund SE-221 00, Sweden

<sup>3)</sup> Hexagem AB, Lund, Sweden

<sup>4)</sup> Future Display Institute of Xiamen, Xiamen 361005, China

\*Corresponding author: Anders.Gustafsson@ff.lth.se

The next generation of displays will use direct emission based on micron-sized light emitting diodes ( $\mu$ -LEDs). [1] In direct emissive displays, each pixel consist of three separate  $\mu$ -LEDs, emitting red, green and blue light. Currently, blue and green  $\mu$ -LEDs in these displays are based on III-nitrides (InGaN) and the red  $\mu$ -LEDs are based on AlGaInP. The holy grail of  $\mu$ -LEDs for display applications is to cover all three colours by III-nitride material. This would simplify the driving circuits for the individual pixels. AlGaInP has the drawback of reduced efficiency when the pixel size is reduced. [2] This is mainly related to a high surface recombination velocity. The issue with red-emitting InGaN is to overcome the large lattice mismatch between the InGaN quantum wells (QWs) and the substrate (typically GaN or GaN-on-sapphire). The mismatch can be the source of structural defects, significantly reducing the efficiency of the  $\mu$ -LEDs. [3] We have investigated the optical properties of  $\mu$ -LEDs based on submicron sized InGaN platelets, covering the entire visible range. We focus this presentation on the technologically challenging red-emitting  $\mu$ -LEDs, where the lattice mismatch with GaN is the largest.

The platelets were grown by selective area growth from an array of submicron-sized holes in a SiN mask on GaN on sapphire substrates. [4] The growth is done by metal-organic chemical vapour deposition, in a two-step process, where the growth is seeded by a GaN nanowire in each hole, just filling the hole and sticking up above the mask. The growth is subsequently switched to InGaN, which results in the formation of pyramids with a hexagonal base. The small footprint and the mask in combination leaves the pyramids virtually dislocation free, as the threading dislocations are blocked from propagating from the substrate into the platelets. [5] The sample with fully formed pyramids is taken out of the reactor and flattened by chemical mechanical polishing, leaving a flat template with a thickness of 50-100 nm, and an extension of 500-800 nm. The sample is loaded back into the reactor and a series of layers are grown on the template. 1) A lower barrier matching the template in composition; 2) A single QW with higher indium content; 3) A top barrier with an indium content matching the lower barrier. Optionally, a transition layer with a slightly higher indium content than in the barrier is grown below the QW to promote indium incorporation into the QW, as well as increasing the carrier injection into the QW.

The optical properties were studied by hyperspectral cathodoluminescence (CL) imaging at room temperature. The typical conditions used were 3 to 5 kV and a probe current of 10 to 50 pA. Hyperspectral images with 1 000 to 20 000 pixels were recorded from both single platelets and arrays. We have investigated platelets emitting in the range from blue to red, but the study is focused on red-emitting platelets.

The CL emission from the platelets is dominated by the emission from the QW, as can be seen in figure 1. There are also weaker contributions from the other layers, most notably from the GaN substrate. The other peaks are from the barriers and the transition layer. The identification of the emission is easily done in using spatially resolved CL imaging at varying acceleration voltages. The QW emission reflects the shape of the platelets (as seen in figure 1) and the GaN substrate emission comes from the area between the platelets. At low acceleration voltage, short penetration depth of the electron beam, the barrier and transition layers appear as hexagonal rings. [6] With increasing acceleration voltage, first the transition layer becomes a filled hexagon and at even higher voltage, the lower barrier becomes a filled hexagon.

When imaging the QW emission in top view, we observe several dark lines, figure 1. These dark lines can also be observed when imaging the barrier emission, leading us to identify these as stacking mismatch

boundaries. [7] A series of samples where each layer was added sequentially reveals that the initial template platelets are defect free, whereas the dark lines appear already in the lower barrier. These dark lines can be studied in the different layers. Due to the different emission energies, it is possible to correlate the location of the dark lines in the different layers. Most of them line up quite well with some minor deviations. The identification of the dark lines as stacking mismatch boundaries was confirmed by a transmission electron microscope (TEM) study, where we performed CL imaging of pre-thinned substrates to make maps of individual platelets selected for TEM imaging. [8] After a final thinning, the dark lines in the CL images were correlated with the structural defects in the TEM images. These structural defects were confirmed to be stacking mismatch boundaries. In high resolution TEM images, the lattice on either side of the boundary are perfect, but are rotated with respect to each other, reflecting the ABAB and ACAC stacking sequence.

One key issue with the red-emitting platelets is that typically half of them are affected by dark lines. As these reduce the efficiency of the light emission, it is essential to determine the origin of the defects and to eliminate the source. The latter is the subject of further investigations.

## References

- [1] T. Jung T, J. H. Choi, S. H. Jang, and S. J Han S J, Symposium Digest of Technical Papers **50**, 442-6 (2019).
- [2] J. H. Park, M. Pristovsek, W. Cai, H. Cheong, T. Kumabe, D. S. Lee, T. Y. Seong, and H. Amano H, Opt Lett **47**, 2250-3 (2022).
- [3] F. Y. Meng, H. McFelea, R. Datta, U. Chowdhury U, Werkhoven C, Arena C, and Mahajan S, Journal of Applied Physics **110** 073503 (2011).
- [4] Z. Bi, A. Gustafsson, F. Lenrick, D. Lindgren, O. Hultin, L. R. Wallenberg, B. J. Ohlsson, B. Monemar, and L. Samuelson, Journal of Applied Physics **123** 025102 (2018).
- [5] Z. Bi, T. Lu, J. Colvin, E. Sjogren, N. Vainorius, A. Gustafsson, J. Johansson, R. Timm, F. Lenrick, R. Wallenberg, B. Monemar, and L. Samuelson, ACS Appl Mater Interfaces **12** 17845-51 (2020).
- [6] A. Gustafsson, Z. Bi, and L. Samuelson, Phys. Status Solidi B **2024** 2400446 (2024).
- [7] J. Bruckbauer, P. R. Edwards, S.-L. Sahonta, F. C. P. Massabuau, M. J. Kappers, C. J. Humphreys, R. A. Oliver, and R. W. Martin, Journal of Physics D: Applied Physics **47** 135107 (2014).
- [8] A. R. Persson, A. Gustafsson, Z. Bi, L. Samuelson, V. Darakchieva, and P. O. Å. Persson, Applied Physics Letters **123** 022103 (2023).

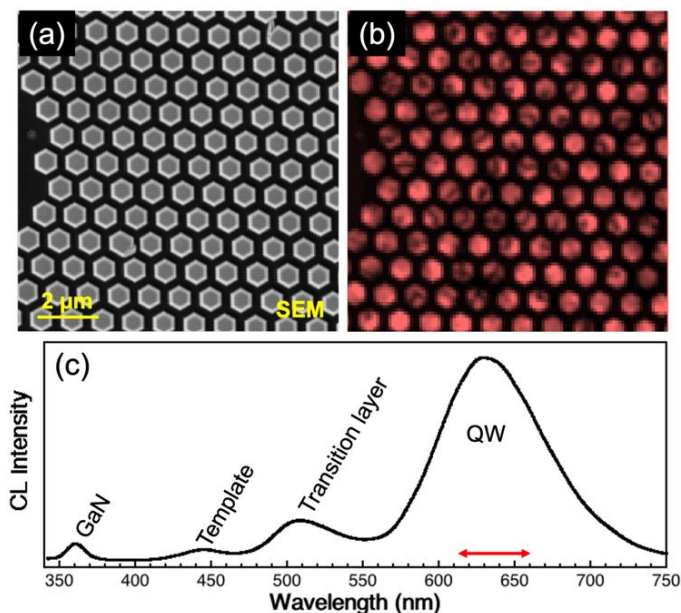


Fig. 1. a) top view SEM image, b) CL image of the QW emission, and c) CL spectrum of the area in (a), with labelling of the emission peaks. The arrow in (c) indicates the spectral width used for the CL image in (b).

## Correlative Scanning Electron Microscopy for exploring Quantum Emitters in Cubic GaN

K. Nicholson,<sup>1)</sup> R. Alshammary,<sup>1)</sup> J.K Cannon,<sup>2)</sup> A.J Bennett,<sup>2)</sup> J. Lee,<sup>3)</sup> K. Chang,<sup>3)</sup> Y.C Chiu,<sup>3)</sup> C. Bayram,<sup>3)</sup> R. W. Martin,<sup>4)</sup> P. R. Edwards,<sup>4)</sup> and N. Gunasekar<sup>1)\*</sup>

<sup>1)</sup> School of Physics and Astronomy, Cardiff University, Queen's Buildings, The Parade, Cardiff, CF24 3AA, UK

<sup>2)</sup> School of Engineering, Cardiff University, Queen's Buildings, The Parade, Cardiff, CF24 3A, UK

<sup>3)</sup> Department of Electrical and Computer Engineering, University of Illinois at Urbana-Champaign, Champaign, Illinois, 61801, USA

<sup>4)</sup> Department of Physics SUPA, University of Strathclyde, 107 Rottenrow East, Glasgow, G4 0NG, UK

\*Corresponding author: [gunasekarn@cardiff.ac.uk](mailto:gunasekarn@cardiff.ac.uk)

Cubic GaN (c-GaN) offer advantages compared to its hexagonal counterpart GaN (h-GaN) such as absence of strong polarization fields which prevents the accumulation of high carrier concentrations promoting Auger recombination [1], making c-GaN a candidate for efficient light emission. However, c-GaN tends to relax to thermodynamically stable h-GaN when grown on foreign substrates. V-groove nanopatterns results in excellent crystal quality but leave large h-GaN wings which have remained unchanged during the phase transition to c-GaN. To suppress this unwanted h-GaN wing, U-grooved nanopatterns has been developed [2]. GaN has also gained attention as a promising material for single photon emitters (SPE), a core element for quantum computing, though the origin of SPE remains unclear [3]. One hypothesis links SPE to point defects found near cubic inclusions within the hexagonal lattice. Unlike h-GaN, where threading dislocation dominate, c-GaN prominently exhibits stacking fault dislocations [4]. In this study, we investigate the possible origin of SPE of U-groove nanopatterned c-GaN on (111) silicon using correlative light-electron microscopy techniques of Cathodoluminescence (CL), Photoluminescence (PL) and Electron channelling contrast imaging (ECCI). PL with HBT interferometer is used to determine the presence of SPE and ECCI to image extended defects. Our preliminary results from CL, show h-GaN present at 365.5 nm, as well as prominent c-GaN peak at 387.5 nm and yellow band (YL) at 509.5nm. We also observe a broad peak at 617 nm which was seen via PL at around 610 nm in previous work. Work is in progress to determine if these emissions are due to single photon sources. Published investigations of c-GaN observe such a peak at 620nm, but it was not attributed to any defects [5]. However, current investigations into green-emitting c-GaN/InGaN/GaN suggest that this may be due to carbon complexes [6].

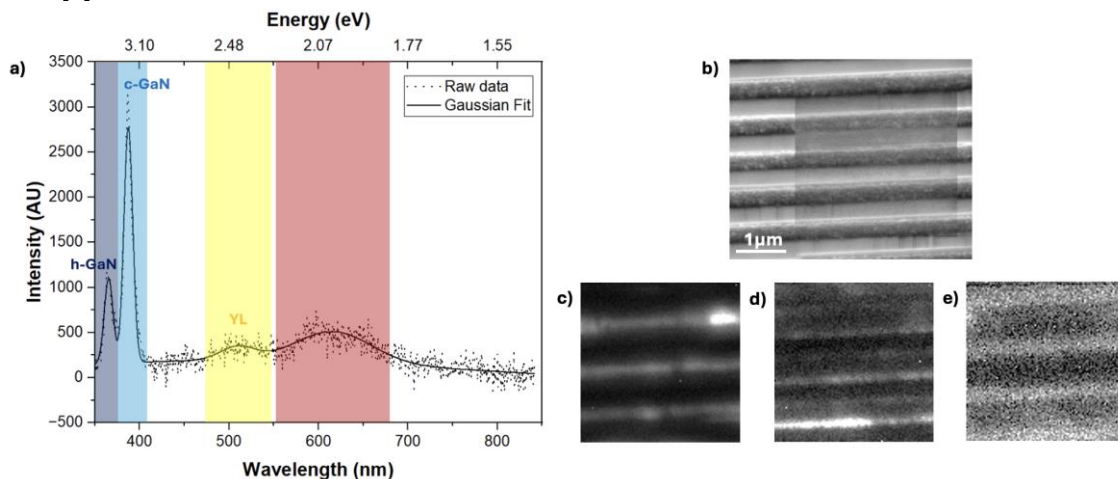


Fig. 1: Figure 1a) Background subtracted mean spectra of the map collected .Figure 1b) SE micrograph of the c-GaN sample with the region of hyperspectral-CL map highlighted. Figure c) – d) monochromatic-CL images of c-GaN, h-GaN and the broad band found at long wavelength, respectively, found through principal component analysis with the same scale seen in Figure 1a).

### References

- [1] K. T. Delaney, P. Rinke, and C. G. Van de Walle, *Appl. Phys. Lett.*, **94**, no. 19, (2009).
- [2] J. Lee, Y. C. Chiu, M. A. Johar, C. Bayram, *Appl. Phys. Lett.*, **121** (3): 032101 (2022).
- [3] S. G. Bishop, J.P Hadden, F. D. Alzahrani, R. Hekmati, D. L. Huffaker, W. W. Langbein and A. J. Bennett, *ACS Photonics* **7**, 7, 1636–1641, (2020)
- [4] D. J. Binks, P. Dawson, R. A. Oliver, D. J. Wallis, *Appl. Phys. Rev.* **9** (4): 041309 (2022).
- [5] Zhou, K., Huang, Y., Wang, Q., Yang, W., Zhang, H. and Liu, B, *Phys. Status Solidi B*, **259** (2022).
- [6] J. Lee, C. Bayram, *Appl. Phys. Lett.* **124**, no. 1, (2024).

## Polarisation-resolved cathodoluminescence study of a zincblende InGaN/GaN single quantum well

X. Xu<sup>1,\*</sup>, M. Frentrup<sup>1</sup>, G. Kusch<sup>1</sup>, Z. S. Pehlivan<sup>1</sup>, M. J. Kappers<sup>1</sup>, D. J. Wallis<sup>1,2</sup>, and R. A. Oliver<sup>1</sup>

<sup>1</sup>Department of Materials Science and Metallurgy, University of Cambridge, United Kingdom

<sup>2</sup>Centre for High Frequency Engineering, University of Cardiff, United Kingdom

\*Corresponding author: xx838@cam.ac.uk

Zincblende (zb) InGaN micro-LEDs have the potential to overcome the low efficiency of long-wavelength emission observed for devices in the conventional wurtzite phase. This is because (001) zb GaN is free of spontaneous and piezoelectric polarization fields and has a narrower bandgap compared to wurtzite GaN [1]. However, zb InGaN suffers from a high density of stacking faults (SFs), which impacts the luminescence from the quantum wells (QWs). Furthermore, optical characteristics typical of quantum wires (QWires) were recently identified in the cathodoluminescence (CL) of a zb InGaN single quantum well (SQW) sample [2]. This was attributed to indium enrichment at the intersection of SFs with the SQW [2]. Meanwhile, previous photoluminescence studies suggested that the QW emission is polarised and may relate to such SF-related QWires [3]. This suggestion implies that the SF density might have a profound effect on the degree of polarization.

In this presentation, we will report on polarisation-resolved CL measurements of zb InGaN/GaN SQW samples with different SF density. The samples were grown on zb GaN buffers with thicknesses varying from 600 nm to 3000 nm by metal-organic vapour phase epitaxy and an X-ray diffraction analysis has previously shown that the SF density reduces with buffer thickness and hence a reduction in polarisation might be expected [4]. However, mean spectra of panchromatic CL maps show that the light emission is mainly from the SQW and is highly polarised. Polarisation-resolved panchromatic CL maps show that the polarised light arises from both SF-rich and defect-free regions, but that the majority of the polarised emission is from regions with no obvious relation to SFs and show no characteristics associated to Qwires. However, elongated features reminiscent of QWires were observed in the panchromatic CL maps at SF locations. The wire-like features were oriented along perpendicular directions in CL maps in which the polarization was in perpendicular orientations, supporting the suggestion QWires can generate polarised light. The degree of polarisation (DoP) was determined to be about 0.625 for the SQW emission peak in the mean spectrum and is approximately independent of the SF density. If the polarised emission were largely related to QWires at SFs, the reduction in SF density with buffer thickness would lead to a lower DoP at larger thicknesses. Hence, this provides further evidence that most of the polarised emission is attributable to defect-free material.

### References

- [1] D. R. Elsaesser et al., J. Appl. Phys. **122**, 115703 (2017)
- [2] Gundimeda et al., J. Phys. D: Appl. Phys. **58**, 025112 (2024)
- [3] S. A. Church et al., Appl. Phys. Lett. **117**, 032103 (2020)
- [4] P. Vacek et al., J. Appl. Phys. **129**, 155306 (2021)

## Characterization of InGaN/GaN Nanowires by Wavelength & Angle Resolved Cathodoluminescence

T. Lassiaz,<sup>1)\*</sup> R. Vermeersch,<sup>1)</sup> A. Rooney,<sup>1)</sup> J. Brochet,<sup>1)</sup> M. Charbonnier,<sup>1)</sup> B. Amstatt,<sup>1)</sup> P. Tchoufian,<sup>1)</sup> and M. Daanouné<sup>1)</sup>

<sup>1)</sup> Aledia, F-38130, Echirolles, France

\*Corresponding author: [timothée.lassiaz@aledia.com](mailto:timothée.lassiaz@aledia.com)

Interest in augmented reality is increasing, with major Tech companies such as Meta, Google, and Samsung actively developing mass consumer solutions in the form of smart glasses based on microdisplays MicroLEDs, particularly based on nanowires, are considered among the most efficient technologies due to their unique physical properties. The nanowires developed by Aledia have dimensions on the order of the wavelength, enabling the formation of a photonic crystal. This property addresses several challenges associated with wearable display applications.

The photonic crystal enables control over the angular and spectral emission of the LEDs. To demonstrate the directivity effects of our sources, as predicted by optical simulations, we employ Wavelength & Angle-Resolved Cathodoluminescence (WARCL). An electron beam excites the material, generating cathodoluminescence (CL) emission. This emission is analysed as a function of wavelength and emission angle, providing detailed insights into the optical properties of the photonic crystal. Angular analysis is essential for understanding how light is trapped, reflected, or coupled within these structures.

The extracted band diagram from this characterization confirms that the photonic crystal effect corresponds well with simulations. The measured intensity is significantly enhanced in a spectral band around 637 nm (red/amber) for a specific set of angles, indicating directional emission (Figure 1). This design achieves:

- A highly pure wavelength emission (red at 637 nm with only 21 nm FWHM) within a  $\pm 20^\circ$  range, exhibiting a characteristic double peak associated with the optical mode.
- Directional extraction compared to Lambertian emission, leading to improved coupling with optical waveguide-based systems. The measured light intensity at normal incidence is enhanced by a factor of  $\sim 2$  compared to a Lambertian source.

Furthermore, we confirm that the band diagram extracted using WARCL is consistent with the band diagram obtained through electroluminescence far-field measurements (Figure 2). These findings validate the potential of nanowire-based MicroLEDs for augmented reality applications by providing improved spectral purity and directional emission control.

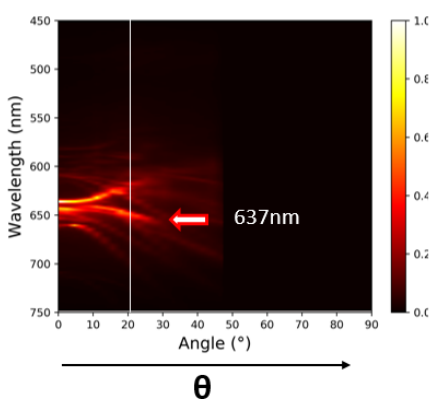


Fig. 1: Result obtain by WARCL measurement  $20^\circ$  is representative of the angle of acceptance of the waveguides).

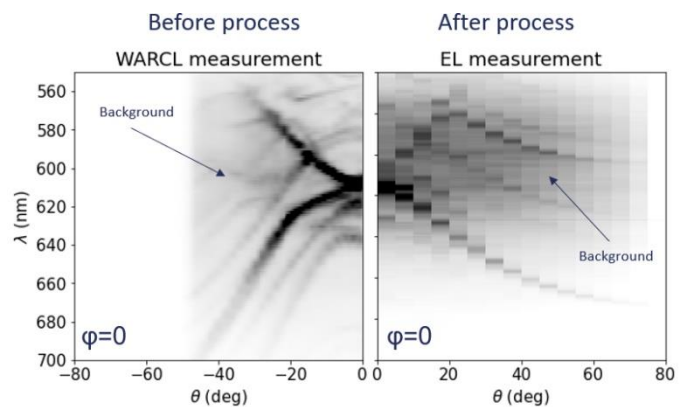


Fig. 2: Validation of WARCL as characterization method: clear correlation between WARCL and EL directivity

## Recombination dynamics of oxygen-related defects in AlN layers studied with time-resolved cathodoluminescence spectroscopy

B. Szafranski,<sup>1)\*</sup> L. Peters,<sup>1)</sup> C. Margenfeld,<sup>1)</sup> S. Wolter,<sup>1)</sup> A. Waag,<sup>1)</sup> and T. Voss<sup>1)</sup>

<sup>1)</sup> Technische Universität Braunschweig, Institute of Semiconductor Technology and Laboratory for Emerging Nanometrology (LENA), 38106 Braunschweig, Germany

\*Corresponding author: [barbara.szafranski@tu-braunschweig.de](mailto:barbara.szafranski@tu-braunschweig.de)

To fabricate AlGaIn-based ultraviolet (UV) light emitting diodes (LEDs) with high quantum efficiency, it is crucial to use a high-quality AlN buffer layer on a sapphire substrate. High temperature annealing (HTA) of sputtered AlN has been proven to significantly enhance crystal quality by reducing the density of threading dislocations propagating through the film. This makes HTA a viable approach for achieving low-defect-density AlN. However, during the annealing process, oxygen diffusion from the sapphire (Al<sub>2</sub>O<sub>3</sub>) substrate introduces a high density of point defects. These oxygen-related defects are considered to cause absorption losses in the deep UV range below ~230 nm. [1] Simultaneously, oxygen acts as a donor in AlN and has a smaller formation energy than the intrinsic donor V<sub>N</sub>. Therefore, the typically observed absorption around 265 nm, which is connected to V<sub>N</sub> donors that compensate C<sub>N</sub> impurities, is suppressed. [2] Since UV LEDs are predominantly designed as bottom emitters, where light outcoupling occurs through the AlN/sapphire template, the optical properties of these templates play a vital role in device performance. [3] A comprehensive understanding of the defect states introduced by oxygen during HTA and their impact on the optical properties of AlN is crucial for optimizing UV LED efficiency.

Therefore, we study the influence of these oxygen-related defects in HTA AlN layers using cathodoluminescence (CL) spectroscopy. For all experiments, we used 350 nm thick AlN layers sputtered on c-plane sapphire substrates. The sputtered AlN layers were annealed at different temperatures (1600 °C – 1750 °C) in N<sub>2</sub> atmosphere at ambient pressure.

At room temperature, CL measurements reveal a broad luminescence band (FWHM = 466 meV) centred around 3.65 eV. We studied the charge carrier recombination dynamics of these oxygen-related defects with temperature-dependent and time-resolved CL spectroscopy. The luminescence associated with these defects exhibits a complex multi-exponential decay, with a fast component of approximately 2 ns and slower components ranging from tens to hundreds of nanoseconds. We attribute the fast decay component to the transition between the conduction band edge states and mainly (V<sub>Al</sub>-O<sub>N</sub>)<sup>2-</sup> and (V<sub>Al</sub>-2O<sub>N</sub>)<sup>1-</sup> defect complexes as acceptors. At low temperatures a donor-acceptor-pair transition between an O<sub>N</sub> donor and the same two acceptors is revealed, which is responsible for the slow decay component. Furthermore, we demonstrate the impact of these oxygen-related defects on the quality and transparency of the AlN templates.

### References

- [1] C. Hartmann, L. Matiwe, J. Wollweber, I. Gamov, K. Irmischer, M. Bickermann, and T. Straubinger, *CrystEngComm*, **22**, 1762 (2020).
- [2] L. Peters, C. Margenfeld, J. Krügener, C. Ronning, and A. Waag, *Physica Status Solidi A* **220**, 2200485 (2023).
- [3] H. Amano, R. Collazo, C. de Santi, S. Einfeldt, M. Funato, J. Glaab, S. Hagedorn, A. Hirano, H. Hirayama, R. Ishii, Y. Kashima, Y. Kawakami, R. Kirste, M. Kneissl, R. Martin, F. Mehnke, M. Meneghini, A. Ougazzaden, P. J. Parbrook, S. Rajan, P. Reddy, F. Römer, J. Ruschel, B. Sarkar, F. Scholz, L. J. Schowalter, P. Shields, Z. Sitar, L. Sulmoni, T. Wang, T. Wernicke, M. Weyers, B. Witzigmann, Y.-R. Wu, T. Wunderer, and Y. Zhang, *J. Phys. D: Appl. Phys.* **53**, 503001 (2020).

## Study of Nanolaser Optical and Structural Properties at the Nanometre Scale

C. Santini,<sup>1)</sup> N. Van Nielen,<sup>2)</sup> T.H Ngo,<sup>3)</sup> V. Brändli,<sup>3)</sup> S. Chenot,<sup>3)</sup> P.M. Coulon,<sup>3)</sup> S. Vézian,<sup>3)</sup> J. Brault,<sup>3)</sup> P.A. Shields,<sup>5)</sup> A. Polman,<sup>2)</sup> B. Damilano,<sup>3)</sup> C. Brimont,<sup>4)</sup> T. Guillet,<sup>4)</sup> S. Meuret<sup>1),\*</sup>

<sup>1)</sup> CEMES, CNRS, 31055 Toulouse, France\*

<sup>2)</sup> AMOLF, Amsterdam, Netherlands

<sup>3)</sup> Université Côte d'Azur, CNRS, CRHEA, Valbonne, France

<sup>4)</sup> L2C, Montpellier, France

<sup>5)</sup> University of Bath, United Kingdom

\*Corresponding author: [sophie.meuret@cemes.fr](mailto:sophie.meuret@cemes.fr)

Since their first demonstration by Huang et al in 2001 [1], semiconductor nanolasers have attracted a lot of interest especially for their application in optoelectronic devices. They have the advantages to be cost-effective, easy to fabricate and of a micron size. Since 2001, various semiconductors and geometries demonstrated lasing properties, for example ZnO [1] or GaN [2] nanowires.

Lasing can be induced by optical pumping, usually it is characterized by a drastic reduction of the emission spectrum width and an increase of the emitted light coherence [3]. The key lasing properties of nanolasers include the emission wavelength, the value of the lasing threshold and the carrier lifetime. The optical modes of the nanolasers observed above the lasing threshold are directly related to the dimensions of the nanolaser, since the cavity is formed by the nanowire itself. Thus, the shape of the nanowire has a direct impact on all laser characteristics. Given that the structural parameters of the nanowires vary at a nanometric scale, electron microscopy is well-suited for their analysis. Moreover, the lasing properties can be directly linked with the nanolaser shape provided that the electron microscope is equipped with a photoluminescence setup.

We aim to probe the near field of optically pumped nanolasers within their lasing regime with a focused electron beam in Ultrafast - STEM. When the electrons interact with the field created by the laser light, electrons absorb or emit quanta of the field energy. By mapping the interactions of the field with the electron beam, Photon-Induced Near-field Electron Microscopy (PINEM) enables us to measure the transversal field intensity [4] and the lasing regime dynamics with a sub-picosecond resolution.

In this presentation, we will discuss how we can study the lasing characteristics of GaN nanolasers at the nanoscale scale within a UTEM using PINEM and photoluminescence.

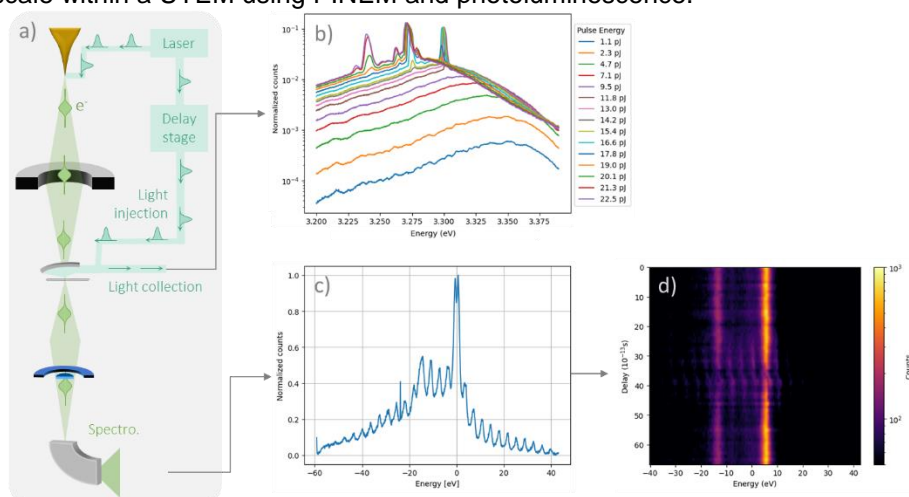


Fig. 1: a) UTEM set-up b) Nanolaser photoluminescence spectrum depending on the pumping power c) PINEM spectrum on Aluminum d) PINEM delay scan on Aluminum.

### References

- [1] M. H. Huang *et al.*, "Room-Temperature Ultraviolet Nanowire Nanolasers," *Science*, vol. 292, no. 5523, pp. 1897–1899, Jun. 2001, doi: 10.1126/science.1060367.
- [2] J. C. Johnson, H.-J. Choi, K. P. Knutsen, R. D. Schaller, P. Yang, and R. J. Saykally, "Single gallium nitride nanowire lasers," *Nat. Mater.*, vol. 1, no. 2, pp. 106–110, Oct. 2002, doi: 10.1038/nmat728.
- [3] L. K. Van Vugt, S. Rühle, and D. Vanmaekelbergh, "Phase-Correlated Nondirectional Laser Emission from the End Facets of a ZnO Nanowire," *Nano Lett.*, vol. 6, no. 12, pp. 2707–2711, Dec. 2006, doi: 10.1021/nl0616227.
- [4] A. Feist, K. E. Echemkamp, J. Schauss, S. V. Yalunin, S. Schäfer, and C. Ropers, "Quantum coherent optical phase modulation in an ultrafast transmission electron microscope," *Nature*, vol. 521, no. 7551, pp. 200–203, May 2015, doi: 10.1038/nature14463.

## V-pits as a source of emission heterogeneity in InGaN/GaN micro-LEDs studied by photon-correlation cathodoluminescence spectroscopy

P. Sáenz de Santa María Modroño<sup>1)\*</sup>, C. Le Maoult<sup>2</sup>, N. Bernier<sup>2)</sup>, D. Vaufrey<sup>2)</sup>, G. Jacopin<sup>1)</sup>

<sup>1)</sup> Univ. Grenoble Alpes, CNRS, Grenoble INP\*, Institut Néel, 38000 Grenoble, France

<sup>2)</sup> Univ. Grenoble Alpes, CEA-LETI, Grenoble INP, 38000 Grenoble, France

\*Corresponding author: [pablossmme@gmail.com](mailto:pablossmme@gmail.com)

GaN-based LEDs are characterized by their remarkable efficiency, exceptionally long operational lifespans, and a tunable bandgap, which could benefit microdisplay applications. However, a series of difficulties stop commercial applications of  $\mu$ -LED displays, like maintaining the high external quantum efficiency and guaranteeing uniform brightness and color.

Here, we have studied the emission properties of InGaN/GaN  $\mu$ LEDs of different sizes and shapes via spatially and spectrally resolved cathodoluminescence (CL) spectroscopy while simultaneously measuring their lifetime via Hanbury-Brown-Twiss (HBT) interferometry measurements, in order to find the origin of this heterogeneity[1]. Fig. 1 shows an example of the measurements performed on a 4  $\mu$ m sample. CL allows us to simultaneously obtain a spatial mapping of the wavelength, lifetime, and intensity. More than 150  $\mu$ LED samples were individually studied, enabling us to compare of pixel-to-pixel emission properties. Fig 1 shows dark intensity spots that do not affect the lifetime, but increase the emission energy. These kinds of structures were found in all the studied samples, and had a significant impact on the total intensity and wavelength, particularly on the smallest samples, of 1  $\mu$ m<sup>2</sup>. These dark spots have been attributed to differences in injection efficiency between samples, caused by V-pit type defects in the active region. V-pits de facto reduce injection efficiency by providing a non-radiative decay [2] path that prevents electron-hole (e-h) pairs inside to produce light. V-pits create an energy barrier [3] that isolates e-h pairs outside the defect from non-radiative path, and cause a local blue-shift via strain relaxation [4]. The variance in the number of V-pits is relatively larger on the smallest samples, explaining their higher heterogeneity in both intensity and wavelength. V-pits are usually considered a desirable defect for large nitride LEDs. In contrast, our results show that for small  $\mu$ LEDs, V-pits can induce a colour and intensity variation between samples.

### References

- [1] P. Sáenz de Santa María Modroño, C. Le Maoult, N. Bernier, D. Vaufrey, and G. Jacopin ACS Photonics **11** (6), 2406-2412, (2024).
- [2] W. Liu, J. Carlin, N. Grandjean, B. Deveaud, G. Jacopin (2016). Applied Physics Letters. **109**. 042101. 10.1063/1.4959832.
- [3] A. Hangleiter, F. Hitzel, C. Netzel, D. Fuhrmann, U. Rossow, G. Ade, P. Hinze, (2005). Physical review letters. **95**. 127402. 10.1103/PhysRevLett.95.127402.
- [4] T. Song Journal of Applied Physics. **98**. 084906 - 084906. 10.1063/1.2108148, (2005).

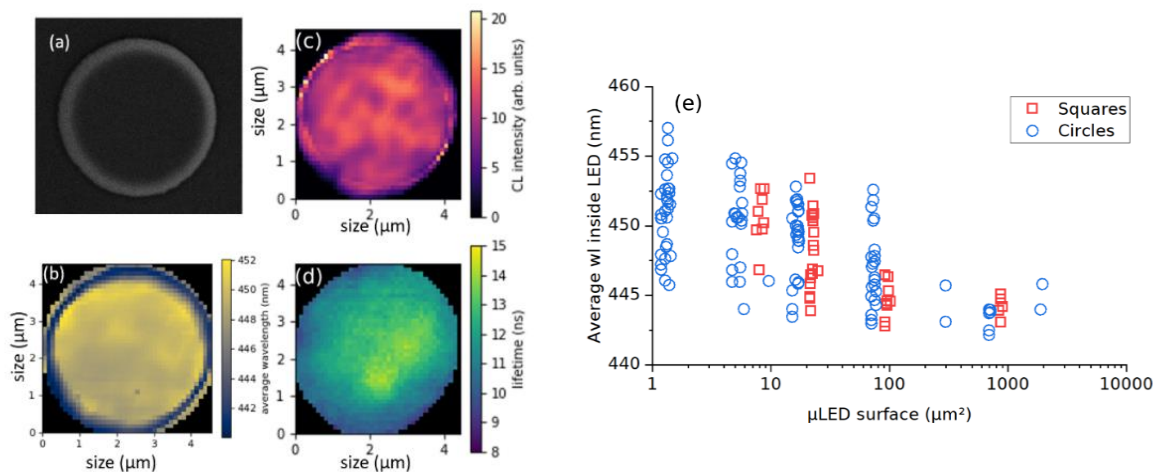


Fig. 1: a) SEM image of a circular 4  $\mu$ m LED. CL mapping of b) average wavelength, c) total intensity, and d) estimated lifetime of the same LED, obtained via CL. e) Arithmetic mean emission wavelength at the center of the  $\mu$ LED as a function of its area.

## Effects of Lamella Preparation on InGaN Quantum Well Luminescence

Nika van Nielen<sup>1)\*</sup>, Delphine Lagard<sup>2)</sup>, Cleo Santini<sup>3)</sup>, Florian Castioni<sup>4)</sup>, Robin Cours<sup>3)</sup>, Andrea Balocchi<sup>2)</sup>, Teresa Hungria<sup>5)</sup>, Andrey Tsatsulnikov<sup>6)</sup>, Alexei Sakharov<sup>6)</sup>, Andrey Nikolaiev<sup>6)</sup>, Nikolay Cherkashin<sup>3)</sup>, Luiz Tizei<sup>4)</sup>, Albert Polman<sup>1)</sup>, Sophie Meuret<sup>3)</sup>

<sup>1)</sup> AMOLF, Amsterdam 1098 XG, The Netherlands

<sup>2)</sup> CNRS, LPCNO, Toulouse 31077, France

<sup>3)</sup> CEMES/CNRS, Toulouse 31055, France

<sup>4)</sup> Laboratoire de Physique des Solides, Orsay 91405, France

<sup>5)</sup> CNRS, Centre de Microcaracterisation Raimond Castaing, Toulouse 31400, France

<sup>6)</sup> Ioffe Institute, Saint-Petersburg 194021, Russia

\*Corresponding author: vnielen@amolf.nl

Despite being a popular method of sample preparation for studies in a transmission electron microscope, the effects on the optical properties of bulk samples thinned into lamellae using Ga-based focused ion beams (FIB), have seldom been studied systematically. In this work, we confront this using correlative cathodoluminescence (CL) microscopy, to investigate the optical properties of high In-content InGaN/GaN quantum wells (QW). The heterostructure is fabricated using a growth-interrupting step that etches the active layer, forming regions of QWs and quasi-quantum dots (QD) that behave as localized emitters [1,2] and furthermore mitigate the strain-induced quantum Stark effect. By exploiting the spatially varying hyperspectral CL signal, we identify the same nanoscale regions of the sample before and after lamella preparation and evaluate changes in the radiative properties. We then employ time-correlated single-photon counting experiments with picosecond electrostatically beam-blanked electron pulses to extract the luminescence decay as a function of position and wavelength and provide insight into the non-radiative recombination dynamics. Our studies show that despite measures undertaken to prevent damage by the FIB, lamella preparation affects both the spectral and time-resolved luminescence properties of the sample. Non-radiative defects introduced by the FIB reduce the emission lifetime, with the QW luminescence component particularly affected due to its weak localization, that allows carriers to migrate to defect areas. These findings underscore the importance of correlating bulk and lamella properties to accurately interpret optical measurements.

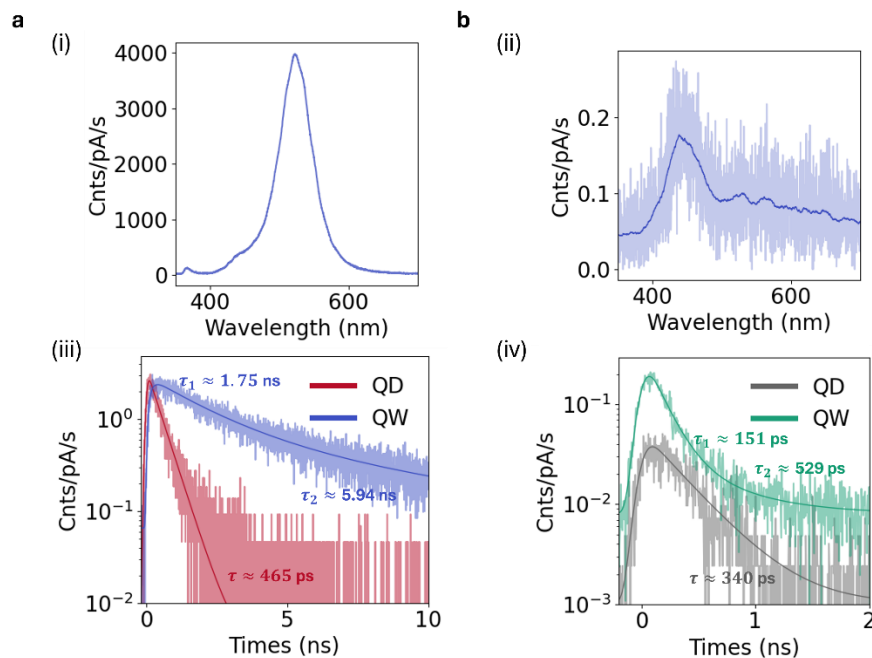


Fig. 2: CL measurements from the sample in (a) bulk and (b) lamella configuration. CL spectra are demonstrated in (i & ii), whereas (iii & iv) demonstrate decay traces of QD and QW emission, isolated using  $450 \pm 20$  nm and  $550 \pm 20$  nm optical filters respectively

[1] A. F. F. Tsatsulnikov et al., *Sci Adv Mater*, 7(8), pp. 1629–1635 (2015)

[2] D. Baretin et al., *Nanomaterials*, 13(8), 1367 (2023)

## Carrier diffusion in Ga(As,Sb) nanowires investigated by continuous and time-resolved cathodoluminescence spectroscopy

M. Gómez Ruiz,<sup>1)\*</sup> G. Kusch,<sup>2)</sup> V. Kaganer,<sup>1)</sup> A. Ajay,<sup>3)</sup> H. W. Jeong,<sup>3)</sup> G. Koblmüller,<sup>3)</sup> R. A. Oliver,<sup>2)</sup> O. Brandt<sup>1)</sup> and J. Lähnemann<sup>1)</sup>

<sup>1)</sup> Paul-Drude-Institut für Festkörperelektronik, Hausvogteiplatz 5–7, 10117 Berlin, Germany

<sup>2)</sup> University of Cambridge, 27 Charles Babbage Road, Cambridge CB3 0FS, United Kingdom

<sup>3)</sup> Walter-Schottky-Institut, Technische Universität München, Am Coulombwall 4, 85748 Garching, Germany

\*Corresponding author: gomez@pdi-berlin.de

Semiconductor nanowire (NW) structures emitting at wavelengths used in optical telecommunications are attractive for the integration on silicon-on-insulator waveguides. To this end, we study Ga(As,Sb) NWs with an axial (In,Ga)As insertion. To assess the potential of these heterostructures as integrated emitters, it is essential to understand the charge carrier transfer to and the recombination in the lower bandgap (In,Ga)As insertions, which can be investigated on a microscopic scale by cathodoluminescence (CL) spectroscopy. The abrupt interface between the Ga(As,Sb) segment and the (In,Ga)As insertion, together with an (Al,Ga)As/GaAs passivation shell enclosing the axial NW heterostructure are prerequisites for an efficient emitter [1].

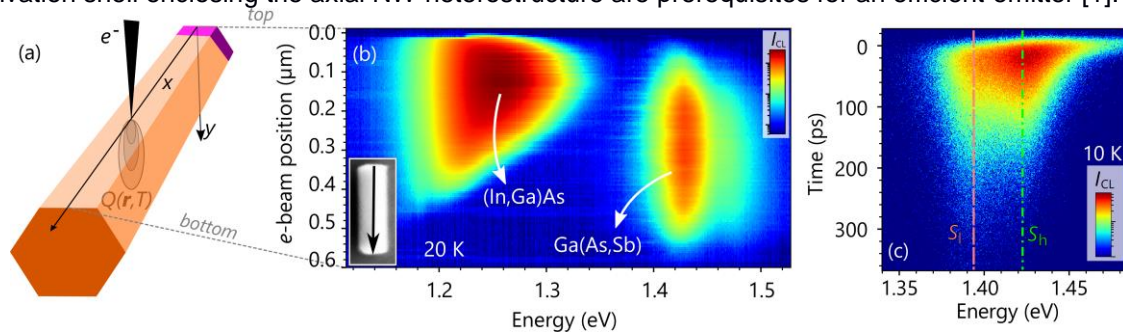


Fig. 1: (a) Schematics of the CL experiment, illustrating the electron beam scanned along the axis ( $x$ ). The (Al,Ga)As shell is omitted for clarity. (b) Representative CL hyperspectral linescan recorded along the axis of a NW, with CL intensity displayed in a logarithmic color-coded style. The secondary electron (SE) image in the inset shows the NW under study and the direction of the linescan. (c) Streak camera image acquired at 10 K, illustrating the spectrally-resolved and temporally-resolved components of the Ga(As,Sb) band.

In our CL experiments the electron beam and thus the volume in which electron-hole pairs are generated, is scanned along the axis of the NW ( $x$ ) [Fig. 1(a)]. After their generation and diffusion, the carriers recombine either in the Ga(As,Sb) segment or in the (In,Ga)As insertion, giving rise to spectrally distinct CL bands. The intensity profiles of both emission bands are recorded as a function of the beam position [Fig. 1(b)]. Although the (In,Ga)As insertion is only about 20 nm long, the corresponding CL band can be observed over a length of more than 400 nm under high excitation conditions. The evolution of these profiles with temperature is analysed using a model that includes the temperature-dependent generation volume and the diffusion of the generated carriers giving a carrier diffusion length of  $L_d \approx 200$  nm at 10 K.

The behavior of the device is constrained by the diffusion length. However, these values alone do not directly reveal the underlying mechanisms limiting diffusive transport. To gain further insights, we extract the diffusivity as a function of temperature by complementary time-resolved cathodoluminescence (TRCL) experiments [Fig. 1(c)]. In these experiments, the effective lifetime of the integrated Ga(As,Sb) transition [ $\tau_{\text{eff,Ga(As,Sb)}}$ ] is measured. The experimentally observed effective decay time  $\tau_{\text{eff,Ga(As,Sb)}}$ , is influenced by the carrier transit time towards the Ga(As,Sb)/air and Ga(As,Sb)/(In,Ga)As interfaces ( $\tau_{\text{tr}}$ ):

$$\frac{1}{\tau_{\text{eff,Ga(As,Sb)}}} = \frac{1}{\tau_1} + \frac{1}{\tau_{\text{tr}}} \quad (1)$$

Here,  $\tau_1$  represents the intrinsic effective lifetime of carriers in Ga(As,Sb) without considering diffusive transport effects, satisfying  $L_d = (D\tau_1)^{1/2}$ . By analyzing the temperature-dependent evolution of  $\tau_{\text{eff,Ga(As,Sb)}}$ , we assess the interplay between carrier recombination and transport processes. We find that twin boundaries play a crucial role in explaining the extracted diffusion parameters, which are significantly lower than those observed in both layers and nanowires of similar materials. This study provides a comprehensive characterization of carrier dynamics within the Ga(As,Sb)/(In,Ga)As heterostructure, complementing findings on diffusion lengths and charge carrier behavior. [1] Jeong H. *et al.*, *Small*, 2207531 (2023)

## Steady-State and Time-Resolved Cathodoluminescence of III-Nitride Semiconductors

K. Loeto,<sup>1,\*</sup> A. F. Campbell,<sup>1)</sup> D. Spallek,<sup>1)</sup> J. Lähnemann,<sup>1)</sup>

<sup>1)</sup> Paul-Drude-Institut für Festkörperelektronik, Berlin, Germany

\*Corresponding author: loeto@pdi-berlin.de

We have recently installed a state-of-the-art time-resolved cathodoluminescence (TRCL) microscope, marking a significant leap in the institute's research capabilities. This TRCL system incorporates an ultra-high-performance scanning electron microscope equipped with a distinctly stable electron source for optimised imaging conditions and the opportunity to operate at very-low acceleration voltages, down-to 0.35 kV, which is critical for achieving high spatial-resolution cathodoluminescence (CL) imaging. An efficient light collection system for enhanced imaging and spectroscopy of low intensity samples is combined with dedicated ultraviolet-optimised detection systems for both continuous-wave and TRCL modes, ideally suited for studying ultrawide bandgap semiconductors. TRCL operation is facilitated by an ultrafast electrostatic beam blaster, paired with either a time-correlated single photon counting (TCSPC) detector or a streak camera. Using the 1 ps temporal resolution of the streak camera, a record short pulse length (full width at half maximum) of down to 23 ps at 5 kV acceleration voltage could be evidenced. Therefore, this cutting-edge setup opens new avenues for studying the dynamic optical properties of advanced semiconductor materials. In this contribution, the focus will be on the III-nitrides, where three different studies each showcase the distinct advantages of the system's capabilities. Firstly, the high spectral resolution ultraviolet-optimised photon detection systems are used to resolve and study spectral and temporal characteristics of excitonic bands in AlN layers. Streak imaging, as seen in Figure 1(a), reveals the distinct decay behaviour for the observed excitonic lines as underscored by the extracted transients. Understanding these decay characteristics will aid in understanding the origins of the excitonic bands, which have seen some debate in the literature [1]. Secondly, CL hyperspectral and TRCL mapping are employed to analyse the optical properties of thick, uniform (In,Ga)N layers, which have potential as pseudo-substrates for red-emitting (In,Ga)N light-emitting diodes [2]. First results, as seen in Figure 1(b), indicate a correlation between dark-regions on the fitted peak intensity map associated with dislocations and regions of fast decay on the lifetime map. Ultimately, such measurements may aid in understanding the interplay between carrier dynamics and localisation in these (In,Ga)N layers. Lastly, the very-low acceleration voltage operation is utilised to map non-radiative recombination at point defects in specially designed ultra-thin (1 nm) AlGaIn quantum-well samples with thin (5 nm) barriers. At 1 kV acceleration voltage, we achieve spatial imaging with a 30 nm resolution, seen in Figure 1(c), notably exceeding the 76 nm reported on (In,Ga)N by [3].

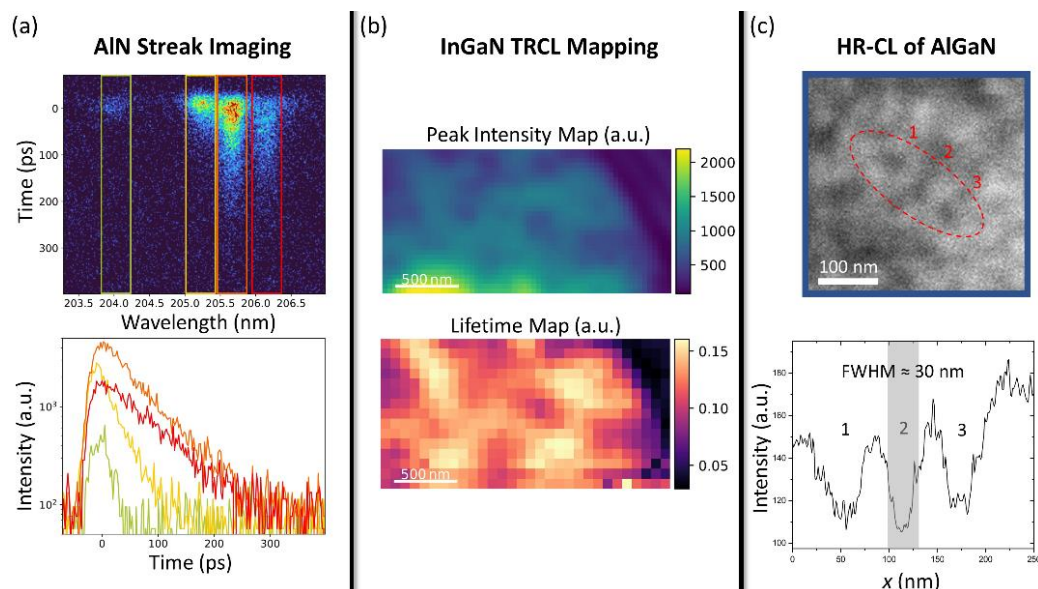


Figure 1: (a) A streak image recorded on an AlN layer (top) and decay transients extracted from the highlighted regions (bottom). (b) Complementary peak intensity (top) and lifetime maps (bottom) recorded from an (In, Ga)N layer. (c) High-resolution CL map of an AlGaIn quantum-well (top) and a linescan highlighting the estimated spatial resolution (bottom).

[1] L. van Deurzen et al., *APL Mater.* **11**, 081109 (2023).

[2] J. Kang et al., *J. Phys. D Appl. Phys.* **58**, 14LT01 (2025).

[3] T. F. K. Weatherley, et al., *Nano Lett.* **21**, 5217–5224 (2021)

## CLEBIC characterisation of deep UV emitting LEDs

Douglas Cameron,<sup>1,4,\*</sup> Marcel Schilling,<sup>2)</sup> Gunnar Kusch,<sup>3)</sup> Paul R. Edwards,<sup>4)</sup> Viesturs Spulis,<sup>3,4)</sup> Tim Wernicke,<sup>2)</sup> Michael Kneissl,<sup>2)</sup> Rachel A. Oliver,<sup>3)</sup> Robert W. Martin<sup>4)</sup>

<sup>1)</sup> Gatan, Inc., Pleasanton, United States

<sup>2)</sup> Technische Universität Berlin, Institute of Solid State Physics, Berlin, Germany

<sup>3)</sup> Department of Materials Science and Metallurgy, University of Cambridge, United Kingdom

<sup>4)</sup> Department of Physics, SUPA, University of Strathclyde, Glasgow, United Kingdom

\*Corresponding author: douglas.cameron@ametek.com

Point defects are particularly problematic in UV LEDs as they can influence the internal quantum efficiency, carrier injection, light extraction as well as reduce device lifetimes through degradation mechanisms. One key variable that can assist in controlling the concentrations of these unwanted defects are the epitaxial growth temperatures. To isolate the effects of growth temperatures on point defect populations, a specific series of samples was produced. Care was taken to ensure consistent layer thicknesses, extended defect densities, and compositions, despite the varying growth temperatures for the active regions.

To study these device-critical defect populations in deep UV emitting LEDs, we employ an array of complementary microscopy techniques. Cathodoluminescence and electron beam induced current (CLEBIC) measurements allow us to create highly detailed maps of the buried active regions. Within these regions point defects, dislocations, step structures and compositional inhomogeneities could all be resolved. We find the defect luminescence in these materials has a strong dependence on excitation density and we use this to our advantage for identifying the spectral signatures of distinct defect species and their distribution. Further time-resolved CL measurements elucidate the role these defects play in carrier recombination within the wells. We find that as the growth temperature increases, certain point defect populations proliferate and migrate, which impacts upon the quantum well luminescence intensity, homogeneity and overall device performance.

Combining CLEBIC measurements with atomic force microscopy (AFM) measurements allows us to identify the growth mechanisms at play and then relate these to the point defect distributions observed at various temperatures. The spiral step structures around screw type threading dislocations were found to be of critical importance, influencing local alloy compositions and defect incorporation.

We explored temperatures in the range of 970°C–1100°C and can report a few core findings. As temperatures were increased the concentrations of both radiative and non-radiative defects around the dislocations increased. Away from the dislocations an improvement in non-radiative populations was gained up to a maximum at 1060°C at which point performance regressed and point defects once again become problematic. The non-radiative species responsible for decreased performance away from dislocations at low temperatures and high temperatures are likely distinct given their unique temperature preferences.

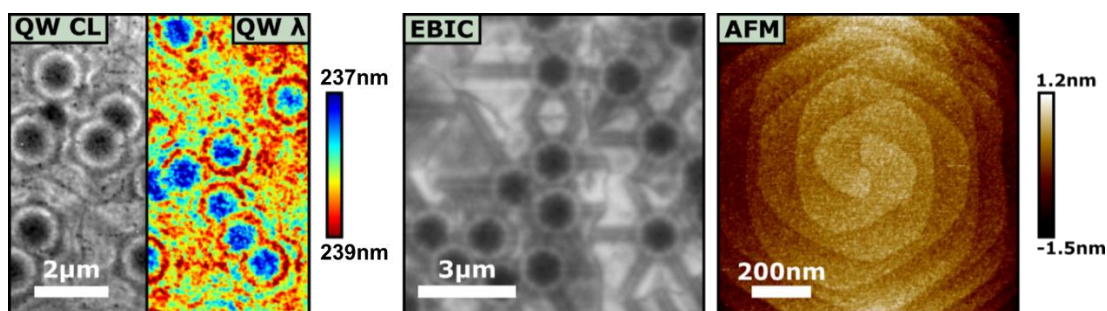


**Fig. 1.** From left to right we have a CL hyperspectral data set, with both the fitted QW intensity and wavelength plotted. The central EBIC image reflects overall recombination (radiative and non-radiative) from within the depletion region. Finally, we display an AFM height map of a single hillock feature with clear atomic step structure.

## Cathodoluminescence of triplet excitons in organic light emitting diode materials

B.G. Mendis<sup>1\*</sup>, A. Danos<sup>1,2</sup> and A.P. Monkman<sup>1</sup>

1. Dept. of Physics, Durham University, South Road, Durham, DH1 3LE, UK

2. School of Physical and Chemical Sciences, Queen Mary University of London, London, E1 4NS, UK

\*Corresponding author: b.g.mendis@durham.ac.uk

Triplet excitons have parallel spins between electrons in their ground and excited orbitals, preventing radiative emission because of the exclusion principle. However, statistically they make up 75% of the excitons produced in an organic light emitting diode (OLED) device. The remaining 25% are singlet excitons, with anti-parallel spins. In the absence of spin-orbit coupling, electronic transitions between the excited triplet state and singlet ground state are spin forbidden. Consequently, radiative decay of triplet excitons only produce weak phosphorescence. Characterising the triplet state is nevertheless important for developing more efficient OLED emissive layers, although doing this through standard photoluminescence requires specialised measurements. A previous report [1] has indicated that triplets can however be readily detected using cathodoluminescence (CL), with an unconfirmed mechanism likely similar to that in OLEDs (recombination of uncorrelated electron-hole pairs).

We have performed scanning electron microscope CL measurements on two room temperature phosphorescence molecules relevant to OLEDs: 22Cz [2] and NPB [3], hosted in a zeonex polymer (1 wt% concentration). Both singlet and triplet luminescence are strongly excited by the electron beam (Figure 1a) and have similar orders of magnitude. The nature of the exciton luminescence is confirmed by blanking the electron beam during hyperspectral CL acquisition, and monitoring the decay of the respective intensities. (Figure 1b). Singlet fluorescence abruptly falls to the background noise level, while triplet emission shows slow decay characteristic of phosphorescence. Since the electron beam can only directly generate singlet excitons, the triplet emission must be due to secondary effects. Apart from electron-hole pair generation, an electron beam can also strongly excite plasmons. We propose that decay of plasmons into electron-hole pairs provides a secondary source of singlets and triplets in 1:3 ratio, as governed by spin statistics. This process is similar to electron and hole injection during operation of an OLED device. A simple kinetic rate model shows that for similar singlet and triplet CL intensities,  $g_e \sim fg_p$ , where  $g_e$ ,  $g_p$  are respectively the electron-hole pair and plasmon generation rates of the electron beam, and  $f$  is the fraction of plasmon decay events leading to exciton formation. Electron energy loss spectroscopy (EELS) measurements on an organic P3HT polymer suggests that  $f \sim 1$ , i.e. excitons are readily produced by plasmon decay. Work is underway to perform similar EELS measurements on the OLED materials in this study. The preliminary results indicate that plasmon decay is an effective source of secondary excitons, which makes CL a promising tool for simultaneously measuring singlet and triplet emission in OLEDs.

### References

- [1] P.J. Wellman, U. Karl, S. Kleber, and H. Schmitt, *J. Appl. Phys.* **101**, 113704 (2014).
- [2] I.A. Wright, A. Danos, S. Montanaro, A.S. Batsanov, A.P. Monkman and M.R. Bryce, *Chem. Eur. J.* **27**, 6545 (2021).
- [3] A. Kirch, M. Gmelch and S. Reineke, *J. Phys. Chem. Lett.* **10**, 310 (2019).
- [4] M. Gmelch, T. Achenbach, A. Tomkeviciene and S. Reineke, *Adv. Sci.* **8**, 2102104 (2021).

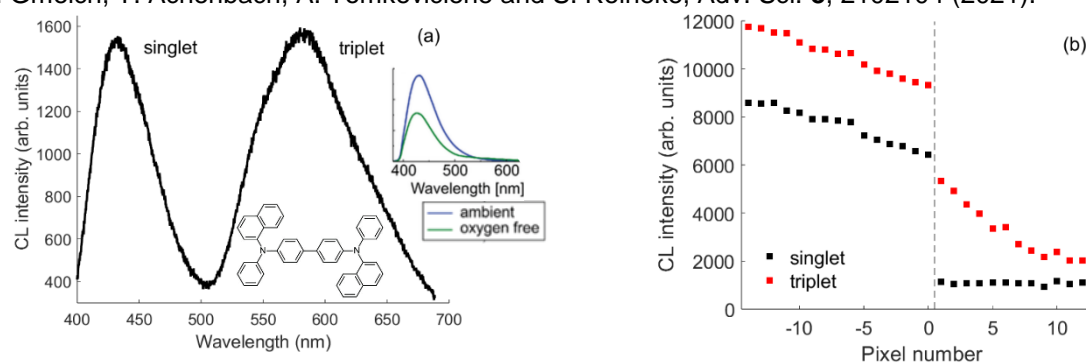


Fig. 1: (a) CL spectrum of NPB (structure inset) and the absence of triplet emission in standard photoluminescence measurements (adapted from [4]) (b) 'decay' curves measured by blanking the electron beam during hyperspectral mapping. The pixel number in the hyperspectral map effectively represents time. The beam was blanked at pixel '0' and the pixel acquisition time was 0.01s. The small decrease in CL intensity prior to beam blanking, i.e. negative pixel number, is due to electron beam damage.

## Morphological Effect on Cathodoluminescence Outcoupling in Perovskite Thin Films

R. Schot,<sup>1)\*</sup> I. Schuringa,<sup>1)</sup> S. Fiedler,<sup>1)</sup> T. Veeken,<sup>1)</sup> B. Ehrler,<sup>1)</sup> and A. Polman<sup>1)</sup>

<sup>1)</sup> NWO-Institute AMOLF, Science Park 104, 1098 XG Amsterdam, The Netherlands

\*Corresponding author: schot@amolf.nl

Metal halide perovskites have emerged as promising materials for solar cells, LEDs and other optoelectronic devices, due to their outstanding optical and electronic properties. To optimize the performance and minimize degradation effects under operation, a detailed understanding of the optoelectronic and structural properties at the micro- and nanoscale is required.

In this study, we utilize cathodoluminescence spectroscopy (CL) to carry out these studies. In CL, a high-energy electron beam (5-30 keV) in a scanning electron microscope (SEM) is raster-scanned over the surface and the light emission is detected and analysed. We investigate the CL emission from polycrystalline CsPbBr<sub>3</sub> films and correlate 2D CL maps with high spatial resolution with the surface morphology at the nanoscale. We find that the CL intensity is significantly reduced at the polycrystalline perovskite film's grain boundaries, hinting at reduced optical quality in these regions. On top of that, a "ring" like pattern is found in samples with larger grains, as shown in the measured CL map in Figure 1.

We then utilise optical near-field simulations with electric dipole sources to simulate the CL emission intensity across the surface, considering the surface morphology around the grain boundaries and the electron-sample interaction distribution beneath the surface. We use surface profiles measured with AFM as input for these simulations, including the silicon substrate. We find that the experimental CL line profiles closely resemble the simulations, indicating that the nano- and microscale surface morphology strongly affects the light outcoupling, leading to reduced CL emission collected from the grain boundaries. Moreover, we find that the "ring" like behaviour in the 2D maps is due to the interference of the dipoles with their own reflected plane waves and reflected evanescent waves. As a result, we conclude that the influence of the surface morphology and substrate on light outcoupling dominate the variation in the detected CL signal.

Our work shows that CL spectroscopy is a powerful tool to study opto-electronic properties of perovskite and other semiconductor materials at the nano- and micro-scale. At the conference we will present additional data comparing simulations with experiments with varying probing depths by varying the electron beam energy. Using Monte Carlo simulations of the electron-sample interaction volume enables estimation of the carrier diffusion length near the grain boundaries. In a further advanced analysis, considering the calculated local density of states near the corrugated surfaces, we use CL spectroscopy to probe the emission quantum efficiency of perovskite films at deep sub-wavelength spatial resolution.

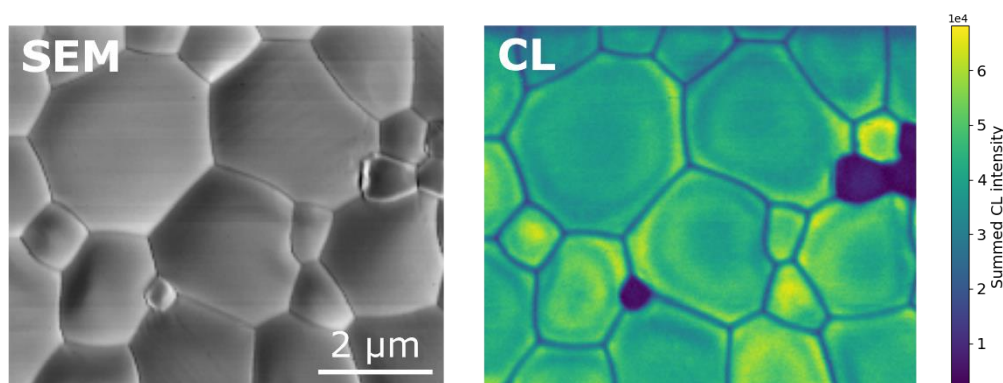


Fig. 1: SEM image and Cathodoluminescence (CL) intensity map of a CsPb<sub>3</sub>Br film on a silicon substrate, measured with an acceleration voltage of 2 keV. Grain boundaries appear "dark", while the grains show a "ring" like pattern.

## Luminescence properties of dislocations in $\alpha$ -Ga<sub>2</sub>O<sub>3</sub>

M. Maruzane,<sup>1)</sup> Y. Oshima,<sup>2)</sup> O. Makydonska,<sup>1)</sup> P. R. Edwards,<sup>1)</sup> R. W. Martin,<sup>1)</sup> and F. Massabuau<sup>1)</sup>\*

<sup>1)</sup> University of Strathclyde, Glasgow, United Kingdom

<sup>2)</sup> National Institute for Materials Science, Tsukuba, Japan

\*Corresponding author: [f.massabuau@strath.ac.uk](mailto:f.massabuau@strath.ac.uk)

Gallium oxide (Ga<sub>2</sub>O<sub>3</sub>) is an emerging ultra-wide bandgap semiconductor showing promising applications for ultraviolet photodetectors and high-power transistors [1]. The material can exist under different phases – namely  $\alpha$ ,  $\beta$ ,  $\kappa$ ,  $\delta$ ,  $\gamma$  – with the monoclinic  $\beta$ -phase being the thermodynamically stable variant. However, the metastable phases, in particular the rhombohedral  $\alpha$ -phase, is receiving increasing interest owing to its wider bandgap (ca. 5.3 eV) and prospects for alloying with isomorphous sesquioxides [2]. However, to unlock the exceptional potential of this material, a better understanding of its properties is necessary.

Defects play a vital role in the development of semiconductor devices, often thought to hamper the full potential of the technology. It is therefore crucial to better understand the properties of defects to identify “killer defects” and implement targeted mitigation methods that will lead to step increase in device performance and reliability. Dislocations is one of the most prominent defects in epitaxial Ga<sub>2</sub>O<sub>3</sub>, yet their properties are to date unknown.

We use hyperspectral cathodoluminescence mapping to analyse the optical properties of dislocations in epitaxial lateral overgrowth (ELOG)  $\alpha$ -Ga<sub>2</sub>O<sub>3</sub> sample. The dislocations are associated with a reduction of self-trapped hole related luminescence (ca. 3.6 eV line) which can be ascribed to their actions as non-radiative recombination sites for free electrons, to a reduction in free electron density due to Fermi level pinning or to electron trapping at donor states. An increase in the intensity of the ca. 2.8 eV and 3.2 eV lines is observed at the dislocations, suggesting an increase in donor-acceptor pair transitions and providing strong evidence that point defects segregate at dislocations [3].

### References

- [1] Pearton et al, Appl. Phys. Rev. **5**, 011301 (2018)
- [2] Oshima et al, Appl. Phys. Lett. **121**, 260501 (2022)
- [3] Maruzane et al, J. Phys. D: Appl. Phys. **58**, 03LT02 (2025)

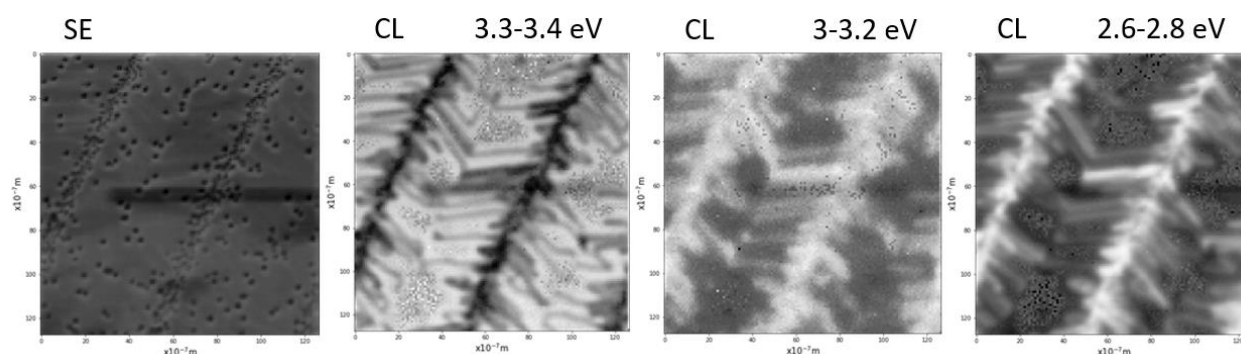


Fig. 1: SE image and bandpass CL images of ELOG  $\alpha$ -Ga<sub>2</sub>O<sub>3</sub>.

## Temperature-dependent interplay between surface GaN quantum wells and two-dimensional MoS<sub>2</sub>

D. Chen,<sup>1)\*</sup> J. Jiang,<sup>2)</sup> J.-F. Carlin<sup>1)</sup>, M. Banerjee,<sup>2)</sup> and N. Grandjean<sup>1)</sup>

<sup>1)</sup> Laboratory of Advanced Semiconductors for Photonics and Electronics, Ecole polytechnique fédérale de Lausanne (EPFL), CH-1015 Lausanne, Switzerland

<sup>2)</sup> Laboratory of Quantum Physics, Ecole polytechnique fédérale de Lausanne (EPFL), CH-1015 Lausanne, Switzerland

\*Corresponding author: danxuan.chen@epfl.ch

The optical properties of hybrid van der Waals (vdW) heterostructures combining two-dimensional (2D) MoS<sub>2</sub> with bulk GaN and surface GaN quantum wells (QWs) shows that MoS<sub>2</sub> enhances GaN surface emission at room temperature (RT) [1]. This effect is stronger for surface QWs and is attributed to passivation of intrinsic surface states (Fig. 1, left). In this study, we performed temperature-dependent cathodoluminescence (CL) measurements on these samples. For MoS<sub>2</sub> on bulk GaN epilayer, GaN CL intensity contrast varies significantly with temperature (Fig. 2), with passivation effect active at RT but quenched at low temperatures, supporting a thermally activated charge transfer across the vdW interface. Additionally, for surface GaN QWs, MoS<sub>2</sub> significantly suppresses emission at low temperatures, particularly for QWs near/at the surface (Fig. 1, right), suggesting a near-field charge or energy transfer between the two. These results highlight CL as a powerful tool for investigating surface effects and near-field interactions in 2D materials/III-nitride vdW heterostructures, paving the way for novel optoelectronic applications.

### References

[1] D. Chen *et al.*, *Nano Lett.*, **24**, 33, 10124–10130 (2024).

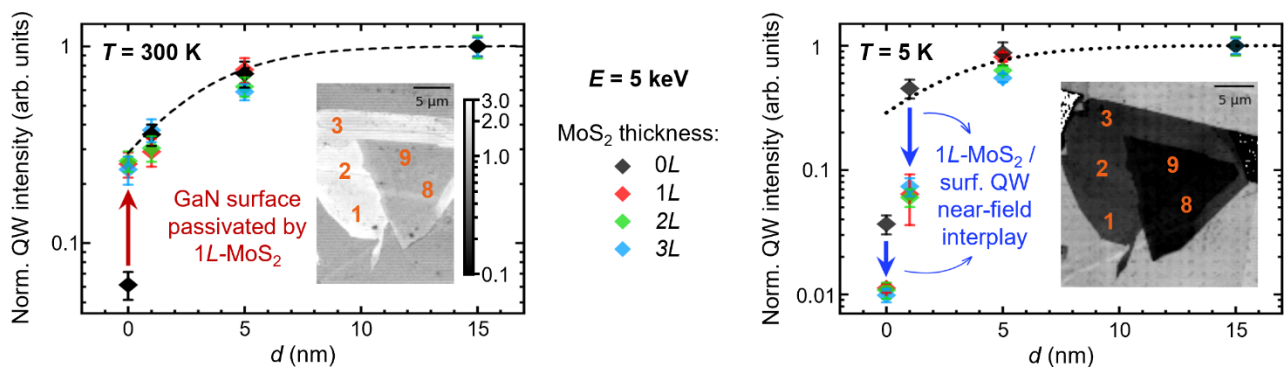


Fig. 3: QW CL intensity as a function of surface barrier thickness ( $d$ ), extracted from regions without and with MoS<sub>2</sub> coating (1–3 monolayers), under 5 keV electron beam excitation at  $T = 300$  K (left) and  $T = 5$  K (right). The dashed/dotted curves represent the spatial distribution of extrinsic surface defects. For comparison, CL intensity maps of the uncapped QW ( $d = 0$ ) coated with an MoS<sub>2</sub> flake of varying thickness (1 to 9 monolayers, as indicated by orange numbers) are shown in the insets for 300 K and 5 K, both normalized to the region without MoS<sub>2</sub> and plotted on a logarithmic scale from 0.1 to 3.

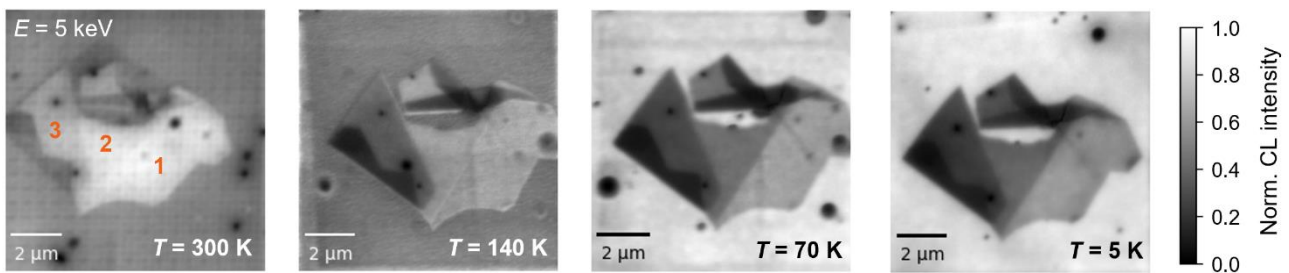


Fig. 4: Normalized GaN CL intensity maps of the MoS<sub>2</sub>-coated bulk GaN epilayer, measured with a 5 keV electron beam at  $T = 300$  K, 140 K, 70 K, and 5 K. Orange numbers in the first map indicate the number of MoS<sub>2</sub> monolayers in the corresponding region. All maps are normalized to their respective maximum and minimum values and plotted on a linear intensity scale from 0 to 1.

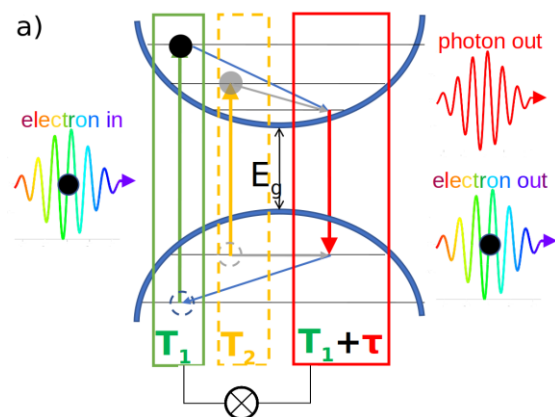
## Cathodoluminescence excitation spectroscopy and the quest of filtering transition radiation

A. Freilinger<sup>1)\*</sup>, F. Castioni<sup>1)</sup>, Y. Auad<sup>1)</sup>, J.-D. Blazit<sup>1)</sup>, X. Li<sup>1)</sup>, M. Kociak<sup>1)</sup>, L. Tizei<sup>1)</sup>

<sup>1)</sup> Univ. Paris-Saclay, CNRS, LPS Orsay, 91400 Orsay, France

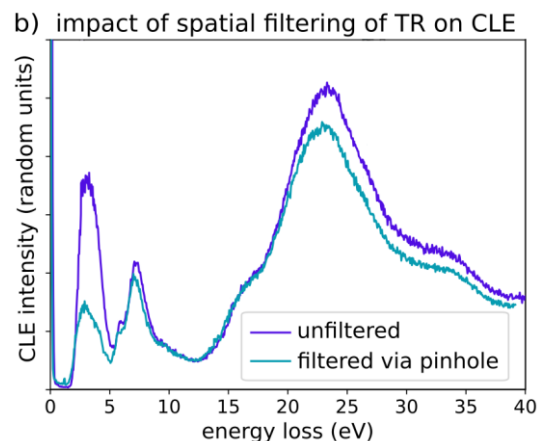
\*Corresponding author: [alissa.freilinger@universite-paris-saclay.fr](mailto:alissa.freilinger@universite-paris-saclay.fr)

Cathodoluminescence excitation spectroscopy (CLE) in Scanning Transmission Electron Microscopy (STEM) is a technique that correlates electron excitation with subsequent photon emission events. These are measured via electron energy loss spectroscopy (EELS) and cathodoluminescence spectroscopy (CL) respectively and correlated via nano-second resolved coincidence detection using a Timepix3 detector for electrons and PMTs for CL. This setup, currently installed on our Nion Hermes STEM, allows for the tracking of which excitation energy leads to a photon emission, crucial for dealing with the broadband nature of the electron-matter interaction. [3] We currently investigate single point defect emitters in nanomaterials like hexagonal Boron Nitride (hBN) and diamond nanoparticles, using electron energies between 60 and 100 keV. Unfortunately, CLE's high sensitivity also picks up transition radiation (TR), which occurs in an energy range overlapping with in-gap excitations we aim to measure [2]. Filtering of TR can be temporal, spectral and spatial. We are currently working on a spatial approach, and plan to explore temporal filtering in the future. The emission angular distribution varies between TR and different excitations [4], allowing potentially not only to filter out TR background, but also to distinguish angular emission distributions of different signals. Complexity is added to the problem by the parabolic mirror used for CL light collection distorting the angular distribution [4]. We are developing an optical system to be integrated in the CL light collection path. By imaging the Fourier plane of the parabolic mirror containing the emission angular distribution [4] and selectively placing a pinhole it will allow to select specific emission angles. To visualize the expected emission angular distributions, find optimal pinhole placements, and estimate possible gains in signal-to-background-ratios, we developed python code simulating the imaging of different excitations or their superpositions in an optical system with a parabolic mirror as in [4]. Already by "blindly" placing a pinhole based on emission peaks optimization, we achieved a signal-to-background ratio enhancement of 2. Remaining challenges are that the parabolic mirror compresses a big part of the angular emission range into a relatively small portion of the resulting image, and so far, rather poor image quality.



filtered (turquoise) to reduce TR

Figure a) Schematics of electron-photon coincidence detection for CLE., Figure b) CLE spectra from hBN, unfiltered (violet) vs spatially



- [1] N Varkentina et al, Science Advances 8 (2022) eabq4947  
 [2] R Bourellier et al, Nano Letters 16 (2016) p. 4317-4321  
 [3] Y Auad et al, Ultramicroscopy 239 (2022), 113539  
 [4] T Coenen, PhD thesis (2014)

## Determination of LED External Quantum Efficiency by electron pumping in a SEM

C.Guérin<sup>1,2</sup>, F. Donatini,<sup>2</sup> Bruno Daudin<sup>1</sup>) and G. Jacopin,<sup>2</sup>)

1) Univ. Grenoble Alpes, CNRS, Grenoble INP, CEA Grenoble, IRIG, PHELIQS, NPSC, 38000 Grenoble, France

2) Univ. Grenoble Alpes, CNRS, Grenoble INP\*, Institut Néel, 38000 Grenoble, France

\*Corresponding author: corentin.guerin@cea.fr

Since the entrance in the age of LEDs, the improvement of the External Quantum Efficiency (EQE), which relates the number of emitted photons to the number of injected electron-hole pairs, is the key issue. However, the question of the measurement of this figure of merit and the reproducibility of the measurement is itself a quest. These measurements usually request to process the full LED, are generally onerous and have to be customized in function of needs. Moreover, in specific range of wavelengths, e.g. deep-UV, the realization of a good EQE for LEDs is drastically depending on the realization of good contacts on the epitaxial structure. Adding to that the difficulty to p-dope wide bandgap materials like AlGaN with high AlN molar fraction, electroluminescence measurement on deep-UV LED is generally dealing with low signals, making their measurement difficult.

Here, we propose a contactless method to measure the EQE of a LED through electron pumping inside a Scanning Electron Microscope (SEM). The key idea of the technique relies on the use of a light-integrative sphere. This technique has the advantage to be easy and reproducible in different SEM. Moreover, it does not require a process for contacting the LED. Then, the LED is not electrically pumped but electronically pumped. One of the main advantage of the technique is the possibility to image directly the LED efficiency inside the sphere without any limitation of field of view compared to standard EQE measurements techniques. This allows one to characterize different patterns in a single measurement.

More precisely, as shown in fig1, the sphere is introduced in the SEM and a Si-photodiode is placed to measure the signal after homogenisation of the light. The sample is introduced at the bottom of the sphere on a grounded metallic plate. This allows one to avoid charge accumulation in the sample. A top aperture of 2 mm allows the electron beam to excite the sample inside the sphere. It is also grounded to mitigate charge effects due to electron accumulation inside the reflective coating of the sphere (see fig1). The photodiode is then connected to a low-noise current preamplifier. In such configuration, each scanned pixel corresponds to a value of current, directly proportional to the real power emitted by the scanned point of the LED. Realization of a scanning allows one to realize a mapping of the light power on the sample (see fig 2.).

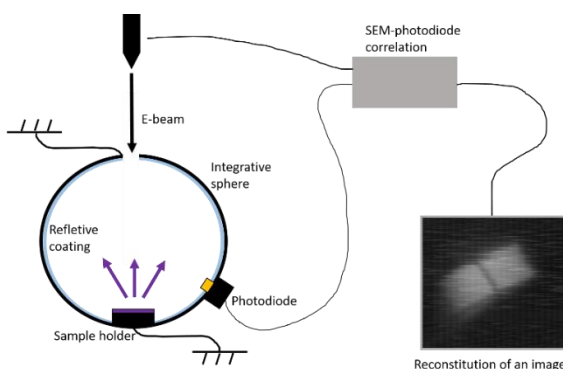


Fig. 1: Schema of the setup inside the SEM

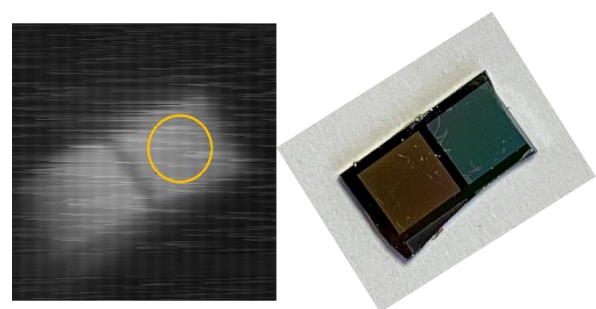


Figure 2: Integrated signal image of the sample inside the sphere (and its picture at right). The bright zones correspond to the growth zones. The signal is a mix of the 245nm active zone emission and 350nm defect related band. The yellow circle represents the averaging of the signal for the EQE measurement

## Photo-Enhanced Cathodoluminescence

Nicolas Tappy<sup>1)\*</sup>, Aurélie Coppex<sup>1)</sup>, Stefano Marinoni<sup>2)</sup>, Nicholas Morgan<sup>1)</sup>, and Christian Monachon<sup>1)</sup>

<sup>1)</sup> Attolight SA, Chemin de la Venoge 11, 1024 Ecublens, Switzerland

<sup>2)</sup> Laboratory of Semiconductor Materials, Ecole Polytechnique Fédérale de Lausanne, 1015 Lausanne, Switzerland

\*Corresponding author: nicolas.tappy@attolight.com

Latest developments of electron microscopy often involve the controlled injection of a laser beam into the microscope's chamber. Applications include in-situ photoluminescence (PL) and Raman spectroscopy, where electron microscopy acts as a correlative imaging technique. Light collection optics designed for cathodoluminescence (CL) measurements are well suited for this purpose thanks to their achromaticity and high numerical aperture. CL scanning electron microscopes (SEM) thus enable combination studies, where CL is perturbed by the presence of a laser beam on the sample (Fig. 1a) during measurement (or vice versa). However, with the notable exception of a study on diamond NV centers [1], such combination studies do not seem to be commonplace. Indeed, for most samples it is expected that luminescence intensity scales linearly with excitation power. In that case, the outcome of simultaneous laser- and electron-beam probing results in summing both signals acquired individually. However, we have observed an interesting deviation from this trivial behaviour even in bulk semiconductor materials, where luminescence mechanisms are generally well understood.

In this work we present that when a GaAs sample is simultaneously excited with a laser, superlinear enhancement of CL signal is observed. This manifests as a clear image of the laser spot on the CL map (Fig. 1b-1d). We discuss probable underlying physical mechanisms for this phenomenon, which has not been described in the literature to the best of our knowledge. We also briefly discuss opposite mechanisms that can lead to decreasing of CL signal under illumination. Finally, we outline the potential for this phenomenon as a new measurement technique, both in material characterization and advanced electron microscopy experiments involving pulsed laser and electron beams, such as ultrafast SEM [2,3].

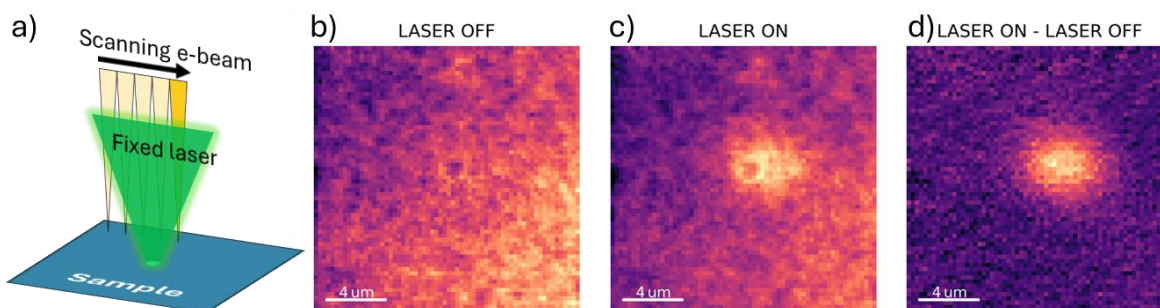


Fig. 1: Principle of photo-enhanced cathodoluminescence measurement. a) shows the principle of the experiment: an electron beam is scanned on the sample to measure a luminescence map, while the laser beam is focused at a fixed position, ideally centered in the field of view. b) – c) are luminescence intensity maps of the GaAs sample acquired via CL-SEM without or with the laser beam, respectively. d) shows the difference between b) and c). The laser used is a 532 nm CW laser. Here, the power absorbed in the sample is about 25  $\mu$ W.

### References

- [1] Solà-Garcia M, Meuret S, Coenen T and Polman A 2020 Electron-Induced State Conversion in Diamond NV Centers Measured with Pump–Probe Cathodoluminescence Spectroscopy *ACS Photonics* **7** 232–40
- [2] Yang D-S, Mohammed O F and Zewail A H 2010 Scanning ultrafast electron microscopy *Proc. Natl. Acad. Sci.* **107** 14993–8
- [3] Garming M W H, Weppelman I G C, Lee M, Stavenga T and Hoogenboom J P 2022 Ultrafast scanning electron microscopy with sub-micrometer optical pump resolution *Appl. Phys. Rev.* **9** 021418

## Towards Laser-Driven Semiconductor Electron Sources: Field-Induced Negative Electron Affinity Gallium Nitride Photocathodes

S. Marinoni<sup>1)\*</sup>, N. Tappy<sup>2)</sup>, V. Piazza<sup>1)</sup>, A. Fontcuberta i Morral<sup>1)</sup> and C. Monachon<sup>2)</sup>

<sup>1)</sup> Laboratory of Semiconductor Materials, Ecole Polytechnique Fédérale de Lausanne, 1015 Lausanne, Switzerland

<sup>2)</sup> Attolight SA, Chemin de la Venoge 11, 1024 Ecublens, Switzerland

\*Corresponding author: stefano.marinoni@epfl.ch

Ultra-bright electron sources are essential for advancing semiconductor nanotechnologies, enabling high-resolution electron microscopy and lithography. These sources must combine long-term stability, excellent coherence and straightforward intensity modulation. With the development of time-resolved techniques, it is also highly desirable to design electron sources capable of generating both continuous and pulsed electron beams. The latter are typically obtained by converting traditional metal cathodes such as Schottky-type emitters into ultrafast lasers-driven photocathodes. This process is inherently time-consuming and imposes significant constraints on both stability and brightness [1-2]. As an alternative, emitters relying on negative electron affinity (NEA) photocathodes based on caesium-activated semiconductor surfaces allow for rapid switching between continuous and pulsed operation while offering excellent brightness and current tunability [3-4]. However, maintaining satisfactory performance requires frequent in situ re-activation of the surface [4].

We explore a novel idea to induce NEA in p-doped gallium nitride (GaN) photocathodes without surface coating. We fabricate 40  $\mu\text{m}$ -tall, high-aspect-ratio GaN micro-pyramids using a scalable, top-down approach, yielding sub-micron apex radii (Fig. 1a). Upon application of a voltage bias, the sharp morphology enhances the electric field around the pyramid apex. Our calculations predict that field-induced NEA should occur at electric fields comparable to or lower than those used in commercial Schottky-type electron guns. To validate this experimentally, we recreate a laser-driven electron gun environment within a scanning electron microscope (Fig. 1b). A UV laser is injected into the microscope and focused onto a 4- $\mu\text{m}$  spot on the pyramid apex. Simultaneously, a biased nanomanipulator approaches the micro-pyramid surface at nanometric distances, inducing electric fields in the range of 1 GV/m. The resulting photoemission current is continuously monitored throughout the experiment.

This work presents the conceptualization, prototyping and first experimental testing of field-induced NEA GaN photocathodes. We discuss both the advantages and challenges of this approach, which integrates the well-established benefits of Schottky virtual sources with the versatility of laser-driven semiconductor photocathodes.

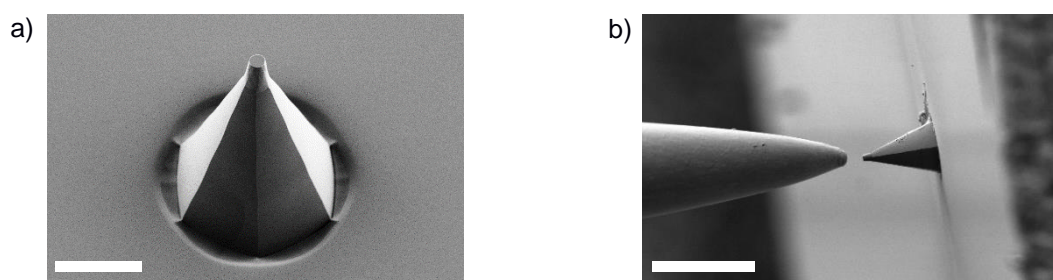


Fig. 5: a) SEM image of a GaN micro-pyramid. The scale bar is 10  $\mu\text{m}$ . b) Experimental testing of field-induced NEA in a GaN micro-pyramid. Inside an SEM, a biased microprobe (left) approaches a grounded photocathode (right). A UV laser is focused onto the photocathode apex. The scale bar is 50  $\mu\text{m}$ .

### References

- [1] L. Zhang, J. Hogenboom, B. Cook and P. Kruit, *Struct. Dyn.* **6**, 051501 (2019)
- [2] D. Yang, O. F. Mohammed and A. H. Zewail, *PNAS* **107** (34), 14993-14998 (2010)
- [3] H. Morishita, T. Ohshima, K. Otsuga, M. Kuwahara, T. Agemura and Y. Ose, *Ultramicroscopy* **230**, 113386 (2021)
- [4] T. Nishitani, Y. Arakawa, S. Noda, A. Koizumi, D. Sato, H. Shikano, H. Iijima, Y. Honda and H. Amano, *J. ac. Sci. Technol. B* **40**, 064203 (2022)

# Cathodoluminescence Hyperspectral Imaging without an Electron Microscope

P. R. Edwards<sup>1)\*</sup> and R.W. Martin<sup>1)</sup>

<sup>1)</sup> University of Strathclyde, Department of Physics, 107 Rottenrow, Glasgow G4 0NG, United Kingdom

\*Corresponding author: paul.edwards@strath.ac.uk

“Optical” cathodoluminescence (CL) setups have long been used as an alternative to electron-microscope-based systems, primarily in the earth sciences [1]. In such setups, a cold-cathode electron gun is used to flood an extended area of a sample with energetic electrons in a small vacuum chamber, with the resultant emission captured through an optical window using a wide-field microscope. Advantages of this approach include: low cost; extremely rapid data acquisition; large field of view; and no requirement for electrical conductivity, due to the charge neutralising effect of positive ions. The main downside is that the spatial resolution is now wavelength-limited due to the effect of far-field diffraction. An additional limitation so far has been the lack of spectral information, with images limited to either RGB colour or a small number of multispectral channels selected through the use of a motorised filter wheel and a set of bandpass filters [2].

In this presentation we report the extension of this technique to the hyperspectral imaging domain. This is achieved through the use of a Lyot-type tuneable bandpass filter, through which multiple monochromatic images are acquired while the peak bandpass wavelength is incrementally shifted, to form a hyperspectral image stack. This is similar to a method we have previously applied to the rapid collection of *electro*-luminescence hyperspectral images from light-emitting diodes [3].

We present initial results of applying the technique to luminescent test structures and LEDs. We discuss the factors affecting the performance of such a system, and its applicability and limitations in the study of light-emitting semiconductors.

Finally, the linearly polarizing nature of the tuneable filter further lends itself to the measurement of polarization anisotropy in the emitted luminescence, and we discuss how the technique would be extended to implement this.

## References

- [1] M.R. Lee, R.W. Martin, C. Trager-Cowan, and P.R. Edwards, *J. Sediment. Res.* **75**, 313–322 (2005)
- [2] B. Charlier, L. de Colnet, and E. Pirard, *Proceedings - Annual Meeting - Belgian Soc. Microscopy* (2001)
- [3] P.R. Edwards, J. Bruckbauer, D. Cameron, and R.W. Martin, *Appl. Phys. Lett.* **123**, 112110 (2023).

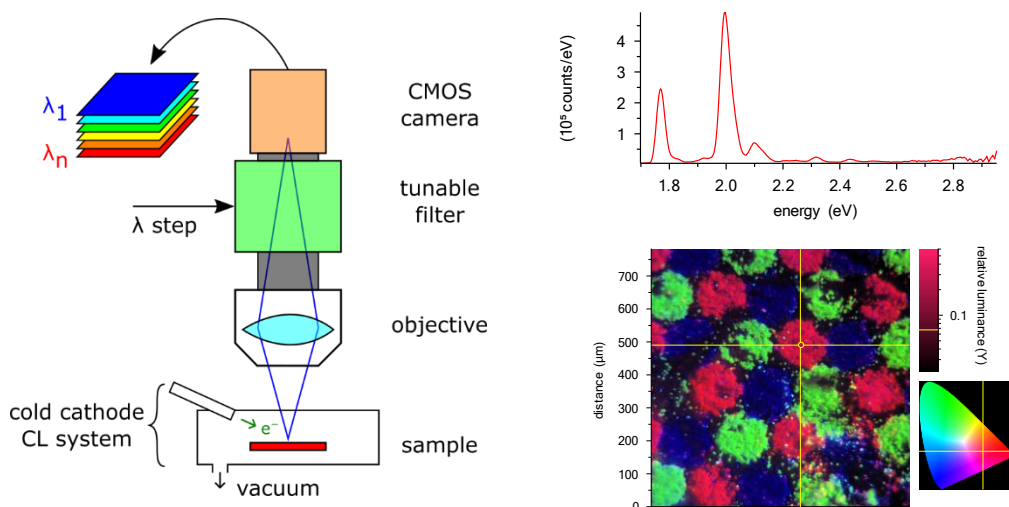
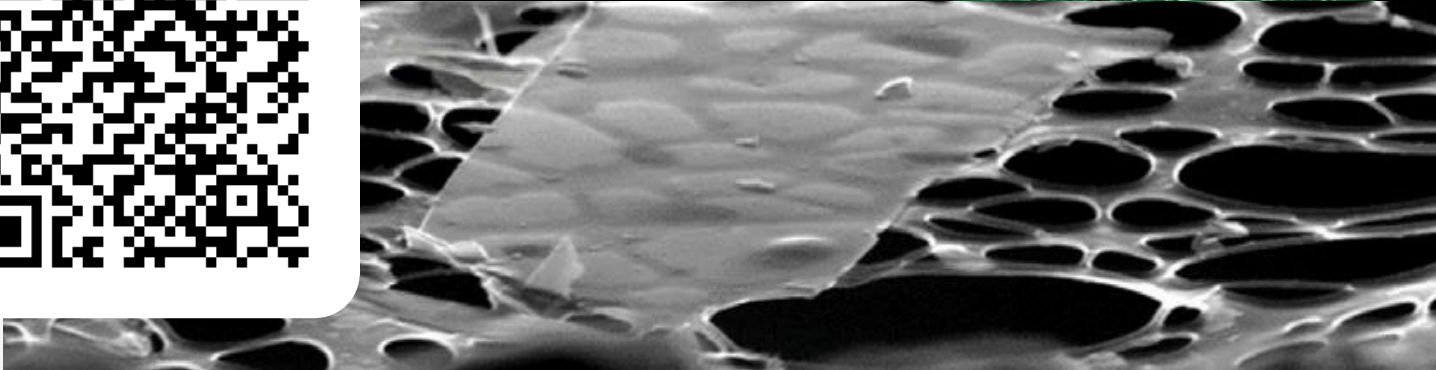
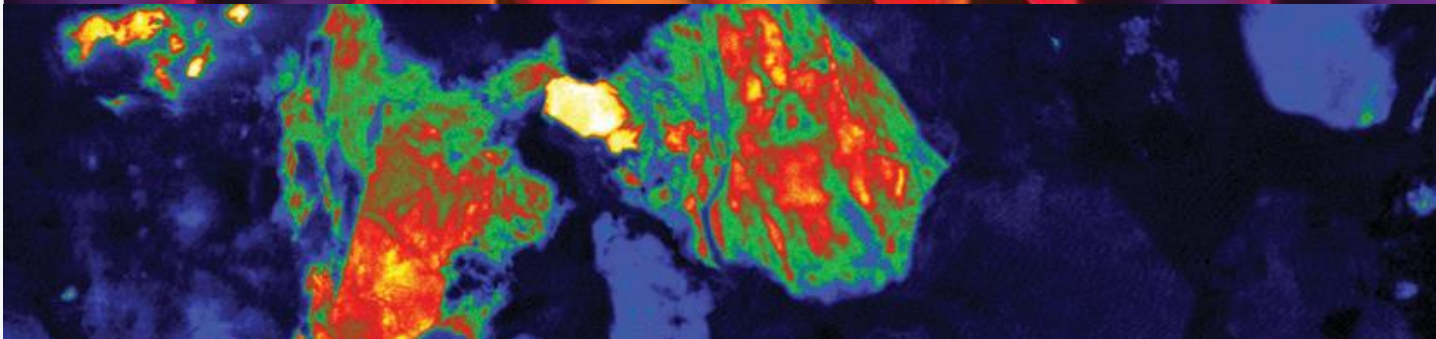
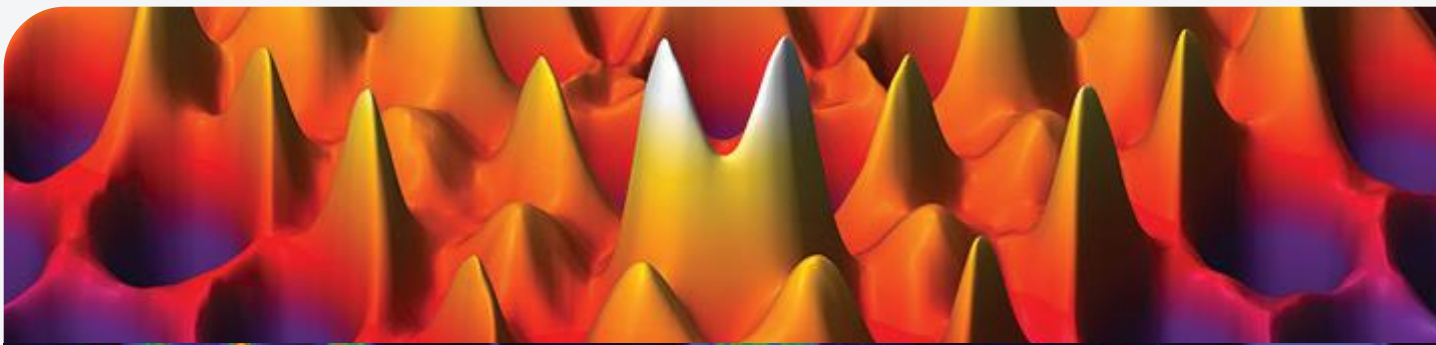


Fig. 1: (Left) Schematic of the cold-cathode CL hyperspectral imaging setup. (Right) Initial results from the measurement of a CRT phosphor, showing two subsets of the data cube: a reconstructed real-colour image and example spectrum.



# Study the fundamental properties of matter in great detail



TEM

# Talos (S)TEM

To make science, not compromise

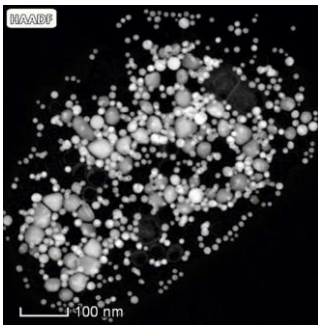
## Key Benefits

- Flexible in configuration  
Options include Cathodoluminescence, EELS, and more
- High throughput  
Fast navigation, imaging and chemistry
- Reproducible & Repeatable  
High stability, trustworthy results
- Easy to use / Intuitive  
Easy to acquire and analyze multimodal data
- Future-proof

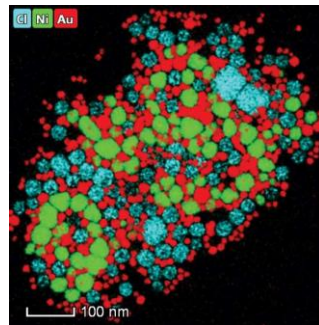


## STEM-EDS

Larger, more sensitive detectors with higher collection efficiency

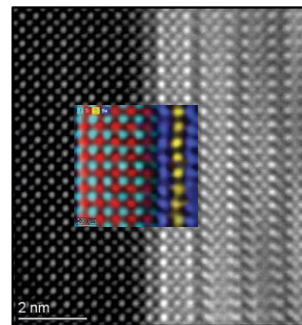


HAADF overview image revealing particle size distribution and morphology variation



EDS map on large field of view, revealing the chemistry of hundreds of nanoparticles

## Atomic resolution EDS with Super-X



Atomic resolution HAADF image and EDS map (central insert) at the interface, revealing the epitaxial relationship of the two materials

Acquired in Velox software on Talos with X-CFEG BYTO-doped YBCO

## Scan QR codes to discover more

Website



Brochure



Nanoparticles Brochure



Talos F200 Datasheet



Application note:  
Advances in Compositional Analysis Using Analytical S/TEM



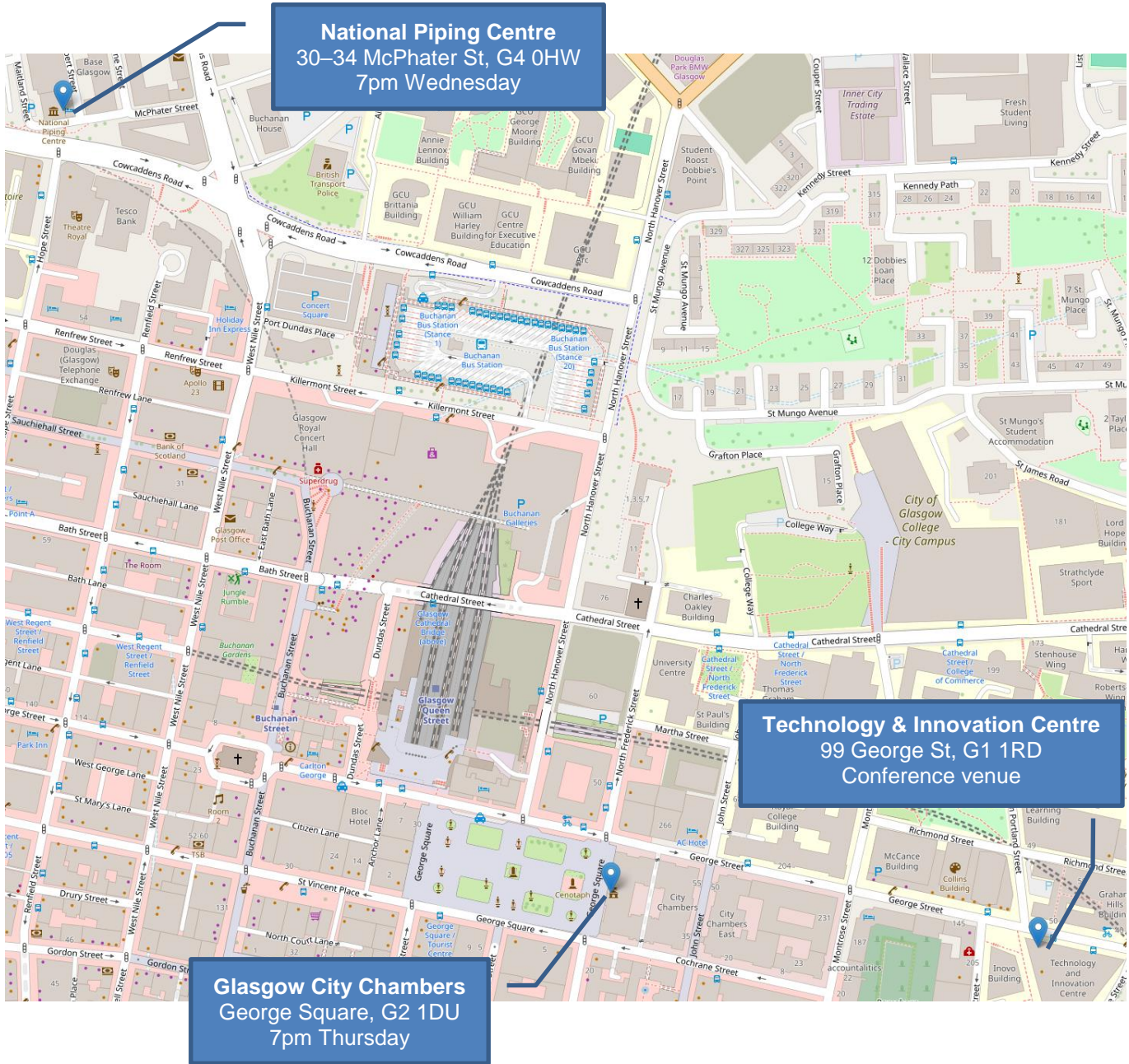
Learn more at [www.thermofisher.com/Talos](http://www.thermofisher.com/Talos)

**thermo**scientific

## Organising committee

- Robert Martin, University of Strathclyde, UK
- Fabien Massabuau, University of Strathclyde, UK
- Paul Edwards, University of Strathclyde, UK
- Gwéno   Jacopin, Institut N  el, CNRS, France
- Jonas L  hnemann, Paul Drude Institute for Solid State Electronics, Germany





Scan QR codes for directions to these venues:



Technology & Innovation Centre  
99 George St, G1 1RD  
Conference venue



National Piping Centre  
30-34 McPhater St, G4 0HW  
7pm Wednesday



Glasgow City Chambers  
George Square, G2 1DU  
7pm Thursday

